Mälardalen University Dissertations
No. 12

A CANONICAL MODEL OF THE PRIMARY VISUAL CORTEX

Baran Çürüklü

2005

National Graduate School in Computer Science
Department of Computer Science, Linköping University

The Department of Computer Science and Electronics
Mälardalen University

ISSN 1651-4238
ISBN 91-88834-51-4
Printed by Arkitektkopia, Västerås, Sweden
Distribution: Mälardalen University Press

Mälardalen University Dissertation
No. 12

A Canonical Model of the Primary Visual Cortex

Baran Çürüklü

Akademisk avhandling

som för avläggande av Teknologie Doktorsexamen vid Insitutionen för Datavetenskap och Elektronik, Mälardalens högskola, kommer att offentligen försvaras 26/4 - 2005, 14:00 i Zeta-salen, Mälardalens högskola.

Faculty opponent: Gaute T. Einevoll, Department of Mathematical Sciences and Technology, Norwegian University of Life Sciences, Ås, Norway.

National Graduate School in Computer Science, Department of Computer Science, Linköping University, SE-581 83 Linköping, Sweden

The Department of Computer Science and Electronics, Mälardalen University, P.O. Box 883, SE-721 23 Västerås, Sweden

Abstract

In this thesis a model of the primary visual cortex (V1) is presented. The centerpiece of this model is an abstract hypercolumn model, derived from the Bayesian Confidence Propagation Neural Network (BCPNN). This model functions as a building block of the proposed laminar V1 model, which consists of layer 4 and 2/3 components.

The V1 model is developed during exposure to visual input using the BCPNN incremental learning rule. The connectivity pattern demonstrated by this correlation-based network model is similar to that of V1. In both modeled cortical layers local horizontal connections are dense, whereas long-range horizontal connections are sparse. Layer 4 local horizontal connections are biased towards the iso-orientation domain, whereas long-range horizontal connections are equally distributed between all orientation domains. In contrast, both local and long-range horizontal connections of the layer 2/3 are biased towards the iso-orientation domains. The layer 2/3 network is axially specific as well. Thus, this V1 model demonstrates how the recurrent connections can be self-organized and generate a cortex like connectivity pattern.

Furthermore, in both layers inhibition operates within a modeled hypercolumn. This is in line with what is found in the V1, i.e. inhibition is mainly local, whereas excitation extends far beyond the inhibitory network. Observe also that neither excitation nor inhibition dominates the network.

Based on this connectivity pattern the V1 model addresses several response properties of the neurons, such as orientation selectivity, contrast-invariance of orientation tuning, response saturation followed by normalization, cross-orientation inhibition. Configuration-specific facilitation phenomena are explained by the axially specific layer 2/3 long-range horizontal connections. It is hypothesized that spike and burst synchronization might aid this process.

The main conclusion drawn is that it is possible to explain connectivity as well as several response properties of the neurons by a general V1 model, which is faithful to the known anatomy and physiology of the neocortex. Thus, when simplicity is combined with biological plausibility the models can give valuable insight into structure and function of cortical circuitry.

Keywords: primary visual cortex, hypercolumn, cortical microcircuit, attractor network, recurrent artificial neural network, Bayesian confidence propagation neural network, developmental models, intracortical connections, long-range horizontal connections, orientation selectivity, response saturation, normalization, contrast-invariance of orientation selectivity, configuration-specific facilitation, summation pools

ISSN: 1651-4238
ISBN: 91-88834-51-4

Abstract

In this thesis a model of the primary visual cortex (V1) is presented. The centerpiece of this model is an abstract hypercolumn model, derived from the Bayesian Confidence Propagation Neural Network (BCPNN). This model functions as a building block of the proposed laminar V1 model, which consists of layer 4 and 2/3 components.

The V1 model is developed during exposure to visual input using the BCPNN incremental learning rule. The connectivity pattern demonstrated by this correlation-based network model is similar to that of V1. In both modeled cortical layers local horizontal connections are dense, whereas long-range horizontal connections are sparse. Layer 4 local horizontal connections are biased towards the iso-orientation domain, whereas long-range horizontal connections are equally distributed between all orientation domains. In contrast, both local and long-range horizontal connections of the layer 2/3 are biased towards the iso-orientation domains. The layer 2/3 network is axially specific as well. Thus, this V1 model demonstrates how the recurrent connections can be self-organized and generate a cortex like connectivity pattern.

Furthermore, in both layers inhibition operates within a modeled hypercolumn. This is in line with what is found in the V1, i.e. inhibition is mainly local, whereas excitation extends far beyond the inhibitory network. Observe also that neither excitation nor inhibition dominates the network.

Based on this connectivity pattern the V1 model addresses several response properties of the neurons, such as orientation selectivity, contrast-invariance of orientation tuning, response saturation followed by normalization, cross-orientation inhibition. Configuration-specific facilitation phenomena are explained by the axially specific layer 2/3 long-range horizontal connections. It is hypothesized that spike and burst synchronization might aid this process.

The main conclusion drawn is that it is possible to explain connectivity as well as several response properties of the neurons by a general V1 model, which is faithful to the known anatomy and physiology of the neocortex. Thus, when simplicity is combined with biological plausibility the models can give valuable insight into structure and function of cortical circuitry.

Keywords: primary visual cortex, hypercolumn, cortical microcircuit, attractor network, recurrent artificial neural network, Bayesian confidence propagation neural network, developmental models, intracortical connections, long-range horizontal connections, orientation selectivity, response saturation, normalization, contrast-invariance of orientation selectivity, configuration-specific facilitation, summation pools

To my dear father

Acknowledgments

I wish to thank my advisor Professor Anders Lansner at NADA, Royal Institute of Technology, for guiding me through the fascinating world of computational neuroscience. I am very grateful for having the opportunity to work with him.

I owe my principal advisor Professor Björn Lisper a dept of gratitude. He has always been helpful; in particular when I needed assistance in solving the well known, and always present 'funding problem'.

I would like to thank Dr. Jacek Malec (now at Lund University) for introducing me to graduate studies. He has also introduced me to the field of artificial intelligence through his course. My interest for artificial intelligence, which later shifted towards computational neuroscience, can be tracked back to that time. I was puzzled by questions, such as 'what would happen if a brain is replaced bit by bit?', and 'can we simulate consciousness just like any other process?'. Finally, I become fascinated by the idea of 'revealing' the computations within the brain by mathematical models.

A special thanks to Dr. Peter Funk who has been a great colleague, and more importantly a real friend. Thanks for everything Peter!

Thank you all at the Department of Computer Science and Engineering (IDt) for making our department such a pleasant place. I especially thank Harriet, Else-Maj, Monica, Åsa, Malin, Roger H, and Jan Ö for always being helpful. I also thank my friends Rikard L, Martin S, Boel, Roger J, Xavier, Jan C, Marcus, Nerina, Thomas L, Mikael S, Markus N, Waldemar, Magnus L, and Ning.

I would like to thank my family, especially my dear wife Ceren. I could not finish this work without her love and support.

This research work was funded by MRTC (the Mälardalen Real-Time Research Centre) at the IDt, and CUGS (the Swedish National Graduate School in Computer Science). This support is hereby gratefully acknowledged.

Baran Çürüklü
Västerås, March 10, 2005

Contributions

[I] Çürüklü B, Lansner A (2001) Spike and burst synchronization in a detailed cortical network model with I-F neurons. In the proceedings of the International Conference on Artificial Neural Networks (ICANN), pp. 1095–1102, Vienna, Springer-Verlag.

[II] Çürüklü B, Lansner A (2002) An abstract model of a cortical hypercolumn. In the Proceedings of the 9th International Conference on Neural Information Processing (ICONIP), pp. 80–85, Singapore, IEEE.

[III] Çürüklü B, Lansner A (2004) A Model of the Summation Pools within the Layer 4 (Area 17). The Annual Computational Neuroscience Meeting 2004, Baltimore, USA.

[IV] Çürüklü B, Lansner A (2003) Quantitative Assessment of the Local and Long-Range Horizontal Connections within the Striate Cortex. In the proceedings of the special session on 'Biologically Inspired Computer Vision', at the 2nd Computational Intelligence, Robotics and Autonomous Systems (CIRAS), Singapore, IEEE.

[V] Çürüklü B, Lansner A (2005) On the development and functional roles of the horizontal connections within the primary visual cortex (V1). Technical Report.

Contents

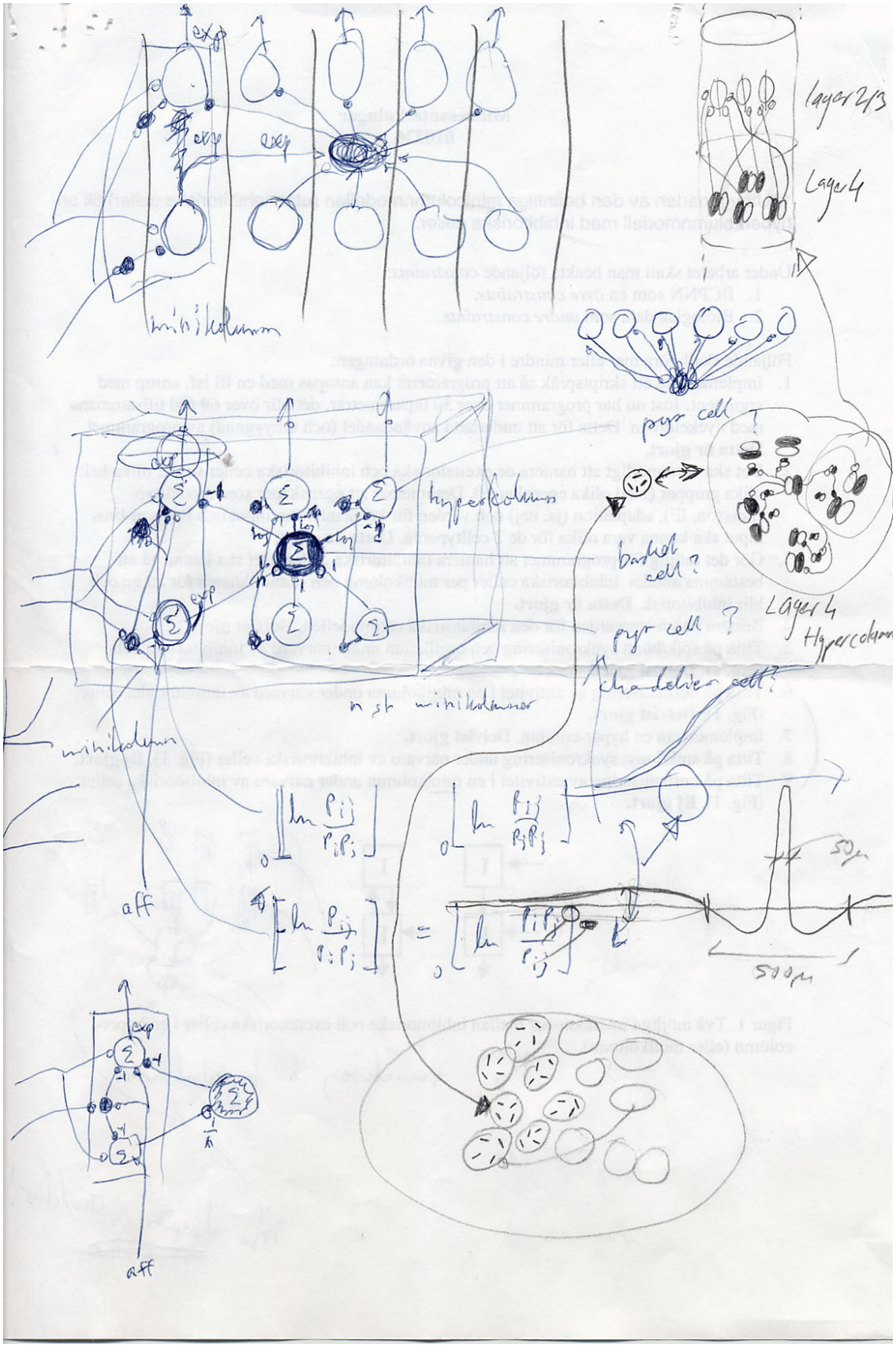
layer 2/3
Layer 4
minikolumn
pyr cell ?
hypercolumn
basket cell ?
Layer 4
Hypercolumn
pyr cell ?
chandelier cell?
minikolumn
aff
50 µm
500 µm
aff

"What chiefly distinguishes the cerebral cortex from other parts of the nervous system is the great diversity of its cell types and interconnections. It would be astonishing if such a structure did not profoundly modify the response of patterns of the fibers coming into it."
Hubel DH and Wiesel TN, (1962) Receptive fields, binocular interaction and functional architecture in the cat's visual cortex. J. Physiol., 160:106–154.

1 Introduction

1.1 Laminar and Modular Organization of the Primary Visual Cortex – Aim and Scope of the Thesis

This thesis presents a canonical model of the primary visual cortex (V1, striate cortex, Brodmann's area 17 of cat). Compared to other parts of the neocortex, the V1 is relatively well documented. It is one of the principal systems for studying the structure and function of the neocortex. In this perspective it is significant to mention that structural similarities between different cortical areas suggest that studies of the V1 (or other areas for that matter) contribute to the general understanding of the neocortex. These structural similarities are manifested by the laminar and modular organization of the neocortex.

A hypothetical structure, which is referred to as the hypercolumn, has been the starting point in the analysis of the V1. This approach leads to one of the ultimate goals of the neuroscience, which is to propose a blue print of the smallest computing unit that is capable of representing a complete set of information (of some kind). In this context this set consists of all possible orientations that can be found in a small spot of the visual field. Such a blue print could eventually help to reveal the organization principles of the whole neocortex, even if the object of study, i.e. the hypercolumn, is highly hypothetical.

Response properties of the V1 neurons, such as orientation selectivity, contrast-invariance of orientation tuning, response saturation followed by normalization, cross-orientation inhibition, and response alternations due to various long-range interactions are among the foremost issues to be addressed by a hypercolumn model. The influence of the cortical circuitry on the emergence of these response properties is still unclear. This should not come as a surprise, since the layout of the intracortical connections is not fully understood. However, as pointed out by

Hubel and Wiesel (1962), it is more likely that the intracortical connections play an active role in representation of the outside world, by modifying the sensory input: 'what chiefly distinguishes the cerebral cortex from other parts of the nervous system is the great diversity of its cell types and interconnections. It would be astonishing if such a structure did not profoundly modify the response of patterns of the fibers coming into it'.

Taken together, based on the hypothesized modular organization of the neocortex, this thesis intends to reveal the link between the intracortical connections, and the processes that create the V1 neuron's response properties. In our view the thalamocortical circuitry plays a minor, but not necessarily insignificant, role in these processes. In order to verify our hypothesis an abstract hypercolumn model, derived from the Bayesian Confidence Propagation Neural Network (BCPNN), is proposed (Paper II). The model addresses interactions within a small region of the V1 that corresponds to a cortical hypercolumn. Later this model is mapped to layers 4 and 2/3 (Paper III–V), for a more detailed analysis of the computations that are carried out within the cortical layers.

With the abstract hypercolumn model comes also the possibility of investigating a larger patch of the V1. Such a two-dimensional patch is possible to construct by tiling the hypercolumn models next to each other. It is well established that the long-range interactions play an important role in information processing within the V1. Thus, different forms of long-range facilitations of the neurons are investigated (Papers I, III–V). Distribution of the intracortical connections within the proposed layer 4 and 2/3 models has been analyzed quantitatively as well (Paper IV). This analysis intends to compare the layout of the connections within the proposed models with the V1. Finally, developmental issues related to the layers 4 and 2/3 have been addressed (Paper V).

1.2 Thesis Structure

This thesis is structured in the following way. Chapter 2 reviews the biological background. Section 2.1 comprises of a brief review of the early stages of vision, which consists of the retina, the lateral geniculate nucleus, and the V1. Modular structure of the V1, and the rest of the neocortex, is reviewed in Section 2.2. The subsequent section reviews issues related to the layout of the intracortical connections within the V1. Section 2.4 reviews emergence of orientation selectivity, as well as other response properties of the V1 neurons. In Section 2.5 functional roles of the long-range horizontal connections in the V1 neurons' responses are reviewed.

Readers who are familiar with neuroscience will notice that some issues, which are significant for understanding information processing within the cortical circuitry, are omitted, e.g. projections from higher cortical areas, connections that

involve layer 5 and 6 neurons. It is considered that these issues would not contribute significantly to the understanding of this thesis. Readers who find this thesis interesting, but is not familiar with visual neuroscience, should turn to university level textbooks in neuroscience (Purves et al., 1997; Kandel et al., 2000; Connors et al., 2002) for a more comprehensive coverage of the theory.

Chapter 3 reviews the BCPNN model and the learning rule. Proposed models of the V1 are derived from the BCPNN. Related work is covered in Chapter 4. In this chapter first two sections review the models that address emergence of orientation selectivity in the V1. Section 4.3 reviews models that address various surround effects. Section 4.4 reviews developmental models of cortical circuits and orientation maps.

Thesis results are described in Chapter 5. Section 5.1 focuses on the findings related to the layout of the intracortical connections, and their development. Section 5.2 summarizes findings related to the emergence of response properties of the V1 neurons. The following section is dedicated to the findings related to the long-range interactions within the V1. Section 5.4 contains a summary of the five papers that are included in the thesis. Chapter 6 sums up the thesis by providing a top-down view of the results described in Chapter 5. Chapters 7–11 contain the papers that are included in the thesis.

Hopefully this thesis will lead to a better understanding of the computations that are carried out within the neocortex, and clarify the challenges that lie ahead, towards more detailed models.

2 Biological Background

2.1 Early Stages of Vision – The Retino-Geniculo-Cortical Pathway

Early stages of vision consist of three structures, i.e. the retina, the dorsal lateral geniculate nucleus (dLGN, or LGN), and the V1. In this section, a brief summary of the properties of the neurons found in these structures will be given. However, some of the properties, which are of special interest, will be explained more thoroughly later (Sections 2.2–2.5). Nevertheless, this summary is limited to those properties, which are relevant to this thesis. Note further that the starting point of this thesis has been the cat V1, consequently if the species is not clear from the context it should be read as cat.

2.1.1 The Retina

The visual field is projected to the two retinae located in the eyes. Thus, the retinae are the first processing steps of the incoming information of the visual field. The retina consists of three granual layers, i.e. the photoreceptor layer, the bipolar (inner nuclear) layer, and the retinal ganglion layer. The bipolar layer consists of bipolar, amacrine, and horizontal cells. Regions between these three layers are referred to as the plexiform layers. Synaptic connections between cells located in different granual layers occur within the two plexiform layers. The outer plexiform layer is located between the photoreceptor layer and the bipolar layer, whereas the inner plexiform layer is located between the bipolar layer and the retinal ganglion layer.

The photoreceptors are divided into two types (rods and cones). These two types of cells are the only elements sensitive to light within the retina. Thus, they form the very first processing step of visual signals within the visual pathway. The specialization into rods and cones reflects different aspects of vision. The rods are

extremely sensitive to light but have poor spatial resolution. These cells are specialized for sensitivity at the expense of resolution. In contrast, the cone system has very high spatial resolution. The cones are, however, less sensitive to light. The cone system is also responsible for color vision.

The bipolar cells receive input from one photoreceptor type only (either rods or cones). Thus, the bipolar cells can be divided into rod- or cone-bipolar cells. Connections between photoreceptors and bipolar cells can be both excitatory and inhibitory. The lateral projections, which target the periphery of the bipolar cells' receptive fields, mediate the opposite to the direct path, which targets the center of the bipolar cells' receptive fields. The term 'receptive field' (RF) is often used when the response properties of the neurons are discussed. In terms of vision this term can be defined as: 'the receptive field of a neuron in the visual system is the region of the retina that influences the firing rate of the target neuron by increasing it (excitation) or decreasing it (inhibition)' (Palmer, 1999).

The connection pattern results in two types of bipolar cells, ON and OFF, with opposite response properties. The ON bipolar cells have ON-center (direct path) and OFF-surround (lateral path) receptive fields, whereas the OFF bipolar cells have OFF-center (direct path) and ON-surround (lateral path) receptive fields.

The bipolar cells make only excitatory connections to the retinal ganglion cells. These connections are of two types, either ON bipolar cells to ON retinal ganglion cells or OFF bipolar cells to OFF retinal ganglion cells. As a result of this wiring pattern, the retinal ganglion cells have similar response properties as the bipolar cells. Retinal ganglion cells are the last processing step within the retina. Thus, they project to the LGN.

Kuffler (1953) discovered receptive field properties described above. The physiological studies done by Kuffler (1953) have shown that the cat retinal ganglion cells respond to small spots of light. This study indicates that each ganglion cell responds to stimulation of a small, circular patch of the retina. This patch defines the receptive field of a single retinal ganglion cell. Kuffler (1953) has discovered two different types of retinal ganglion cells (ON and OFF). When the center of an ON retinal ganglion cell is stimulated with a light spot, the cell responds by generating a burst of spikes as a result of increased activity. When the light stimulus, which covers the center of the ON retinal ganglion cell, is moved to the periphery of the cell's receptive field, the cell is inhibited (decreased activity). The OFF retinal ganglion cells have opposite response properties. These cells prefer dark spots in the center of their receptive fields, which is surrounded by a light region. The receptive fields of the bipolar and the retinal ganglion cells can be mathematically described with a so-called 'Mexican Hat' function.

Note however that the activity of the retinal ganglion cells depends on the contrast, i.e. the difference in the amount of light that falls on their receptive field centers and surrounds. Both types of retinal ganglion cells are equally numbered, and are distributed equally in the retina.

The retinal ganglion cells are not only divided into ON or OFF cells. There is also a morphological (based on form and structure) classification of these cells. According to this classification best known retinal ganglion cells are either α (5%) or β (55%) cells (Wässle et al., 1975). The remaining 40% are γ retinal ganglion cells (Boycott and Wässle, 1974). The γ retinal ganglion cells are further subdivided into groups. Not much is known about their functional impacts on vision.

The α and β retinal ganglion cells show functional differences as well. Thus, based on their physiology they are classified as Y (α) and X (β) cells, respectively. The γ retinal ganglion cells are classified as W cells. The α retinal ganglion cells act as novelty detectors, they are fast and sensitive to motion, and they can operate during poor light conditions. On the contrary, the β retinal ganglion cells are specialized for a more detailed analysis of a stationary scene.

Distribution of the different types of photoreceptors (rods and cones) and retinal ganglion cells (α and β) reveals different aspects of vision. The cones are the only photoreceptors located in the fovea, whereas the rods dominate the periphery of the retina. The fovea is a region located in the center of the retina, about 2º of visual angle in diameter. There are only photoreceptors in this part of the retina, thus the structure that lie between the outer plexiform layer and the retinal ganglion layer is displaced. As a result, the light rays can penetrate the photoreceptors with minimum scattering. This region provides the brain with visual information that has very high spatial accuracy. The convergence between photoreceptors and the retinal ganglion cells is also very small within the fovea. It is thus not a surprise that the β retinal ganglion cells dominate the fovea, whereas the α retinal ganglion cells dominate the periphery of the retina. With increasing retinal eccentricity the density of photoreceptors and retinal ganglion cells decrease, and the sizes of receptive fields of all ganglion cells increase. Furthermore, the fraction of rods and α retinal ganglion cells, as well as convergence rate increase.

2.1.2 The LGN

The primary target of the retinal ganglion cells is the LGN of the thalamus (Hubel and Wiesel, 1977). Neurons in the thalamus send their axons to the cerebral cortex. The retinotopic representation of the visual field, which emerges in the retina, is preserved throughout the retino-geniculo-cortical pathway. Hubel and Wiesel (1977) have shown that the fibers that start from the neighboring retinal ganglion cells within the retina converge to neighboring geniculate cells. These cells project in turn to neighboring regions within the V1 (Hubel and Wiesel 1977).

The LGN consists of four parvocellular (or P-cell) and two magnocellular (or M-cell) layers. The ipsalateral eye drives two parvocellular and one of the magnocellular layers. The contralateral eye drives the remaining LGN layers.

Axons from the α retinal ganglion cells converge to the magnocellular layers, whereas the β retinal ganglion cells converge to the parvocellular layers.

The retinotopic maps within the LGN and the V1 are distorted, since the central retina needs higher resolution and more computing power than the parts on the periphery.

Note that also the LGN cells respond to point like stimuli (Kaplan and Shapley, 1982). The receptive field properties of the geniculate P and M cells are similar to those of β and α retinal ganglion cells, respectively. The LGN cells are also classified as ON and OFF cells. The antagonistic center surround receptive field profile of the bipolar cells is preserved in the LGN. As a result the LGN is often seen as a relay between the retina and the V1. However, the LGN also receives input from two other sources than the retina. These two modulatory sources are, the V1 and the inhibitory cells located in the thalamic reticular nucleus. These inputs can affect the gain of the signal transmission (Coenen and Vendrik, 1972) and the mode of the firing of the LGN cells (burst or continuous firing) (Steriade et al., 1993).

Recently, a biologically plausible model of the LGN input to simple cells has been presented (Troyer et al., 2002). This model addresses responses of the LGN cells to moving sinusoidal gratings. According to this model LGN input can be approximated by two components. The first component depends on the stimulus contrast, and the phase difference between the stimulus and the neuron's RF. This is the linear component of the LGN input. The second, nonlinear, component of the input is the mean activity level averaged over all spatial phases. Thus, this component is solely a function of the stimulus contrast. In this thesis the Troyer et al. (2002) model has been modified and extended to fit the proposed V1 model (Paper III–V) (see Section 11.5 Paper V for a detailed description of the model).

2.1.3 The Primary Visual Cortex

The cerebral cortex is a thin folded structure that covers the cerebral hemispheres (Purves et al., 1997). The neocortex is a six-layered structure, which takes up most of the cerebral cortex. The laminar division of the neocortex is based on the properties of the neurons of different kinds that populate the neocortex. These properties are size, shape and density. Some of the neocortical layers (laminea) are divided further into sublayers (See the excellent book by Braitenberg and Schüz (1998) for a comprehensive review on the cortex). The neocortex of cat is ~1.3 mm thick (~0.08 mm in mouse, ~1.6 mm in monkey, ~3 mm in human).

Approximately 80% of the neurons are pyramidal or spiny stellate cells. These neurons are excitatory (non-GABAergic). Remaining neurons are classified as GABAergic inhibitory cells. These neurons are referred to as interneurons (they are also mentioned as sparsely spinous cells, local circuit neurons, stellate cells) (Gabbott and Somogyi, 1986). Each neuron makes and receives thousands of

synaptic connections to neurons located nearby and neurons in other parts of the brain.

The rest of the cerebral cortex is made up of phylogenetically older structures (Purves et al., 1997). These structures are paleocortex, which has four layers, and archicortex (hippocampus), which has three layers.

The neocortex is composed of different areas, which are dedicated to different tasks such as vision, hearing, sense of smell, reasoning, etc. These areas are distinguishable from each other, based on their properties. The V1, which is a part of the visual cortex, is one such area. It has (i) distinct architecture, (ii) a unique connectional signature with other parts of the brain, (iii) functional maps with unique characteristics, (iv) a unique inventory of receptive field properties, (v) a distinct catalog of contributions to visual processing and visually guided behaviors (Payne and Peters. 2002).

As mentioned above the primary cortex is composed of six layers. The most superficial layer is referred to as layer 1. This very thin layer is also known as the plexiform layer, since the density of the neurons is relatively low (compared to other layers). The small numbers of neurons that populate layer 1 are mostly inhibitory (Gabbott and Somogyi, 1986).

The border between layer 1 and layer 2 is easy to define. Upper layer 2 is populated with pyramidal cells. All the way through layer 2 and layer 3 the pyramidal cells increase in size. There is no clear border between layer 2 and layer 3. Most often these two layers are referred to as layer 2/3. However, layer 2 pyramidal cell axons are short, whereas layer 3 pyramidal cell axons are long and go through the deeper layers into the white matter, and continuous to other cortical areas (O'Leary, 1941). It has been shown that besides the projections to other cortical areas, the axons of the pyramidal cells can extend horizontally for several millimeters (Rockland and Lund, 1982; 1983; Gilbert and Wiesel, 1983; 1989; Rockland, 1985; Amir, 1993; Malach et al., 1993; Fitzpatrick, 1996; Durack and Katz, 1996; Bosking et al., 1997; Kisvárday et al., 1997; Schmidt et al., 1997; Yousef et al., 1999; Chisum et al., 2003). These axons seem to form clusters of terminals, which mainly target dendritic spines (Kisvárday et al., 1986). The functional implication of these horizontal projections seems to be to spread the activity to other pyramidal cells, which have similar receptive field properties (Section 2.5). The effect of these horizontal projections is emergence of reciprocally connected patches. Thus, they have a considerable facilitative effect.

Layer 4 is the thickest of the layers, and takes up one third of the cortex. It is mainly populated with small and closely packed spiny stellate cells, and some pyramidal cells. The spiny stellate cells are similar to the pyramidal cells. However, they lack the typical apical dendrite of the pyramidal cells, and hence make symmetrical synapses around the cell body. Layer 4 is further divided into two sublayers (layers 4A and 4B). Layer 4A borders to layer 3, whereas layer 4B borders to layer 5. Spiny stellate cells found in layer 4A are bigger and more evenly placed than those in layer 4B. Layer 4A spiny stellate cells project to layer

3 and deeper layers. Layer 4B spiny stellate cells project mainly to layer 5 and layer 6.

One more fundamental difference between the two sublayers is the type of the thalamic afferents. Layer 4A is dominated by the Y-visual signals from the LGN, whereas layer 4B receive exclusively X-visual signals. Ahmed et al. (1994) propose a quantitative assessment of the excitatory inputs to a spiny stellate cell. They suggest that 45% comes from layer 6, 28% from other spiny stellate cells, and 6% from the thalamic afferents. The remaining 21% could not be classified. They suggest also that up to 84% of the inhibitory connections might come from the small basket cells (see below).

Layer 5 is divided into two sublayers. Layer 5A contains irregular discontinuous clusters of small and medium size pyramidal cells (O'Leary, 1941). These neurons send their axons to the layer 2/3. The upper part of the layer 5B contains large pyramidal cells. The apical dendrites of these neurons pass all the layers and terminate at layer 1. On their way the apical dendrites of these neurons branch in layer 4 and later in layer 2/3. However, the small pyramidal cells dominate layer 5B. Their apical dendrites terminate in layer 1 without branching. Some of their axons terminate in layers 5 and 6, whereas some enter the white matter.

Layer 6A contains small and medium size pyramidal cells. These neurons are arranged into vertical columns. According to Katz (1987) these neurons can be divided into two groups. The claustrum-neurons, which have apical dendrites that reach layer 1 and have fine axonal collateral branches that arborize only in layer 6 and lower layer 5, and corticothalamic neurons, which have apical dendrites that never reach higher than layer 3. Axons of these neurons send widespread collaterals into layer 4. Layer 6B borders to the white matter. Not much is known about the neurons that populate this sublayer.

In summary, the signals from the LGN that enter layer 4A are distributed within layer 4A, later to layer 2/3 and to the deeper layers. From layer 2/3 the signals are sent to layers 5B and 6. Signals entering layer 4B are projected to deeper layers, and back to layer 4B or to layer 2/3.

Only ~20% of the cortical neurons are classified as interneurons (Gabbott and Somogyi, 1986). The distribution of the interneurons is not uniform across the cortical layers. The lowest density of interneurons is found in layer 5, followed by layer 2, upper parts of layer 3 and layer 6. The highest density of interneurons is found in layer 4 (note that this layer is the main recipient of the thalamic input) and lower parts of layer 3. Until now no morphological scheme has been generally accepted to classify these neurons. Below the interneurons that are of special interest are reviewed. These are chandelier cells, small and large basket cells.

Chandelier cells are multipolar cells (Tömböl, 1978). These neurons are more common in layer 2/3, and to some extent in layer 5. These neurons are characterized by their axons, which give rise to short, vertically oriented string of boutons. These neurons are also referred to as axoaxonic cells, since they synapse with the axons of the postsynaptic neurons. Based on the strategic placement of the

axon terminals, it is assumed that these neurons are powerful inhibitors of the postsynaptic neurons.

Large basket cells are common in all layers except in layer 1 (O'Leary, 1941; Tömböl, 1978). These neurons have vertically oriented dendrites. Their axons form up to five branches. These branches extend up to 1.5 mm, parallel to the pial surface (horizontal projections). Main postsynaptic targets of these neurons are both excitatory cells and other basket cells within the layer where they are located. Inhibition of other basket cells can be used for indirect facilitation of excitatory cells. Kisvárday et al. (1987) suggest that the basket cells do also target neurons found in other layers as well.

Small basket (multipolar) cells are found in layer 3 (Meyer, 1983) and layer 4 (Kisvárday et al., 1987). Results by Kisvárday et al. (1987) suggest that these neurons inhibit excitatory cells found in layer 4. The targets of their axons are the dendrites of the postsynaptic neurons.

In this section some of the properties of the V1, which are highly significant to this thesis, are left out. In the following sections these properties will be review in detail. In Section 2.2 the modular structure of the neocortex is explained. This hypothesis is founded on the vertical organization of the apical dendrites of the larger pyramidal cells within layer 5. Section 2.3 focuses on the layout of the horizontal connections within layer 4 and the superficial layers (layer 2/3). Sections 2.4–2.5 focus on the response properties of the neurons that are found within the V1.

2.2 Modular Structure of the Neocortex

2.2.1 Neocortical Mini- and Macrocolumns

The vertical organization of the neocortex is as evident as the laminar organization. The neocortex is composed of repetitive structures referred to as the minicolumns (Mountcastle, 1957; 1978; 1997; Powell and Mountcastle, 1959; Hubel and Wiesel, 1962; 1977; Buxhoeveden and Casanova, 2002; Lund et al., 2003). The minicolumns are positioned orthogonally to the cortical surface, and go through all cortical layers, i.e. from the pial surface of layer 1 to layer 6, which borders to the white matter. A minicolumn contains roughly some 100 neurons. Minicolumns found within the V1 have 2–3 times higher density of neurons than minicolumns elsewhere in the neocortex.

Mountcastle (1957) have reported the very first evidence of the columnar organization of the neocortex (cat's somatosensory cortex). It was also the first time the term 'column' was used. Later, Mountcastle and Powell (1959) have revealed that also the monkey's somatosensory cortex is based on same organization principals. Vertical penetration through the cortical layers of cat

somatic sensory cortex revealed that neurons in each layer have similar properties of place and modality. However, penetrations oblique or parallel to the cortical surface showed that the properties change continuously.

Hubel and Wiesel (1962; 1977) have revealed the columnar organization of the V1. They have discovered that neurons respond selectively to 'line orientations' (Hubel and Wiesel 1962). They found that the orientation preference of the neurons along the vertical axis, i.e. perpendicular to the cortical surface, is almost constant. Note that the layer 4 neurons of monkey (Hubel and Wiesel, 1977; Blasdel and Fitzpatrick, 1984; Hawken and Parker, 1984), tree shrew (Humphrey and Norton, 1980), and ferret (Chapman and Stryker, 1993) are weakly selective to orientations. However, the parallel and the oblique penetrations revealed the systematic change of orientation preference of the neurons with distance. Their study reveals that these changes are either clockwise or counterclockwise with steps of ≤10º, roughly every 50 μm. During several penetrations, one full sequence of orientations, corresponding to 180º, or more is completed. Hubel and Wiesel have named the region that corresponds to a full sequence the 'orientation hypercolumn'. The length of a full sequence is approximately 500–850 μm on cortical surface.

The columnar organization of other heterotypical areas, such as the auditory cortex (Woolsey and Waltz, 1942), and the motor cortex (Meyer, 1987) is also prominent. The homotypical cortical areas, i.e. the association cortex, do also show same organization principles. Columnar organization of the homotypical cortical areas is highly interesting. Note that the modalities of the neurons found in these areas are created within the neocortex, through intrinsic connections, since neurons that populate these structures do not receive sensory input directly.

A more recent evidence of existence of the minicolumn structures is presented by Peters and colleagues (Peters and Yilmaz, 1993; Peters and Sethares, 1996) based on the arrangement of the pyramidal cells of cat and monkey V1. Their analysis is based on the layout of the apical dendrites of larger layer 5 pyramidal cells of cat area 17. Peters and Yilmaz (1993) have shown that the apical dendrites of these neurons form clusters, and are joined by the apical dendrites of layer 2/3 pyramidal cells, while they continue to pial surface. The result is an axis of dendrites going from layer 5 to layer 1. Layer 6A pyramidal cells do, however, not participate in this arrangement. A similar pattern is also found within the monkey V1 (Peters and Sethares, 1996). In monkey V1 the center-to-center cluster distance is 23 μm, whereas in cat the distance between the clusters is 56 μm (these values are roughly constant). It seems that the minicolumns within the monkey's neocortex are smaller and more densely packed than those found in the cat's neocortex.

Neurons within a small patch receive input mainly from one eye. Horizontal penetrations show that there is a transition between regions of different eye dominations (Hubel and Wiesel, 1977). However, penetrations perpendicular to the

cortical surface shows that the same eye dominates all neurons within an orientation minicolumn. Layer 4 neurons are, however, driven exclusively from one eye, and hence are classified as monocular cells, whereas neurons in other layers are classified as binocular. These findings gave birth to the 'ocular dominance columns'. Ocular dominance columns run parallel to the cortical surface and alternate with each other (right eye and left eye). Later, Hubel and Wiesel have integrated orientation and ocular dominance columns into one general model. The result is the highly idealized 'ice cube' model (Hubel and Wiesel, 1972; Hubel, 1988). Inside the ice cube model, columnar systems of orientation and ocular dominance are positioned orthogonally to each other. Ice cube modules are hypothesized to analyze small spots of the visual field. According to this scheme, adjacent ice cube modules analyze adjacent small spots of the visual field, with some overlap between them. Note however that the hypercolumns are not physical entities with well-defined input and outputs such as components in electrical circuits.

During the late seventies a circular-shaped centric model was proposed (Braitenberg, 1979). Within this circular-shaped model, orientation minicolumns are organized around the middle points, which correspond to the orientation 'singularities'. The orientation singularities are regions where all orientations meet (Swindale, 1982). Around this middle point of the model, the orientation changes continuously. Braitenberg (1979) have proposed that during one lap around the middle point same orientation should be encountered twice. Thus, on the 'opposite side' of an orientation singularity point, neurons that have the same orientation preference are located. Blasdel and Salama (1986) have named this model the 'pinwheel model'.

Later, the pinwheel model has received renewed attention after the discovery of the cytochrome oxidase blobs in cat (Wong-Riley, 1979) and in monkey V1 (Hendrickson et al., 1981; Horton and Hubel, 1981). Neurons within the blobs are poorly tuned for orientation. Thus, it is tempting to speculate that blobs are located at the orientation singularities of the pinwheel model. After the discovery of blobs several circular-shaped models have been proposed (Horton, 1984; Gotz, 1987; 1988; Baxter and Dow, 1989) (see the reviews by Erwin et al. (1995) and Dow (2002)). However, most of them have been ruled out after the voltage-sensitive dye examinations of the monkey V1.

Despite their ripe age, the ice cube and the pinwheel models are still very popular among the modelers. In the literature, these two and more recent models are referred to as models of cortical microcircuits, cortical columns, macrocolumns, cortical modules, hypercolumns (this term is reserved for microcircuits found in the visual cortex (Hubel and Wiesel, 1977)) and segregates (this term is reserved for microcircuits found in the somatosensory cortex (Favorov and Diamond, 1990)), etc.

2.2.2 The Orientation Map

A more careful analysis of the distribution of the orientation minicolumns and how they are related, in terms of geometry, to the ocular dominance columns and the singularities becomes possible first after the voltage-sensitive dye examinations of the monkey V1 (Blasdel and Salama, 1986; Blasdel, 1992; Obermaiyer and Blasdel, 1993). Through these studies, several features of the orientation map are revealed. The singularities, described by several independent groups, are apparently located in the center of the ocular dominance columns. During clockwise movement around a singularity point, the orientation rotates either clockwise (positive singularity) or counterclockwise (negative singularity). One lap around the singularity point corresponds to 180º, and not to 360º, as proposed by the original pinwheel model (Braitenberg, 1979). Thus, cross-orientation domains are positioned on the opposite sides of a singularity point.

Besides the orientation singularities the orientation map has other features, such as 'linear zones', 'saddle points', and 'fractures'. Linear zones are frequently located on the borders between the ocular dominance columns. Within these zones the iso-orientation lines are parallel to each other. Furthermore, these lines are roughly orthogonal to the ocular dominance columns. Saddle points are found within the ocular dominance columns. The saddle points are relatively large zones where the orientation selectivity remains almost constant. Most often these areas are found between two adjacent singularity points that are within the same ocular dominance column. Fractures are small local discontinuous patches where orientation selectivity changes irregularly (Hubel and Wiesel, 1977).

It is not clear how and when the orientation map develops and takes its final form. The majority of the studies suggest that the neurons respond selectively to orientations at the eye opening. This finding has been demonstrated on newborn kittens (Hubel and Wiesel, 1962; 1963; Blakemore and Van Sluyters, 1975; Buisseret and Imbert, 1976; Frégnac and Imbert, 1978; Albus and Wolf, 1984; Gödecke et al., 1997; Crair et al., 1998), ferrets (Chapman and Stryker, 1993; Chapman et al., 1996), and monkeys (Wiesel and Hubel, 1974). However, as pointed out in Chapman and Stryker (1993), reported values on the degree of orientation selectivity at the eye opening vary, even within the same species (in this case the cat). According to Hubel and Wiesel (1963) all neurons are orientation selective at the eye opening, whereas others are more conservative and suggest that 25–30% of the neurons respond selectively to orientations (Blakemore and Van Sluyters, 1975; Buisseret and Imbert, 1976; Frégnac and Imbert, 1978; Albus and Wolf, 1984). In contrast, Barlow and Pettingrew (1971) suggest that orientation selectivity is absent in young kittens. Chapman and Stryker (1993) point out that the variations in the reported values on the fraction of the orientation selective neurons might be explained by the fact that the experiments are made on young animals, which are fragile by nature. These experiments are not easy to conduct, and hence several factors can influence the results easily. Consequently,

Chapman and Stryker (1993) conclude that the reported values on the fraction of the orientation selective neurons might be an underestimation.

It has been reported the overall shape of the orientation map remains unchanged when the newly opened eyes are subject to normal visual experience (Chapman et al., 1996; Crair et al., 1998; White et al., 2001). Thus, it seems that the genetic factors play an important role in the emergence of the orientation map, and hence the impact of the environment on the development of the orientation map is small (Gödecke et al., 1997; Crair et al., 1998; Chapman et al., 1999; Miller et al., 1999).

However, after eye opening the neurons' selectivity to orientations increases significantly (Blakemore and Van Sluyters, 1975; Frégnac and Imbert, 1978; Chapman and Stryker, 1993; Chapman et al., 1996; Gödecke et al., 1997; Crair et al., 1998). Furthermore, dark rearing or binocular deprivation can alter the normal development of the orientation map (Imbert and Buisseret, 1975; Chapman and Stryker, 1993; Chapman et al., 1996; White et al., 2001). These studies indicate that the orientation map continues to develop after that the eyes are opened. Recently, White et al. (2001) have reported that the orientation maps are present in the dark-reared ferrets. However, the neurons are less selective to orientations than if they were subject to normal visual experience. When the animals are lid-sutured the normal development of the orientation map is disturbed so much that neurons are not orientation selective any longer. Furthermore, dark-reared and lid-sutured ferrets develop horizontal connections, which are abnormal (White et al., 2001). It seems that the initial (prenatal) orientation map provides an important bias to the postnatal development process. As a result robust orientation maps can be developed in different environments.

DeAngelis et al. (1993) report that neurons are orientation selective but both the spatial and temporal properties develop after eye opening. Thus, it seems that normal visual experience facilitates the maturation of the already existing orientation map, whereas abnormal visual experience can have devastating effects on its development. Yet another factor that affects the maturation of the orientation map is the horizontal connections, especially those that are found in the layer 2/3, since they link distant iso-orientation domains to each other (Section 2.3.1). The horizontal connections continue to expand after eye opening, and hence play an important role in the determination of the final form of the orientation map (Section 2.3.4).

The adult cortex can adapt itself to new circumstances, thus reorganization is not restricted to young animals (Merzenich et al., 1984; Jenkins et al., 1990; Gilbert, 1992; Gilbert and Wiesel, 1992; Pettet and Gilbert, 1992; Kapadia et al., 1994). Merzenich and colleagues (Jenkins et al., 1990) have shown that practice can modify the representation of the digits within the primary somatic cortex, since those digits that are more active need larger parts of the cortex. Merzenich et al. (1984) have also investigated the effects of removing one digit from the hand on the primary somatic cortex of an owl monkey. As a result, the region of the primary somatic cortex, which previously represented the removed digit (number

3), is now dedicated to the digits 2 and 4. Gilbert and Wiesel (1992) have shown that also the orientation map can reorganize itself. Retinal lesions made on the both eyes of a cat first silenced an area of the V1. However, after two months of visual experience the RFs in the lesion area of the V1 were reorganized. As a result, the lesion area was reduced in size (Gilbert and Wiesel, 1992).

The two-dimensional orientation map is often used as a starting-point when the organization of the neocortex is analyzed. The orientation map reveals the orientation preference of the neurons located in different regions on the cortical surface. It can also be used to link the visual field, covered by both eyes, to cortical dimensions. The orientation map is also a perfect tool for the visualization of the layout of the intracortical connections. This is done by mapping the connections, within a specific cortical layer, on an orientation map, which holds information on the orientation preference of the regions exposed to projections from the injection site.

2.3 Layout of the Intracortical Connections within the Primary Visual Cortex

In this section, a brief review of the layout of the local and long-range horizontal connections within V1 will be given. This review is based on the qualitative assessments of the connections within cat area 17. The focal point is the intracortical connections within layer 4 and the superficial layers (layer 2/3). Remember that layer 4 is the main recipient of the thalamic input. Furthermore, in cat area 17 orientation selectivity emerges in layer 4 (Section 2.4).

The superficial layers are interesting for the analysis of the computations within the V1, since long-range horizontal connections within these layers extend more than in any other layer of the neocortex (perhaps with the only exception of the layer 5 horizontal connections, which are as long as layer 2/3 connections). Thus, they integrate information that is spread over a large region.

In the literature the local connections are defined as connections within a region, which roughly corresponds to a hypercolumn (‘Diameter’ of a hypercolumn is in the range of 0.5–1.2 mm depending on the area and species. Cat hypercolumns are larger than monkey, and area 17 hypercolumns are larger than area 18 (V2)). Thus, according to this concept an imaginary border isolates a hypercolumn from the rest of the neocortex. Connections crossing this imaginary border are defined as long-range horizontal connections. (These connections are also referred to as long-range intracortical (intrinsic, lateral) connections, distal projections, etc.). It is hypothesized that those connections link neurons, which are located in different hypercolumns, even though the distances covered by the axons might be relatively small.

One important consequence of this division is to be able to distinguish the functional role of the neurons located in the immediate surrounding of a neuron, and neurons located elsewhere within the neocortex, in altering the response properties. It is obvious that the term 'local' is highly subjective and depends on the intention of the author. In some cases local is defined as a region that is composed of up to four or five hypercolumns.

2.3.1 Patchy Layout of the Layer 2/3 Long-Range Horizontal Connections

During the early eighties, Rockland and Lund (1982) discovered the patchy layout of the long-range horizontal connections of the tree shrew visual cortex. These patches were located periodically several millimeters from the injection sites. Since the discovery of their patchiness, the long-range horizontal connections have received increased attention. It is now widely accepted that the patchy long-range horizontal connections of layer 2/3 are a prominent feature of the visual cortex.

The patchy, iso-orientation biased, layout of the long-range horizontal connections have been shown on a variety of species including cat (Gilbert and Wiesel, 1983; 1989; Kisvárday et al., 1997; Schmidt et al., 1997; Yousef et al., 1999), tree shrew (Rockland and Lund, 1982; Fitzpatrick, 1996; Bosking et al., 1997; Chisum et al., 2003), ferret (Rockland, 1985; Durack and Katz, 1996), and monkey (Rockland and Lund, 1983; Amir, 1993; Malach et al., 1993). These connections, which mainly arise from pyramidal and spiny stellate cells, extend up to 4 mm on cortex surface (in one direction). However, most connections are within an area of ~2.5 mm from the injection site (Kisvárday et al., 1997).

Long-range horizontal connections are also found in other neocortical areas, such as auditory, motor, somatosensory, and prefrontal cortex (Schmidt and Löwel, 2002).

2.3.2 Quantitative Assessment of the Layer 2/3 Long-Range Horizontal Connections

A qualitative assessment of the intracortical connections has been possible to do only recently. Excitatory pyramidal cells and inhibitory cells of different kinds such as the chandelier cells and the basket cells populate the superficial layers. Kisvárday et al. (1997) report that in layer 2/3, 56.2% of the local excitatory connections target the iso-orientation (±30º) domain. Oblique- (±30–60º) and cross-orientation (±60–90º) domains receive 28.4 and 15.3 per cent of the connections respectively. Long-range connections show a similar pattern. The distribution of excitatory connections shows that 40.0% are located at the distal iso-orientation domains, 36.9% at the distal oblique-, and 23.1% at the distal cross-orientation domains. Note that roughly every second connection targets the

iso-orientation domains. It is clear that the projections that target the iso-orientation domains do not dominate.

The inhibitory long-range horizontal connections extend only one third to one half of the excitatory network. Furthermore, the excitatory connections outnumber them. It is also assumed that large basket cells make these inhibitory long-range horizontal connections. Thus, the majority of the long-range connections are considered to be excitatory in both layer 4 and layer 2/3 (Kisvárday et al., 1997). Inhibitory local connections target mainly the iso-orientation domain, similar to the excitatory local connections. Roughly 48.0% of them are found within the iso-orientation domain. 29.2% are located at the oblique-orientation domain, and 22.8% are located at the cross-orientation domain. Long-range projections are even less orientation specific, with only 47.7% targeting the distal iso-orientation domains. 21.7% are located at the oblique-, and 30.6% at the cross-orientation domains.

The pattern shown by the excitatory and inhibitory connections is that the inhibitory projections are less specific for orientation. Both networks are biased towards the iso-orientation domain, however, as pointed out by Kisvárday and colleagues (Kisvárday et al., 1997) this bias is moderate.

2.3.3 Quantitative Assessment of the Intracortical Connections of Layer 4

Surprisingly, the layout of the long-range horizontal connections found within the layer 4 has drawn much less attention (compared to those found within the layer 2/3). The findings suggest that the layout of the layer 4 long-range horizontal connections is different from those found within layer 2/3 (Chisum et al., 2003; Kisvárday et al., 1997; Yousef et al., 1999; Schmidt and Löwel, 2002). Their extent is only 50% of the connections of the layer 2/3 (Kisvárday et al., 1997).

Yousef et al. (1999) found that layer 4 long-range connections (of area 18) are hardly biased towards the iso-orientation domains. The patches projections, which characterize the superficial layers, are absent. Thus, only 35.4% of the connections (>740 μm) target the distal iso-orientation domains. Oblique- and cross-orientation domains receive 33.7% and 30.9% of the connections respectively. The pattern shown by the local connections (<740 μm) is different. The local iso-orientation domain receives 60.0% of the connections, whereas 22.0% of the connections are targeting the oblique- and 18.0% the cross-orientation domains. Note that 40% of the local connections target other than the iso-orientation domain.

It seems that independent of the layer, the excitatory long-range horizontal connections are neither random nor restricted to the iso-orientation domains. Cross-talk between different orientation domains is a prominent feature of both the layer 4 and the superficial layers.

2.3.4 Emergence of the Horizontal Connections

Emergence of the horizontal connections within different cortical layers has been addressed thoroughly by Callaway and Katz (1990; 1992). In layer 2/3, the process of emergence and maturation of the horizontal connections is as follows (Callaway and Katz, 1990): At postnatal days 4–6 (P4–6) the extent of the layer 2/3 connections is 2 mm and the patches, which are the distinguishing feature of this layer, are absent. However, already at P8 the patches are taking form and the connections reach longer distances. One week later (P12–15), the patches are more evident and the number of labeled neurons increases. Furthermore, the increase of labeled neurons is more dramatic in the patches than in the labeled region.

During P12–21 the horizontal connections reach their maximum extent, however, the inter-patch regions are populated by far more labeled neurons than previously. After this period the pruning of the horizontal connections starts. This period continues for approximately 3 weeks and at the end of P38 inter-patch regions contain less labeled neurons than previously. Maturation of the orientation map coincides with the phase.

Layer 4 spiny neurons project either to the layer 4 and 2/3 or downward, to the infragranular layers (5 and 6) (Callaway and Katz, 1992). Those connections that target the layers 4 and 2/3 are denser and mature later than those that target the infragranular layers. The connections that terminate in the infragranular layers mature at P15. Connections within the layer 4 continue to expand until P20, whereas the connections that target the layer 2/3 continue to develop another 13 days. Axons of the layer 4 spiny neurons cross into layer 3 first after P11. Note that by that time, the patches of the layer 2/3 are already evident. Thus, the patchy layout of the layer 2/3 is not a consequence of the interlaminar projections that emerge from the layer 4. However, during the following weeks, these interlaminar projections increase in density, and at the same time the patches of the layer 2/3 are reshaped.

Emergence of the orientation map indicates that the thalamocortical circuitry is taking form. Apparently, this procedure coincides in time with the development of the horizontal connections (Luhmann et al., 1986; Gödecke et al., 1997; Callaway and Katz, 1990; 1991; 1992; Katz and Callaway, 1992; Burkhalter et al., 1993). It is thus hypothesized that the orientation map and the horizontal connections influence each other during this process, which starts before eye opening and accelerates when the brain is subject to visual input. Recall that dark-reared and lid-sutured ferrets develop shorter and less patchy layer 2/3 long-range horizontal connections (White et al., 2001).

2.4 Emergence of Orientation Selectivity within the Primary Visual Cortex

Neurons found in the V1 respond selectively to the orientations of bar-like stimuli (Hubel and Wiesel, 1962), whereas the retinal ganglion cells and the LGN cells do only respond to point like stimuli (Kuffler, 1953; Kaplan and Shapley, 1982). Since its discovery for over 40 years ago, the orientation selectivity property of the V1 neurons has drawn much attention. Emergence of this property demonstrates the brains way of representing incoming sensory information (Das, 1996; Sompolinsky and Shapley, 1997; Ferster and Miller 2000).

In cat V1, orientation selectivity is evident already in the layer 4, which is dominated by the simple cells (Hubel and Wiesel, 1962). According to the earliest model of orientation selectivity (Hubel and Wiesel, 1962), the RFs of these neurons are composed of alternated ON and OFF subfields, i.e. light preferring and dark preferring, respectively (in the text, this model is referred to as the Hubel-Wiesel model). The Hubel-Wiesel model assumes that ON subregions of simple cells emerge through projections of the ON-center LGN cells. OFF subregions of the simple cells emerge similarly, through the projections that originate from the OFF-center LGN cells. Furthermore, the subfields are hypothesized to be elongated along the axis that coincides with the simple cell's preferred orientation. The anisotropy seen in the subfields is explained solely by the projections from the LGN. Thus, it is hypothesized that an elongated region of the visual field is covered by the RFs of the LGN cells that project to a simple cell's subfield.

The Hubel-Wiesel model explains emergence of orientation selectivity without any involvement of the intracortical connections, and hence is classified as a feedforward model. There is some support for this model, at least qualitatively. A number of studies have shown that the subfields of the simple cells are elongated both in cats (Jones and Palmer, 1987; Pei et al., 1994; Reid and Alonso, 1995) and in ferrets (Chapman et al., 1991). Furthermore, Reid and Alonso (1995) have shown that the simple and the LGN cells that are correlated have also overlapping receptive fields.

These results support the existence of a thalamocortical circuitry, which is in line with the Hubel-Wiesel model. On the other hand, they cannot explain sharp tuning, which is demonstrated by the V1 neurons (Orban, 1984). In average a simple cell responds selectively to a narrow band of orientations of ~20° at half-width at half-height (Orban, 1984). This requires stronger anisotropy than what is indicated (Jones and Palmer, 1987; Chapman et al., 1991; Pei et al., 1994; Reid and Alonso, 1995). Jones and Palmer (1987) have shown that on average a simple cell's RF is composed of 2–3 subfields. Furthermore, mean width-to-length aspect ratio of a simple cell RF is 1:1.5 (Jones and Palmer, 1987).

Silencing of the cortical activity has been done to address the impact of the LGN input on the emergence of orientation selectivity (Ferster et al., 1996; Chung

and Ferster, 1998). In Ferster et al. (1996) the activity of the cortex is reduced by cooling down the cortex to ~9ºC. The cooling procedure reduces the amplitudes of the EPSPs. Furthermore, the latency of an EPSP increases to 5 ms. The most important result of this study is that the neurons are orientation selective even after the cooling of the cortex. However, the reported tuning widths are significantly broader than what has been reported (Orban, 1984). In Ferster et al. (1996) neurons respond selectively to a broad band of orientations of ~45° at half-width at half-height. Furthermore, the tuning curve in (Ferster et al., 1996) is calculated based on the F1 (first harmonic) of the responses, and hence responses that are untuned for orientation are ignored. Thus, as also pointed out in Sompolinsky and Shapley (1997) the results of Ferster et al. (1996) are inline with low aspect ratios.

When the number of synapses that target a layer 4 neuron is concerned, between ~4% (Garey and Powell, 1971; Hornung and Garey, 1981; Winfield and Powell; 1983; LeVay, 1986; Peters and Payne, 1993; Ahmed et al., 1994), and ~24% (LeVay and Gilbert, 1976; Einstein et al., 1987) originate from the LGN.

The thalamocortical synapses are, however, relatively strong (Ahmed et al., 1994; Stratford et al., 1996). Ahmed et al. (1994) report that the thalamocortical synapses are larger than the intracortical synapses, and hence contain more release sites. Stratford et al. (1996) have compared the EPSPs that originate from LGN, layer 4 and the infragranular layers (5 and 6). The target neurons were spiny stellate cells, which are common in layer 4 of cat V1. LGN inputs generate highest amplitudes (1,97 μV). Layer 4 EPSPs were 1,06 μV, whereas infragranular EPSPs were 0,28 μV. It seems that the excitatory input that originate from the nearby and distal neurons is the main input to layer 4 spiny stellate cells, even if the thalamic EPSPs are relatively strong.

Taking together these results it is reasonable to assume that the thalamocortical circuitry is not solely determinant of emergence of orientation selectivity.

2.4.1 Simple, Complex and Hypercomplex Cells

As mentioned above, Hubel and Wiesel (1962; 1977) have discovered and named three types of neurons, which have fundamentally different response properties. The simple cells, which mainly populate layer 4 of cat, have ON- and OFF-subregions that reflect the thalamic inputs. Hubel and Wiesel (1962; 1977) have discovered that these neurons' responses to complex stimuli can be predicted from their responses to individual spots of lights. As a consequence, a simple cell's receptive field can be exposed based on its response to small light spots positioned on different locations on the retina. A light, which is positioned at the neurons' ON-subregion, excites the cell, whereas a light spot positioned at the neurons OFF-subregion inhibits the neuron. The responses to 'dark' spots are opposite to light spots.

'Absolute spatial phase' and 'relative spatial phase' are two definitions that are useful when the RF of a simple cell is described in terms of its subfields. Relative

spatial phase refers to the position of the ON- and OFF-subregions with respect to the center of a receptive field. Absolute spatial phase refers to the position of the ON- and OFF-subregions with respect to the visual field. These concepts are also useful when two RFs are related to each.

Complex cells are the single most common cell type in the V1. Approximately 75% of the neurons are classified as complex cells. It is assumed that projections originating from layer 4 simple neurons form the receptive fields of these neurons (Hubel and Wiesel, 1962; 1977; Alonso and Martinez, 1998). Complex cells do not have the linear receptive fields like the simple cells. The nonlinear receptive field properties of the complex cells are much harder to predict. They do not respond to light spots at all. They respond to lines (bars or gratings) located within their receptive fields. The location of the stimuli within the receptive field seems to have less importance compared to the simple cells. Complex cells are highly sensitive to motion though. They have also larger receptive fields than the simple cells.

Hypercomplex cells (end-stop cells) are named after their odd responses to lines that are positioned in their receptive fields. Surprisingly, lines that normally excite the hypercomplex cells inhibit them if they extend beyond their receptive fields. Now it is widely believed that the hypercomplex cells are actually end-stopped simple or complex cells.

2.4.2 On the Interplay between the Thalamocortical Circuitry and the Intracortical Connections

It is reasonable to assume that the RF properties of the neurons are formed within a complex network, which consists of the thalamocortical circuitry and the intracortical connections. Cat layer 4 neurons are orientation selective (Hubel and Wiesel, 1962). These neurons have widespread lateral connections (Martin and Whitteridge, 1984; Yousef et al., 1999), which extend up to two hypercolumn distances from the cell body (Yousef et al., 1999). In monkey, layer 4Cβ cells are not selective to orientation, whereas their counterparts in the layer 4Cα respond selectively (less prominent than in cat) to the orientations of the bar-like stimuli (Hubel and Wiesel, 1977; Blasdel and Fitzpatrick, 1984; Hawken and Parker, 1984). One possible explanation of this important difference might be that the lateral projections in layer 4Cα are more prominent than those that are found in layer 4Cβ. Thus, there seems to be a correlation between lateral extent of the horizontal connections and orientation selectivity displayed by the neurons.

Yet another support for horizontal connections and orientation selectivity comes from the layer 2/3. Layer 4 neurons in tree shrew (Humphrey and Norton, 1980), and ferret (Chapman and Stryker, 1993), are poorly tuned for orientation, whereas their counterparts in the layer 2/3 respond selectively to stimulus orientation. Since the LGN afferent rarely target layer 2/3 (Bullier and Henry, 1979; Ferster and

Lindstrom, 1983; Martin and Whitteridge, 1984), it is reasonable to assume that the horizontal connections are responsible for the emergence of orientation selectivity in these species. The patchy, iso-orientation biased, layout of the long-range horizontal connections within the layer 2/3 of tree shrew (Rockland and Lund, 1982; Fitzpatrick, 1996; Bosking et al., 1997; Chisum et al., 2003), ferret (Rockland, 1985; Durack and Katz, 1996) is a reasonable explanation to the fact that neurons in tree shrew and ferret layer 2/3 are selective to orientation.

2.4.3 Spatial Frequency Selectivity

Moving and static sinusoidal gratings with different spatial and temporal configurations are often used to reveal response properties of the neurons. The 'spatial frequency' of a sinusoidal grating is defined as the width of the light and dark bars, which a sinusoidal grating is composed of. A sinusoidal grating that has low frequency is composed of thick light and dark bars. High frequency implies that the sinusoidal grating consists of thin bars.

It has been shown that the neurons respond selectively to spatial frequencies (Campbell et al., 1969; Maffei et al., 1973). They behave like band-pass filters, and hence prefer frequencies that are within a narrow range. Their responses to sinusoidal gratings, which have lower or higher spatial frequencies than the preferred ones are lower. Recall that the neurons respond similarly to orientations.

Tootell et al. (1981) suggest that spatial frequency is organized in a columnar fashion, such as orientation and ocular dominance. It is, however, not clear how spatial frequency columns are topologically related to orientation and ocular dominance columns. Shoham et al. (1997) have shown that low spatial frequency neurons are positioned at cytochrome oxidase blobs, which coincide with the singular points (Section 2.2), and that these regions are surrounded by neurons that prefer higher spatial frequencies (Shoham et al., 1997). Remember that the singular points are positioned in the middle of ocular dominance columns (Section 2.2). One year earlier, the same group has revealed that LGN Y-cells project predominantly to the blobs, whereas interblob areas receive input mainly from LGN X-cells (Hübener et al., 1996). Recall that the LGN X-cells are tuned for higher spatial frequencies than the LGN Y-cells (Derrington et al., 1979).

Issa and colleagues (2000) suggest that neurons that are selective to the extremes of the spatial frequency continuum (either low or high spatial frequencies) are located at the singular points. They point out that Shoham and colleagues (1997) classify spatial frequencies as 'low' or 'high', whereas their approach is based on three classes of spatial frequencies (low, high and intermediate). They also remark that they test a larger (and especially higher) range of spatial frequencies than Shoham et al. (1997). Everson et al. (1998) on the other hand proposes that the spatial frequencies are organized in a pinwheel fashion around singular points, in the same manner as orientation selectivity.

2.4.4 Contrast Gain Functions of the LGN Cells

It seems that the parvocellular cells do have roughly linear contrast gain functions, whereas the magnocellular cells have logarithmic contrast gain functions (Derrington and Lennie, 1984; Sherman et al., 1984; Movshon et al., 1994). Note further that 90% of the LGN cells are found in the parvocellular layers of the LGN (Dreher et al., 1976).

Since the LGN P cells dominate the input to the cortex (Peters and Payne, 1993) the hyperbolic contrast gain functions of the neurons (Section 2.4.5) cannot be explained by the saturation of the thalamic cells.

2.4.5 Contrast Gain Functions of the Neurons

Several groups have investigated the contrast gain functions of the neurons (Maffei et al., 1973; Dean, 1981; Albrecht and Hamilton, 1982). Albrecht and Hamilton (1982) have quantified the contrast gain functions of the neurons found within both the cat's and the monkey's V1. During the experiments, 247 simple and complex neurons from cat and macaque monkey are recorded. It is found that the contrast gain functions of the neurons have the form of a hyperbolic function. Thus, the first phase of this function is a linear increase of response. This phase is followed by a rapid saturation, and later by total saturation, i.e. normalization or division.

Albrecht and Hamilton (1982) have also shown that the saturation level seems to be determined by the properties of the stimuli, i.e. orientation and spatial frequency, and not by the electrical properties of the neurons. Furthermore, maximum response to non-preferred stimulus is reported to be lower than to preferred stimulus.

Note that the neurons saturate more than the LGN cells (Derrington and Lennie, 1984; Sherman et al., 1984; Movshon et al., 1994; Maffei et al., 1973; Dean, 1981; Albrecht and Hamilton, 1982). This finding reveals the existence of the intracortical inhibition. Carandini and Heeger (1994) propose that normalization of the activity comes from a pool of inhibitory cells that represent all orientations and spatial frequencies. This pool generates the shunting inhibition, which is required to divide the excitatory input from the thalamus. The effect is saturation of the responses of the neurons. However, the shunting inhibition requires that the membrane time constant of the neurons decreases ~60 ms. This is not possible, since the resting time constant of the most neurons are ~20 ms. Nevertheless it seems that the intracortical inhibition is indeed responsible, in one form or another, for shaping the contrast gain functions of the neurons.

2.4.6 Contrast-Invariance of Orientation Tuning

The Hubel-Wiesel model cannot solely predict many of the response properties of orientation selective neurons (Ferster and Miller, 2000). Contrast-invariance of

orientation tuning shown by these neurons is perhaps the most striking example. As contrast increases the height of the neurons' response curves increase. However, the half-width at half-height of the response curve remains almost constant (Sclar and Freeman, 1982; Skottun et al., 1987). Loosely speaking, these neurons can detect a line (bar, edge) and 'tell' its orientation, also in poor light conditions.

The study carried out by Sclar and Freeman (1982) shows that orientation tuning of a neuron is independent of the contrast of the stimulus. The stimuli, which were used during the experiment, are sine-wave gratings. Data obtained from 45 neurons (19 simple and 26 complex) in the cat V1 shows that orientation tuning is indeed independent of stimulus contrast. Furthermore, saturation of activity when the stimulus contrast is increased is evident in all 45 cases.

2.4.7 Cross-Orientation Inhibition

One last interesting finding is related to responses of neurons to superimposed stimuli. When two stimuli are superpositioned, the response of a cell is less than to the sum of each stimulus alone. During the experiment two gratings stimulate the neuron. The first grating is of the preferred orientation, and the second grating is of the orthogonal orientation. It is shown that the second grating inhibits a cell, which is of orthogonal orientation (Morrone et al., 1982; Bonds, 1989). Morrone et al. (1982) suggest that this inhibition arises from a pool of neurons with different orientations.

2.4.8 Degree of Invariance within the Orientation Map

A study conducted by DeAngelis et al. (1999) reveals the degree of invariance of several response variables within a small patch of cat V1. Both adult cats and kittens were included in this study. This study indicates that there are great variations between the receptive fields of neurons that are close to each other in space. The authors point out that a small patch of the cortex, e.g. a cortical minicolumn, might be more heterogeneous than what it is considered previously. This study reveals also that neurons that have similar receptive fields show correlated activity.

Relative to other response variables, the highest degree of clustering is shown by orientation selectivity, closely followed by spatial frequency (DeAngelis et al. 1999). One response variable did, however, not show any evidence of clustering, namely, the spatial phase. The authors propose that high degree of variance between the receptive fields of the neurons within a small patch might be an indication of mechanisms that are involved in response pooling. The effect of this response pooling is to reduce noise (DeAngelis et al. 1999).

Results on heterogeneity were also reported earlier (Murphy and Sillito, 1986). This study, which was restricted to orientation selectivity, revealed that there are variations in orientation preferences of the neurons that are found in an orientation minicolumn. Orientation preference inside an orientation minicolumn can vary 9–18º between the neurons (Murphy and Sillito, 1986). Recall also that, each cell responds selectively to a broad range of orientation.
Given the evidences that orientation selectivity, which varies considerably within a small patch, is the most clustered response variable, it is evident that orientation minicolumns are highly heterogeneous.

2.5 Putative Functional Roles of the Long-Range Horizontal Connections in Responses of the Neurons

Even though the extent and shape of the long-range horizontal connections are relatively well documented, their functional roles in cortical processing are still not clearly understood. It is believed that in the V1 these connections are responsible for a variety of surround effects. Depending on stimulus configuration, these effects can be facilitatory or suppressive (Howell and Hess, 1978; Robson and Graham, 1981; Polat and Sagi, 1993; 1994a; 1994b; Polat and Norcia, 1996; 1998; Kastner et al., 1997; Polat and Tyler, 1999; Solomon et al., 1999; Solomon and Morgan, 2000; Yu et al., 2002; Chisum et al., 2003). These effects are exposed by psychophysical studies on humans and neurophysiological studies on other species.

It is also hypothesized that the long-range horizontal connections are responsible for spike and burst synchronization, which is believed to play an important functional role in perceptual grouping (Gray and Singer, 1989; Gray et al., 1989; Singer, 1993; 1999).

2.5.1 Summation Pools and Contour Integration

The influence of the horizontal connections over the response properties of the neurons extends beyond emergence of OS as well as other response properties. It has been reported that the visibility of a grating stimulus improves when its size increases (Howell and Hess, 1978; Robson and Graham, 1981). Furthermore, this improvement in visibility seems to be closely related to the stimulus configuration (Polat and Sagi, 1993; 1994a; 1994b; Polat and Norcia, 1998; Polat and Tyler, 1999; Chisum et al., 2003).

Polat and Norcia (1998) have addressed configuration-specific facilitation phenomena in human visual cortex during low-contrast conditions. Based on measurements of visually evoked potentials in human visual cortex, the authors

have shown that elongation of a foveally viewed circular Gabor patch has a positive effect on its visibility. Furthermore, elongation that is along the orientation axis of the neurons (collinear configuration) results in a more prominent improvement in visibility than orthogonal elongation. Polat and Norcia (1998) propose that elongated summation pools, which are hypothesized to be related to the long-range horizontal connections (Section 2.3; Rockland and Lund, 1982; 1983; Gilbert and Wiesel, 1983; 1989; Rockland, 1985; Amir, 1993; Malach et al., 1993; Durack and Katz, 1996; Fitzpatrick, 1996; Bosking et al., 1997; Kisvárday et al., 1997; Schmidt et al., 1997; Yousef et al., 1999; Chisum et al., 2003), can explain phenomena related to configuration-specific facilitation phenomena.

A recent support for the hypothesized link between configuration-specific facilitation phenomena and the layout of the long-range horizontal connections (Polat and Norcia, 1998) is from the study conducted by Chisum et al. (2003). This study shows that neurons in the layer 2/3 of tree shrew V1 have elongated RFs and are sharply tuned for orientation. In addition, they perform length summation, which indicates that these neurons can integrate information from remote locations. Chisum et al. (2003) have shown that along the orientation axis of the neurons the size of these summations pools coincides well with the coverage of the layer 2/3 long-range horizontal connections. In the same study Chisum et al. (2003) show that responses to the collinearly positioned Gabor patches are stronger than responses to noncollinear constellations of Gabor patches. This second results is interpret as an indication of the axial specificity of the layer 2/3 long-range horizontal connections. Thus, the results of Chisum et al. (2003) are in line with configuration-specific facilitation experiments conducted by Polat and Norcia (1998).

A recent study carried out by Ernst and colleagues (Ernst et al., 2003) relate psychophysical investigations to information theoretical modeling of contour integration. More precisely, the intention of this study is to compare quantitatively the performance of monkeys on detection simple contours with an ideal observer defined by Williams and Thornber (2001). Simple contours compromise of aligned Gabor patches. Ernst et al. (2003) reveal that monkeys perform close to what is defined as an ideal observer. Their results indicate that the mechanisms within the visual cortex of monkey are highly specialized for contour integration. Thus, monkeys perform equally well as humans on contour integration. Furthermore, Ernst et al. (2003) stress that the gap between a heuristical explanation of the Gestalt criteria and a solid mathematical framework of the Gestalt properties remains. However, according to Ernst et al. (2003) the work by Williams and Thornber (2001) helps to narrow this gap. Williams and Thornber (2001) have shown that a contour can be defined as the outcome of a stochastic process with a known probability distribution. When this relation is inverted the model can take an arbitrary collection of elements, e.g. Gabor patches, and calculate the relative probability of them to belong to a contour. The result is the performance of an

optimal observer on contour detection. These calculations give an upper limit, which can be compared to real observers as humans or monkeys, and hence give an indication on the performance of various species and individuals within a species.

Solomon et al. (1999) have studied the facilitation from collinearly positioned flanks in human visual cortex. In this experiment both the target and the two flanks were Gabor patches. This study show that even tough the flanks have opposite sign, relative to the target, the effect of presence of flanks is facilitation. However, this facilitation is not as prominent as if the flanks have the same sign as the target. Furthermore, Solomon and Morgan (2000) have reported that when the flanks extend to surroundings the target the facilitation is reduced dramatically. This finding is interesting, since non-collinear flanks by themselves do not mask the target prominently.

Yu et al. (2002) have recently studied modulatory effects of cross-orientation. In this study the stimulus that is positioned in the surroundings has orthogonal orientation relative to the target stimulus. They report that cross surround facilitation is a surround-contrast dependent effect. This effect is more evident at low surround-contrasts. Thus, when the full-surround has low contrast threshold is lowered. Surprisingly, collinear surround facilitation is unaffected by surround contrast (Polat and Sagi, 1993). Yet another interesting result of the study by Yu et al. (2002) is related to the tuning of spatial frequency and orientation. The results indicate that on the contrary to the orientation, surround facilitation is narrowly tuned for spatial frequency. Yu et al. (2002) hypothesize that the target neurons receive surround input from a group of neurons narrowly tuned for target spatial frequency but loosely tuned for cross-orientation, indicating signal pooling over a large range of orientations.

Kastner et al. (1997) have investigated the neuronal responses to static and moving texture in area 17 of anaesthetized and paralyzed cats. The motivation is to investigate the neural basis of visual pop-out of orientation and motion. In the orientation test the stimulus that is positioned in the classical receptive field (CRF) is either orthogonal or parallel (uniform pattern) to the other bars that surround it. Their results indicate that orthogonal configuration enhances pop-out, since during this configuration the neurons respond more strongly compared to the uniform pattern. In the motion test all bars have same orientation, however, center and surround elements move either in the same or opposite directions. The results indicate that when the center element moves in the opposite directions the neurons respond stronger than if all patterns move in the same direction. As a result, Kastner et al. (1997) conclude that static and moving patterns positioned outside the CRF may alter the response properties of the neurons.

2.5.2 Synchronization and its Putative Functional Role in Perceptual Grouping

Neurons in the visual cortex of anesthetized and awake animals (cat and monkey) tend to synchronize with each other, with near-zero phase lag and in the millisecond range, when activated with a single contour (Gray and Singer, 1989; Gray et al., 1989; Singer, 1993; 1999; Singer and Gray, 1995; Kreiter and Singer, 1996; Engel et al., 1997; Usrey and Reid, 1999; Friedman-Hill et al., 1999; 2000; Haig et al., 2000; Maldonado et al., 2000). Furthermore, the synchronized neurons oscillate in the γ frequency range, which is 30–50 Hz (Singer and Gray, 1995). However, this precise synchronization is absent if the stimulus is composed of different contours moving in different directions (Gray et al., 1989).

Neurons that are synchronized are found several millimeters from each other (and are even located in different hemispheres). It is assumed that the reciprocal long-range horizontal connections play a prominent functional role in emergence of this behavior (Engel et al., 1991; Löwel and Singer, 1992; König et al., 1993). One consequence of synchronization is enhancement of the incoming signals. This has been shown in hippocampus (Stevens and Zador, 1998), along the thalamocortical (Alonso et al., 1996; Usrey and Reid, 1999) and the intracortical pathway (Alonso and Martinez, 1998).

According to the Gestalt physiologists the cognitive system of humans tends to relate objects (or events) to each other if they are connected in time and space (Köhler, 1930; Koffka, 1935). Events that happen simultaneously are more likely to be related to each other than events that are separated in time. The same idea is also valid for objects. Contours (or contrast edges) that have a similar contrast or move with the same speed and direction are more likely to be part of the same object. It is assumed that synchronization in the early stages of vision is a result of internal dynamics. It is also believed that synchronization is context-dependent and probably reflects Gestalt criteria for perceptual grouping (Gray et al., 1989; Kreiter and Singer, 1996).

3 The Bayesian Confidence Propagation Neural Network

The environment where the animals and the humans live in is ever changing and highly complicated. The information, which is available on the environment, is often noisy and incomplete. Furthermore, several events occur simultaneously, and on different time scales. Biological learning systems seem to cope with these properties of the real world successfully. These systems are adapted to specific habitats and are formed by millions of years of evolution.

Sandberg et al. (2002) have recently developed an incremental learning rule derived from the Bayesian confidence propagation neural network (BCPNN) (Lansner and Ekeberg, 1987; 1989; Lansner and Holst, 1996; Holst, 1997). This learning rule mimics biological learning systems remarkably well. Furthermore, the network, which is subject to learning, has several properties that are generally accepted as key properties of the neocortex (Section 2.3).

As demonstrated by Sandberg et al. (2002) the network has 'palimpsest' properties when configured as a recurrent attractor network (see also Sandberg (2003)). Thus, recently learned patterns are more stable than older patterns to avoid catastrophic forgetting. The recurrent network, which is subject to learning, consists of dense local and sparse long-range connections (Sandberg et al., 2002). Thus, it fits well the known connectivity of the neocortex (Section 2.3). In the same study it is shown that this recurrent network does not suffer from catastrophic forgetting. Furthermore, the network's capacity depends on the learning time constant, and it recalls newer patterns faster than the older ones, during the retrieval mode that is.

The BCPNN has been developed in analogy with the known columnar structure of the neocortex (Mountcastle, 1957; 1978; 1997; Powell and Mountcastle, 1959; Hubel and Wiesel, 1962; 1977; Buxhoeveden and Casanova, 2002; Lund et al., 2003). The network consists of units that correspond to cortical minicolumns. The

units are grouped into hypercolumn-like modules and the summed activity within each hypercolumn module is normalized to one. The normalization is a way of controlling the total activity of the network. The normalization scheme is supported by the studies on the response saturation properties of the neurons (Maffei et al., 1973; Dean, 1981; Albrecht and Hamilton, 1982; Section 2.4.5).

The BCPNN learning rule is based on a probabilistic view of learning, and is derived from Bayes' rule (Bayes, 1958). Units receive input from all other units in the network representing confidence of feature detection. Based on the input, the units calculate posterior probabilities of outcomes. The learning rule is based on Hebb's ideas on synaptic plasticity and emergence of cell assemblies (Hebb, 1949). Thus, correlated activity reinforces the connections between pairs of units. Anti-correlated activity results in weakening of a connection, and emergence of an inhibitory one. Connections between units that are neither correlated nor anti-correlated weaken and disappear. A brief derivation of the BCPNN architecture and the incremental learning rule can be found in the next section (see Sandberg et al. (2002) and Sandberg (2003) for a more detailed derivation).

3.1 Derivation of the Network Architecture and the Incremental Learning Rule

As mentioned above the starting point is Bayes' rule and the naive Bayesian classifier (Good, 1950). Using the naive Bayesian classifier (NBC), probabilities of attributes y_j, can be calculated given other attributes x_i. It is assumed that both these two sets of attributes are discrete. Furthermore, the variables x_i are assumed to be independent ($P(x_1,\ldots,x_n)=\prod_{i=1}^{n}P(x_i)$), and conditionally independent given y_j ($P(x_1,\ldots,x_n \mid y_j)=\prod_{i=1}^{n}P(x_i \mid y_j)$).

Based on the properties of x_i and y_j Bayes' rule gives

$$\pi_j = P(y_j \mid x) = P(y_j)\prod_{i=1}^{n}\frac{P(x_i \mid y_j)}{P(x_i)} = P(y_j)\prod_{i=1}^{n}\frac{P(x_i, y_j)}{P(y_j)P(x_i)}.$$

This can be extended to the case where some information is missing. Suppose we are given completely known observations x_i when $i \in A \subseteq \{1,\ldots,n\}$ and have no information about the attributes x_k when $k \in \{1,\ldots,n\} - A$, then for the NCB

$$\pi_j = P(y_j \mid x_i, i \in A) = P(y_j)\prod_{i \in A}\frac{P(y_j, x_i)}{P(y_j)P(x_i)}.$$

Taking the logarithm of π_j eliminates the product

$$\log \pi_j = \log P(y_j) + \sum_{i \in A} \log \left[\frac{P(y_j, x_i)}{P(y_j)P(x_i)} \right] = \log P(y_j) + \sum_{i \in A} o_i \log \left[\frac{P(y_j, x_i)}{P(y_j)P(x_i)} \right]$$

where the indicator o_i represent whether there is information about a feature i or not

$$o_i = \begin{cases} 1 & i \in A \\ 0 & i \notin A \end{cases} = I_A(i) .$$

The equations above can be implemented as a one-layered feedforward neural network with the weights w_{ij}= log[P(y_j,x_i)/(P(y_j)P(x_i))] and the biases β_j = log P(y_j). The input layer activations are o_i. The one-layered feedforward neural network calculates the posterior probabilities π_j using an exponential transfer function, given the input attributes.

The one-layered feedforward neural network becomes modular when the discrete attribute values are represented by the indicator variables. Continuous valued attributes can be interval coded. Note that this scheme is common within the neocortex (Mountcastle, 1957; 1978; 1997; Powell and Mountcastle, 1959; Hubel and Wiesel, 1962; 1977; Buxhoeveden and Casanova, 2002; Lund et al., 2003). A classical example is the V1 where the orientation minicolumns respond selectivity to a narrow interval of orientations (Hubel and Wiesel, 1962; 1977). Thus, all orientations within a small patch of the visual field are represented by a collection of such orientation minicolumns (that together form an orientation hypercolumn).

Assume now that the representation of the attributes is changed so that each attribute i can take M_i different values. The observation of a given value of a given attribute as a new binary value is defined (marked with double indices)

$$\pi_{jj'} = P(y_{jj'}) \prod_{i \in K} \frac{P(y_{jj'}, x_{ik})}{P(y_{jj'})P(x_{ik})}$$

where for each attribute $i \in \{1,...,n\}$ a unique value x_{ik} is known, where $k \in \{1,...,M_i\}$. Similarly is follows that

$$\pi_{jj'} = P(y_{jj'}) \prod_{i=1}^{n} \sum_{i'=1}^{M_i} \frac{P(y_{jj'}, x_{ii'})}{P(y_{jj'})P(x_{ii'})} o_{ii'} .$$

with indicator $o_{ii'} = 1$ if $i' = k$ and zero otherwise

Consider now the attributes X_i as stochastic variables with values $\{x_{i1},\ldots,x_{iM_i}\}$, which are explicitly represented in the network. Now $o_{X_i}(x_{ii'}) \coloneqq o_{ii'}$ can be viewed as a degenerate probability $o_{X_i}(x_{ii'}) \coloneqq \delta_{x_{ik}}(x_{ii'})$, which is zero for all $x_{ii'}$ except for the known value x_{ik}. When o_{X_i} is replaced with a general probability P_{X_i} we get

$$\hat{\pi}_{jj'} = P(y_{jj'}) \prod_{i=1}^{n} \sum_{i'=1}^{M_i} \frac{P(y_{jj'}, x_{ii'})}{P(y_{jj'})P(x_{ii'})} P_{X_i}(x_{ii'})$$

$$\log(\hat{\pi}_{jj'}) = \log P(y_{jj'}) + \sum_{i=1}^{n} \log\left[\sum_{i'=1}^{M_i} \frac{P(y_{jj'}, x_{ii'})}{P(y_{jj'})P(x_{ii'})} P_{X_i}(x_{ii'}) \right].$$

If the outcomes $x_{ii'}$ of different attributes are independent of each other when conditioned on X_i, $\hat{\pi}_{jj'}$ will be the expectation of $\pi_{jj'}$ given input X_i.

The resulting equations reveal that the network has a modular structure. The unit *ii'* represents explicitly values $x_{ii'}$ of X_i, which can be viewed as a hypercolumn. By definition the total activity within a hypercolumn *i* is normalized

$$\sum_{i'=1}^{M_i} P_{X_i}(x_{ii'}) = 1.$$

The probability of $y_{jj'}$ can be calculated given the uncertain information related to $x_{ii'}$. The probability $P_{X_i}(x_{ii'})$ reflects the uncertainty. The network setting of these relations is

$$h_{jj'} = \beta_{jj'} + \sum_{i}^{n} \log\left(\sum_{i'}^{M_i} w_{ii'jj'} P_{X_i}(x_{ii'}) \right).$$

In this network setting $h_{jj'}$ is defined as the support of unit *jj'*. The output of a unit *jj'* is given by $\hat{\pi}_{jj'} = f(h_{jj'}) = e^{h_{jj'}}$. The biases of the units and the weights between the pairs of units are defined as

$$\beta_{jj'} = \log(P(y_{jj'}))$$

$$w_{ii'jj'} = \frac{P(x_{ii'}, y_{jj'})}{P(x_{ii'})P(y_{jj'})}$$

The independence assumption is too strong and can only be approximately fulfilled as we deal with approximations of probabilities. As a consequence the outputs within each hypercolumn is normalized

$$\hat{\pi}_{jj'} = f(h_{jj'}) = \frac{e^{h_{jj'}}}{\sum_{j'} e^{h_{jj'}}}.$$

Note that both the input and the output of the units are probabilities. It is now possible to configure the network as a fully recurrent network, which can work as an autoassociative memory. The procedure starts with the currently observed probability $P_{X_i}(x_{ii'})$, which is used as an initial approximation of the true probability $X_{ii'}$. From $P_{X_i}(x_{ii'})$ the posterior probability is calculated, which tends to be a better approximation than $P_{X_i}(x_{ii'})$. In the following step, the posterior probability is fed back to the process to calculate an even better approximation. This procedure is iterated until a stable state is reached. Sandberg et al. (2002) explain the procedure with: 'this represents a heuristically estimated probability closest to the observed data and consistent with the already acquired knowledge, that is prior information represented by the learning parameters $\beta_{jj'}$ and $w_{ii'jj'}$'.

The continuous time updating rule is defined as

$$\tau_c \frac{dh_{jj'}(t)}{dt} = \beta_{jj'} + \sum_{i}^{n} \log\left(\sum_{i'}^{M_i} w_{ii'jj'} f(h_{ii'}(t)) \right) - h_{jj'}(t)$$

where the parameter τ_c is the 'membrane time constant' of each unit.

The BCPNN has two modes. During the learning mode the weights and the biases are modified, whereas during the retrieval mode these parameters are static and a pattern is being retrieved. At the start of the retrieval mode the units are initiated with probabilities. These values propagate through the network during the retrieval mode (see above).

The original BCPNN learning rule (Lansner and Ekeberg, 1989; Lansner and Holst, 1996) uses counters for calculating the probabilities $P_{X_i}(x_{ii'})$. Whenever a unit is active the counter it is associated with is updated. Later, when the training is finished, the counters are divided with the total number of examples that was used during the training. Probabilities $P_{X_i}(x_{ii'jj'})$ associated with co-activations of units are calculated in the same way. Whenever the units *ii'* and *jj'* are active (due to a training example) the counter associated with the weight between them is updated. Later this counter is divided with the total number of training examples. When the estimations $P_{X_i}(x_{ii'})$ and $P_{X_i}(x_{ii'jj'})$ are calculated the weights and the biases of the units can be calculated. Afterwards the network can be used in the retrieval mode.

A continuously operating learning system operates in a fundamentally different way. Such a system learns new patterns and updates the weights and the biases

continuously. Estimations $P_{X_i}(x_{ii'})(t)$ and $P_{X_i}(x_{ii'jj'})(t)$ need to be estimated given the information that $\{x(t'), t' < t\}$. Such a system must fulfill three requirements. First, it should converge towards $P_{X_i}(x_{ii'})(t)$ and $P_{X_i}(x_{ii'jj'})(t)$ in a stationary environment. Later, more recently learned patterns must be more stable than older ones. Finally, it should smooth or filter out noise and adapt to longer trends.

These requirements are achieved by the incremental BCPNN learning rule by approximating $P_{X_i}(x_{ii'})(t)$ and $P_{X_i}(x_{ii'jj'})(t)$ with the exponentially smoothed running averages $\Lambda_{ii'}(t)$ of the activity $\hat{\pi}_{ii'}$ and $\Lambda_{ii'jj'}(t)$ of coincident activity $\hat{\pi}_{ii'}\hat{\pi}_{jj'}$.

The continuous time version of the update and learning rule is defined as

$$\hat{\pi}_{ii'} = \frac{e^{h_{ii'}}}{\sum_j e^{h_{ij}}}$$

$$\frac{d\Lambda_{ii'}(t)}{dt} = \alpha([(1-\lambda_0)\hat{\pi}_{ii'}(t) + \lambda_0] - \Lambda_{ii'}(t))$$

$$\frac{d\Lambda_{ii'jj'}(t)}{dt} = \alpha([(1-\lambda_0^2)\hat{\pi}_{ii'}(t)\hat{\pi}_{jj'}(t) + \lambda_0^2] - \Lambda_{ii'jj'}(t))$$

$$\beta_{ii'}(t) = \log(\Lambda_{ii'}(t))$$

$$w_{ii'jj'}(t) = \frac{\Lambda_{ii'jj'}(t)}{\Lambda_{ii'}(t)\Lambda_{jj'}(t)}$$

The parameter α is defined as the inverse of the learning time constant τ_L. During the retrieval mode α is set to zero, and hence the weights and the biases are not updated.

The parameter λ_0, which corresponds to noisy background activity, is introduced primarily to avoid logarithmic zero. In the absence of input the parameters $\Lambda_{ii'}(t)$ and $\Lambda_{jj'}(t)$ converge towards λ_0 and $\Lambda_{ii'jj'}(t)$ converges towards λ_0^2. Thus, the weight between two units becomes $w_{ii'jj'}(t) = 1$, i.e. no connection since log(w)=0.

4 Related Work

There are several types of network models that address vastly different aspects of information processing within the V1. Consequently, these network models address different response properties of the neurons that populate the V1, such as response saturation followed by normalization (Albrecht and Geisler, 1991; Heeger, 1992; Carandini et al., 1997), emergence of orientation selectivity (Hubel and Wiesel, 1962; Somers et al., 1995; Troyer et al., 1998; Adorján et al., 1999; McLaughin et al., 2000; Wielaard et al., 2001; Kayser and Miller, 2002), and various surround effects (Somers et al., 1998; 2002; Yen and Finkel, 1998; Li, 1998; Grossberg and Raizada, 2000) (see (Das, 1996; Sompolinsky and Shapley, 1997; Ferster and Miller, 2000; Martin, 2002) for a review).

Most of these models are of either cat (Hubel and Wiesel, 1962; Somers et al., 1995; 1998; 2002; Troyer et al., 1998; Grossberg and Raizada, 2000) or monkey (Adorján et al., 1999; McLaughin et al., 2000; Wielaard et al., 2001) V1. Some network models address the interactions within a small region, which consists of an iso-orientation domain (Troyer et al., 1998; Kayser and Miller, 2002) or a hypercolumn (Somers et al., 1995; Adorján et al., 1999), whereas others focus on interactions within patches that include several hypercolumns (Somers et al., 1998; 2002; Yen and Finkel, 1998; Li, 1998; Grossberg and Raizada, 2000; McLaughin et al., 2000; Wielaard et al., 2001).

Most often these models are classified after the importance of the thalamocortical circuitry in shaping the response properties of the neurons. The recurrent models assume that the thalamic input is weak and poorly tuned for orientation, and hence assume that the intracortical connections play an important role in every aspect of information processing within the V1 (Section 4.2). On the contrary, the feedforward models rely heavily on the thalamocortical circuitry (Section 4.1). The normalization models, which can be seen as a sub-class of the feedforward models, address mainly the contrast gain functions of the neurons. Various surround effects are reviewed in Section 4.3.

The models that are mentioned above (see Sections 4.1–4.3 for the details) do not deal with the development of the V1, since they assume a fully developed adult brain. Thus, connections between modeled entities, which correspond to neurons

or populations of neurons, are fixed. In Section 4.4 developmental models that are relevant to this thesis work are reviewed. These models address the mechanisms behind map building and emergence of horizontal connections (Miikkulainen et al., 1997; Miller et al., 1999; Shouval et al., 2000; Bartsch and van Hemmen, 2001; Kayser and Miller, 2002; Bednar and Miikkulainen, 2004).

4.1 Feedforward and Normalization Models of Orientation Selectivity

Hubel and Wiesel (1962) have proposed the original feedforward model (Section 2.4). LGN cells of the same type (ON-center or OFF-center) converge to form elongated regions, which becomes the subregions of the simple cells. This model addresses the emergence of orientation selectivity in an elegant way, and has some quantitative support. However, it cannot explain contrast-invariance of orientation tuning (see Paper II). Nevertheless, this elegant model is still used for studying the thalamocortical circuitry.

Miller and colleagues (Troyer et al., 1998; Kayser and Miller, 2002; Lauritzen and Miller, 2003) have shown that contrast-invariance of orientation tuning of cat layer 4 simple cells can be achieved within a very small patch of the V1. They assume that the input from the thalamus is strong and well tuned for orientation. In this models the intracortical recurrent connections, especially the long-range horizontal connections, play a minor functional role in shaping the response properties of the neurons. Interactions inside the modeled small patch are based on the spatially opponent inhibition theory (Ferster, 1988). According to the study by Ferster (1988) inhibitory simple cells mediate local inhibition between excitatory simple cells, which have opposite absolute spatial phase. Miller and colleagues (Troyer et al., 1998; Kayser and Miller, 2002) assume that the neurons participating in this assembly are located inside a very small region corresponding to a couple of orientation minicolumns. As a consequence this model assumes that inhibition is local. Recently this model has been extended with inhibitory complex cells (Lauritzen and Miller, 2003). The role of these neurons is to compensate for the part of the thalamic input, which only depends on the contrast of the stimulus (Troyer et al., 2002; Lauritzen and Miller, 2003).

Well tuned and strong thalamic input are the main assumptions of the feedforward models. As mentioned earlier these assumptions are in contradiction with the reported values on aspect ratios of the subfields (Jones and Palmer, 1987; Chapman et al., 1991; Pei et al., 1994; Reid and Alonso, 1995) and relative strength of the thalamic input (Garey and Powell, 1971; LeVay and Gilbert, 1976; Hornung and Garey, 1981; Winfield and Powell; 1983; LeVay, 1986; Einstein et al., 1987; Peters and Payne, 1993; Ahmed et al., 1994; Stratford et al., 1996) (see

Section 2.4 for the details; note that the opposed view is taken in Ferster and Miller (2000)).

A sub-class of the feedforward models is the normalization models (Albrecht and Geisler, 1991; Heeger, 1992; Carandini and Heeger, 1994; Heeger et al., 1996; Carandini et al., 1997). The primary goal of these models is to address the contrast gain functions (response saturation) of the neurons. Thus, these network models assume that input from the LGN grows linearly with contrast of the stimulus. The geniculate input is divided by a linearly growing inhibitory input, which is of cortical origin and depends of the contrast of the stimulus. The effect is division of the input from the LGN.

Carandini and Heeger (1994) proposed that the inhibition would take the form of a shunting inhibition. This inhibition would originate from a pool of neurons with all possible orientation and spatial frequency preferences (the so-called normalization pool). The shunting effect corresponds to the lowering of the time constants of the neurons, and as a result the neurons' integration times decreases. However, the shunting inhibition requires that the membrane time constants of the neurons decreases ~60 ms. This is not possible, since the resting time constants of most neurons are ~20 ms, and membrane time constants cannot decrease below zero. Nevertheless, it seems that the intracortical inhibition is indeed responsible, in one form or another, for shaping the contrast gain functions of the neurons, since most thalamic cells saturate only mildly (Sections 2.4.4 and 2.4.5).

4.2 Recurrent Models of Orientation Selectivity

Recurrent models are fundamentally different in their approach on addressing response properties of the neurons (Ben-Yishai et al., 1995; 1997; Somers et al., 1995; 1998; 2002; Hansel and Sompolinsky, 1996; Adorján et al., 1999; McLaughin et al., 2000; Wielaard et al., 2001). In these network models the intracortical recurrent connections play an important functional role in achieving orientation selectivity and contrast-invariance of orientation tuning. The geniculate input is assumed to be weak and poorly tuned for orientation (Jones and Palmer, 1987; Chapman et al., 1991; Pei et al., 1994; Stratford et al., 1996).

Somers and colleagues (1995; 2002) assume that inhibition originates from a pool of neurons with more spread in orientation selectivity than the excitatory input. Furthermore, iso-orientation inhibition is stronger than oblique- and cross-orientation inhibition as proposed by Ferster (1986). This network topology helps to prevent the spread of a local excitatory activity. A prominent feature of the recurrent models is the emergence of the Mexican Hat function (Somers et al., 1995; 2002; Ben-Yishai et al., 1995; 1997; Hansel and Sompolinsky, 1996). The effect of the Mexican Hat functions is that neurons in close surroundings receive net excitatory input, whereas neurons located further away receive net inhibitory

input. As a consequence of this connections pattern, the orientation tuning becomes a property of the recurrent cortical circuitry, and does not depend on the tuning of the geniculate input. Note also that the layout of excitatory and inhibitory connections define the tuning width of the neurons.

However, the recurrent models that are described above (Somers et al., 1995; 2002; Ben-Yishai et al., 1995; 1997; Hansel and Sompolinsky, 1996) violate the cortical connectivity. They assume that the inhibitory network extends more than the excitatory one. This is in direct contradiction with what is generally accepted (Kisvárday et al., 1997; Roerig and Chen, 2002; see also the critical review of the hypercolumn models by Martin (2002)).

The network model of macaque V1 (layer 4Cα) by Adorán et al. (1999) is based on the anisotropic intracortical excitatory connections within the V1 of the macaque monkey. These connections provide both the initial orientation bias and its subsequent amplification. Note further that the thalamic input from the M cells does not provide any orientation bias, even though this possibility is not ruled out (Adorán et al., 1999).

Yet another model of the layer 4Cα macaque V1 has been proposed by McLaughlin and colleagues (McLaughin et al., 1999; Wielaard et al., 2001). In this model the Mexican Hat connectivity near the orientation singularities provide the neurons with broadly tuned local inhibition. The result is sharpening of the orientation tuning of the neurons. However, as pointed out by Martin (2002) this model assumes very strong inhibition. In the model inhibitory synapses are 5–10 times stronger than the excitatory synapses (McLaughin et al., 1999; Wielaard et al., 2001). Strong inhibition compensates for the fact that the inhibitory neurons are only ~20% of the total number of neurons (Gabbott and Somogyi, 1986).

In Paper V emergence of OS has been addressed. The model assumes that the LGN input is poorly tuned for orientation, and hence explains emergence of OS through lateral interactions mediated by horizontal connections.

4.3 Models that Address Various Surround Effects

Besides contrast invariance of orientation tuning, Somers and colleagues (Somers et al., 1995; 1998; 2002) address several other phenomena, such as contrast-dependent length tuning (end-stop cells), supersaturation and facilitation suppression based on the local and long-range synaptic interactions. Contrast-dependent length tuning is the effect of increase in excitatory receptive field size of a cell with decreased contrast. Supersaturation, which is related to contrast-dependent length tuning, means that increased contrast of a stimulus can actually cause decreased activity of a neuron. Facilitation suppression reveals the modulatory effects of the (uniform or orthogonal) surround grating to the center

grating. When the center grating has low contrast surround grating has facilitatory effect independent of the configuration. However, during high contrast an orthogonal surround grating has more prominent facilitatory effect.

Several groups have addressed contour integration and perceptual grouping (Grossberg and Raizada, 1998; Yen and Finkel 1998; Li, 1998). Grossberg and Raizada (1998) present a laminar model of areas V1 and V2 that addresses contrast-sensitive perceptual grouping and attention. Their highly detailed model pools and sharpens raw contrast edge signals, which become closed boundaries that are 'filled-in' by neuronal activity representing color. In this model, above-threshold firing layer 2/3 complex cells are responsible for perceptual grouping. The model also demonstrates that in V2 long-range excitation and disynaptic inhibition is sufficient for explaining emergence of illusory contours.

Yen and Finkel (1998) address the extraction of salient contours within the V1. Their model relies heavily on temporal synchronization, which is a result of strong facilitation of the modeled neurons. This facilitation is mediated by the long-range horizontal connections. Furthermore, the level of temporal synchronization between modeled neurons determines perceptual salience. Li (1998) address contour integration within the V1. The initial activity is amplified so that edges that form smooth contours oscillate in synchrony. In this model V2, which is involved in perceiving illusory contour, is absent. However, the author points out that the model could easily be modified to include other (higher) cortical areas.

4.4 Developmental Models of Cortical Circuits and Orientation Maps

Kayser and Miller (2002) have proposed a correlation-based developmental model of the layer 4, which is the main recipient of the thalamic input. The proposed developmental model is based on their earlier work (Troyer et al., 1998). Connections between simple cells develop according to Hebbian plasticity. The input consists of correlated activity that originate from the retina. The model addresses also the development of the thalamocortical circuitry, which occurs simultaneously as the intracortical connections. However, the model cannot produce a truly periodic orientation map.

Parallel development of the thalamocortical circuitry and the intracortical connections has also been addressed by Bartsch and van Hemmen (2001). Hebbian plasticity governs the development of the connections. Bartsch and van Hemmen (2001) demonstrate that the orientation maps can be generated in the absence of the thalamic input, through spike-spike correlations of spontaneous activity, within the layer 4. The authors propose that the orientation map, which is created through intracortical interactions, can guide the development of the thalamocortical circuitry. The model explains also reverse lid-suture experiments. These

experiments demonstrate that the right and left orientation maps are identical even though the eyes never receive the same visual input (Gödecke, Bonhoeffer, 1996; Sengpiel et al., 1998). This model does not address development of a local cortical circuit.

Experience based plasticity within the cat and ferret primary visual cortex is addressed by Shouval et al. (2000). It is proposed that a non-isotropic scaffold does exist before the V1 is subject to visual experience. This scaffold is made of the layer 2/3 long-range horizontal connections. The function of the scaffold is to guide the thalamocortical connections that begin to emerge after the eye opening. With the maturation of the thalamocortical circuitry neurons become sharply tuned for orientations. Stimulus consisting of natural images is used during training. The model does not address modification of the horizontal connections, since the scaffold is static. However, this possibility is not ruled out as pointed out by the authors.

Miikkulainen and colleagues have addressed the combined prenatal and postnatal development of the horizontal connections and emergence of orientation maps (Miikkulainen et al., 1997; Bednar and Miikkulainen, 2004). During the prenatal phase spontaneous neuronal activity generated the orientation map. During the following postnatal phase the orientation map is refined by visual activity (Bednar and Miikkulainen, 2004). The overall shape of the orientation map is, however, not subject to change after that it is developed during the prenatal phase. Bednar and Miikkulainen (2004) point out that similar orientation maps can be generated with a variety of stimulus types. According to the authors this indicated that the information on the orientation maps does not need to be genetically coded. Miikkulainen et al. (1997) propose that during development the horizontal connections learn the activity between the neurons. Furthermore, the same connections act as filters when V1 is subject to visual experience.

5 Results of the Thesis

5.1 Issues Related to Development and Layout of the Horizontal Connections

The abstract hypercolumn model in Paper II is derived from the BCPNN architecture (Chapter 3). The model addresses interactions within a region, which corresponds to hypothesized cortical hypercolumns. This is a highly general model, which can be mapped to whole cortical hypercolumns (Paper II), as well as circuitry of individual cortical layers. In Papers II–V this model is mapped to layers 4 and 2/3.

The BCPNN architecture requires that the activity within a hypercolumn-module is limited to a certain level. This requirement is founded on the normalization mechanism within V1 (Section 2.4.5). The basket cells, which are positioned between the two layers (not to mix with cortical layers) of the hypercolumn-module, address this requirement (Paper II; Section 5.2). These cells correspond to a uniformly distributed population of large basket cells within a cortical layer. This mechanism is referred to as normalization inhibition (Papers II and V).

Large basket cells are known for sending out horizontally aligned axons up to 1.5 mm (Kisvárday et al., 1997), whereas other interneurons, such as bipolar, chandelier, and small basket cells target neurons in their near surroundings. The model assumes that large basket cells can inhibit a region, which is roughly as large as a cortical hypercolumn. It is further assumed that the excitatory cells within the same region can drive these large basket cells. Note that in the model there are no restrictions on the relationship between the lateral extents of inhibition and excitation. The outcome of this scheme is local inhibition for controlling the total activity of a region, which corresponds to a cortical hypercolumn (see Section 5.2 for the details). This scheme can occur both in layer

4 and layer 2/3, since large basket cells are found in both these layers (O'Leary, 1941; Tömböl, 1978).

In Paper V the development of the horizontal connections (in layers 4 and 2/3) has been addressed by a laminar model of the V1. The simulations mimic the situation, which start with the eye opening and continue for some weeks. During this period the horizontal connections develop and mature. The correlation-based developmental models of layers 4 and 2/3 in Paper V (see also Paper III) propose an excitatory network of horizontal connections that is responsible for excitation as well as inhibition. According to this scheme unit pairs that are correlated develop excitatory connections that link them, whereas anti-correlated unit pairs develop excitatory connections that target inhibitory interneurons located at the target units (Ferster, 1988; Hirsch et al., 2000; 2003). These two horizontal connections are referred to as E→E and E→I connections. Observe that the result of the second type of connection is inhibition.

In the laminar model presented in Paper V layer 4 RF were contrast edge detectors. Each layer 4 anti-phase unit pair projected to a layer 2/3 unit to generate a complex cell like RF. Since RF profiles are dependent of modeled layer, the BCPNN learning rule generates two different networks. In the layer 4 network both types of horizontal connections prefer the iso-orientation domain. The quantitative assessments of the connections show that every second connection targets the iso-orientation domain. Observe that in the model strongest inhibition is between iso-orientation domains. This result is in line with what has been reported (Ferster, 1986; 1988). Furthermore, due to uncorrelated activity direct cross-orientation inhibition is very weak (Paper V). In this network long-range connections are equally distributed between different orientations. These results are in line with the distribution of the connections in the layer 4 (Yousef et al., 1999).

Input from layer 4 generates a patchy, axially specific layer 2/3 network (Paper V), similar to the layer 2/3 of V1 (Kisvárday et al., 1997). Presence of patches located at iso-orientation domains is an indication of correlated activity between units that are selective for similar orientations. The network does not develop E→I connections, which indicates absence of anti-correlated activity between unit pairs. Recall that these connections are common in the layer 4 network, especially between anti-phase unit pairs. Quantitative assessment of layer 2/3 reveals that approximately half of the connections are between iso-orientation domains. There are minor differences between the distribution of the local and long-range connections. The former are somewhat more selective for the iso-orientation though. These results are in line with Kisvárday et al. (1997).

Observe that in the model normalization inhibition operates within a hypercolumn-module. In layer 4 network there is an additional source of inhibition mediated by the (excitatory) E→I connections. These connections target local inhibitory interneurons, thus this form of inhibition is local as well. These assumptions are in line with what is found in V1, i.e. inhibition is mainly local,

whereas excitation extends far beyond the inhibitory network. Observe also that neither excitation nor inhibition dominates the network.

5.2 Horizontal Connections Account for emergence of OS, Contrast-Invariance of Orientation Tuning, and Response Saturation followed by Normalization

It is shown that the neurons start to saturate when the stimulus contrast is increased beyond a certain level (Maffei et al., 1973; Dean, 1981; Albrecht and Hamilton, 1982; Section 2.4.5). For most neurons this saturation, which occur rapidly, starts at 50–60% of their theoretical response ranges. As a result, the contrast gain functions take the form of a hyperbolic function (Albrecht, 1982).

The mechanisms behind this rapid saturation are not known. It seems, however, that the gain functions of the LGN cells cannot explain this behavior. Results by Movshon et al. (1994) indicate that the M cells have logarithmic contrast gain functions, whereas, the majority of the LGN cells, i.e. the P cells, have roughly linear contrast gain functions, and hence show very little sign of saturation due to increase in stimulus contrast (Section 2.4.4). It is further known that most neurons (especially those found in lower parts of layer 3, layer 4A and layer 6A) receive a mixture of P and M signals. Thus, the hyperbolic contrast gain functions of the neurons cannot be explained solely by the saturation of the LGN input to the cortex. In Paper II it is assumed that the normalization inhibition can explain emergence of this behavior.

In Paper II, a possible mechanism behind rapid response saturation followed by normalization is proposed. The large basket cells that are positioned in between the layers of a BCPNN hypercolumn-module, integrate the total activity of the excitatory cells located in the hypercolumn-module's input layer. Thus, these inhibitory cells estimate the total input from the LGN and the cortex to a patch, which corresponds to a cortical hypercolumn. The strength of this input is primarily a function of stimulus contrast, since the large basket cells integrate the activity of all excitatory cells in the input layer of the hypercolumn-module (independent of their orientation preferences). In the next step, the large basket cells inhibit excitatory cells in the output layer of the hypercolumn-module. As a result, the output of these excitatory cells' is controlled. It is assumed that this circuitry, which is limited to a hypercolumn-module, is sufficient to explain the machinery needed to control response saturation followed by normalization in V1 neurons.

The same local circuitry addresses contrast-invariance of orientation tuning as well as cross-orientation inhibition (Morrone et al., 1982; Bonds, 1989) (Paper II).

As an effect of increase in stimulus contrast the large basket cells increase their activities. The result is stronger inhibition of the excitatory cells found in the output layer. For those output layer excitatory cells, whose orientation preferences differ more than ~45º relative the stimulus, the inhibition increases more rapidly than the excitation from the LGN and the V1. As a result, stimulus contrast increase causes these neurons to decrease their activities. The outcome is contrast-invariance of orientation tuning.

The proposed layer 4 network addresses OS by assuming normalization inhibition for controlling the total activity of the hypercolumn-modules, and long-range E→E connections, which provide units with information from a larger region than their CRF. These two factors seem to be the key components. However, as a result of increase in the strengths of the E→E connections units become less orientation selective. In this context the E→I connections play a major role in stabilizing the activity of the units. Increasing the strengths of these connections prevents the drop off in OS without affecting convergence times. Observe that the layer 4 network addresses OS by assuming V1 like connectivity, i.e. the network is not dominated by extremely strong inhibition, and the excitatory network encloses its inhibitory equivalent. Earlier, other recurrent models of OS (see Section 4.2) have been criticized for violating this (Martin, 2002).

The study of configuration-specific facilitation (Paper V) also gives insight into the emergence of OS in species whose layer 4 neurons are poorly tuned for orientation, e.g. tree shrew (Humphrey and Norton, 1980; Chisum et al., 2003), ferret (Chapman and Stryker, 1993), and monkey (Hubel and Wiesel, 1977; Blasdel and Fitzpatrick, 1984; Hawken and Parker, 1984). Anisotropy in the layer 2/3 iso-orientation dominated long-range inputs compensates for the poorly tuned inputs to the layer 2/3 from layer 4 (see 5.3.2).

The proposed layer 4 network is unique in that it addresses emergence of OS, contrast-invariance of orientation tuning, and response saturation followed by normalization within the framework of a conceptual model, which is in line with the known anatomy and physiology of the neocortex.

5.3 Findings Related to the Functional Roles of the Long-Range Horizontal Connections

5.3.1 Long-Range Horizontal Connections Account for Spike and Burst Synchronization

The simulations in Paper I are intended to show that spike and burst synchronization phenomena may occur between neurons that are located several

millimeters from each other. This study addresses the facilitatory effects of synchronization as well.

Synchronized activity is demonstrated in a biologically plausible network model of tree shrew V1 (layer 2/3). The network model consists of six sub-sampled orientation minicolumns. Each orientation minicolumn consists of twelve integrate-and-fire neurons. All neurons are selective for the same orientation. Their RF are positioned in a collinear manner. The intention of the network layout is to mimic axial specificity of the summation pools found in layer 2/3 of V1 (Sections 2.5.1 and 2.3.2; Papers III and V).

Connections between modeled neurons inside the orientation minicolumns are dense, whereas connections between neurons located in different orientation minicolumns are sparse. In both cases connection probability is a function of the distance between neuron pairs. On average, each modeled neuron receives six connections from others that are positioned in the same orientation minicolumn, whereas two connections are received from those positioned in other five orientation minicolumns.

This study demonstrates that burst as well as zero-lag (γ frequency) spike synchronization is possible to achieve in a biologically detailed network model. Spike synchronization is however fragile, since it can be destroyed by repetitive firing. The network recovers fast though, and returns back to the spike synchronization mode after some tens of milliseconds. In the network model spike synchronization is only slightly tighter between neurons spatially closer to each other, e.g. neuron pairs positioned inside an orientation minicolumn. Nevertheless, zero-lag spike synchronization is possible to achieve between arbitrarily chosen neuron pairs. Note that the maximum distance between two neurons in the model is ~2.5 mm. The minimum spike propagation delay between such a pair is ~4 ms. Observe that in some cases there were no direct connections between zero-lag spike synchronized neuron pairs. In larger network models (maximum span is ~8 mm) lag in spike synchronization is present between neuron pairs at the extremes of the network model. This lag was, however, only ~2–3 ms, whereas the delay in those larger models was more than 12 ms. Thus, it seems that the network attempts to spike synchronize the neurons.

The modeled neurons were clearly facilitated due to synchronized activity (Paper I). It is possible that synchronization seen in visual cortex plays a similar role (Sections 2.5.2 and 4.3). Such a mechanism might be useful, e.g. in low-contrast conditions, since facilitation is even more vital when the external input is weak (in this case due to low stimulus contrast). Layer 2/3 network in Paper V demonstrates how (burst) synchronization might operate to facilitate BCPNN units. This study demonstrates that when the number of populations that participate in synchronization increases facilitation effects become more prominent.

5.3.2 Findings Related to the Summation Pools

Several groups have addressed the putative functional role of the long-range horizontal connections in response facilitation phenomena in V1 of humans and other species (Polat and Sagi, 1993; Polat and Norcia, 1996; 1998; Yu et al., 2002; Chisum et al., 2003; Sections 2.5.1 and 4.3). These experimental studies link detection or improved visibility of abstract figures, such as contours or Gabor patches, to response facilitation of the V1 neurons. Facilitation effects are dependent on stimulus configuration though. This finding is highly interesting since it might reveal the layout of the long-range connections that are found in the V1. Note that the intention of these studies is somewhat different from those that focus on synchronization (Section 2.5.2).

In Papers III–V the functional role of the long-range horizontal connections in response facilitation of the V1 neurons is investigated. These simulations are primarily influenced by the experiments of Polat and colleagues (Polat and Sagi, 1993; Polat and Norcia, 1996; 1998) who suggest that elongated physiological summation pools can explain configuration-specific facilitation phenomena in visual cortex (see Section 2.5.1 for the details). The authors assume that these summation pools emerge through long-range interactions within V1. In Paper V it is assumed that the axially specific long-range horizontal connections are responsible for these interactions. These connections are common in layer 2/3 (Section 2.3.1).

Two assumptions are made in Papers III–V. First, the total activity of the units inside a hypercolumns is constant, as required by the BCPNN incremental learning rule. The abstract hypercolumn model addresses this requirement (Paper II). Furthermore, during the simulations activities of the units are calculated without taking the delays between the units into account. Paper I shows, however, that synchronization on different levels between groups of neurons located several millimeter from each other can be achieved despite delays. Thus, it is assumed that excluding the time factor does not influence the results considerably.

Paper V addresses configuration-specific facilitation phenomena in layer 2/3. The simulation results suggest that increase in stimulus area results in response facilitation. The consequence is improved visibility of the stimulus. Furthermore, the way the stimuli are configured affects the degree of facilitation as well. Collinearly configured stimuli are easier to detect than orthogonally configured stimuli. Interestingly, differences in facilitation effects due to stimulus configuration are more prominent in low-contrast. In high-contrast there are only minor differences in the degree of facilitation due to stimulus configuration. Independent of stimulus configuration increase in facilitation is linear as a function of log contrast, as reported by Polat and Norcia (1998). This suggests fast improvement of facilitation as a function of contrast in low-contrast conditions.

It is assumed that layer 2/3 is responsible for these phenomena, since the layer 4 network is local and isotropic. It is not likely that the layer 4 network can detect

the differences between the stimuli. The situation is, however, different for the layer 2/3 network, since in this case units receive input from an anisotropic region. This is explained by the axially specific layout of the long-range horizontal connections (this region is referred to as the elongated summation pool by Polat and Norcia (1998)). As a consequence of this network layout, input from collinearly positioned units (with similar orientation preferences, due to modular specificity) is stronger than from all other units in the layer 2/3 network. Recall also that horizontal connections are reciprocal, thus units along the line, which overlaps with the stimulus, excite each other in a positive feedback loop.

Response facilitation is evident in layer 4 as well. The correlation-based model of V1 in Paper III represents layer 4 circuitry. BCPNN units' receptive fields are defined as contrast edge detectors. As in Paper V the stimuli used during training are randomly positioned contrast edges. The end result is an overlapped circuitry that comprises units located in several hypercolumn-modules and operates as contour integrators. Such a network can efficiently reinforce relatively weak and noisy input from LGN (Paper III–V). Units along a contrast edge are facilitated or inhibited by their neighbors depending on differences in orientation preferences as well as spatial phases. Yet another effect of response facilitation is to sharpen the orientation selectivity of the units (Section 5.2).

5.4 Summary of the Papers

5.4.1 Paper I

In this paper it has been shown that phenomena like spike and burst synchronization are possible to simulate with a biologically detailed network of integrate-and-fire neurons. One of the most important conclusions of this paper is that high precision spike synchronization (<10 ms) is possible to achieve with a constant current input. However, when the strength of the current input is above a certain level neurons display repetitive bursting. This behavior enhances population oscillation but destroys high precision spike synchronization.

The network behavior is relatively independent of the input type. It is further assumed that more pronounced spike synchronization is possible to achieved for the one bar stimulus simulation, if the stimulus configuration is different.

Long-range horizontal connections play an important functional role for synchronization. Even with very few connections it is possible to spike synchronize neurons situated in minicolumns 2.5 mm from each other. During the simulations there have been at most two connections between neurons in orientation minicolumn one and six. These two orientation minicolumns are positioned on the extremes of the network.

Spike synchronization is slightly tighter between neurons spatially closer to each other. This finding is detectable when much larger networks are simulated (up to 8 mm between orientation minicolumns on the extremes).

This paper was presented at the ICANN – International Conference on Artificial Neural Conference in Vienna, August 2001.

5.4.2 Paper II

In this paper we derived and presented a model of a cortical hypercolumn from the BCPNN architecture. This model replicates important experimental findings related to the orientation tuning mechanism in the V1. Properties of the orientation selective neurons in the V1, such as contrast-invariance of orientation tuning and response saturation (followed by normalization) are demonstrated by computer simulations.

One important assumption was made on the LGN input to the network model. It was assumed that the LGN input increases in a linear fashion to linear increase in stimulus contrast, since the LGN input is mainly from the P-cells (see Section 2.4.4). Based on this assumption, it is shown that the response saturation (followed by normalization) behavior of the modeled neurons in the output layer is possible to explain by the local horizontal connections inside the abstract hypercolumn model.

The divisive inhibition of the excitatory cells in the output layer (by inhibitory cells) results in sharpening of the orientation tuning curves and normalization of their activities. The inhibitory cells represent a pool of large basket cells with a mixture of preferred orientations. It is assumed that these large basket cells are distributed homogenously within the layers of area 17. The activity level of the large basket cells is a function of the excitatory cells in the input layer and the LGN input. Thus, it samples the total activity inside the hypercolumn.

This paper was presented at the 9th ICONIP – International Conference on Neural Information Systems in Singapore, November 2002.

5.4.3 Paper III

A patch of layer 4 of cat area 17 has been modeled. This developmental network model is based on the modular structure of the neocortex. The BCPNN incremental learning rule develops the connections between the units. The correlation-based network captures some of the known properties of area 17 of cats, such as dense local and sparse distal connectivity.

The network has two different types of interneurons. Large basket cells are responsible for keeping the total activity within a hypercolumn constant. The second group of interneurons, the inhibitory simple cells, mediate local and distal inhibition through targeting excitatory cells that are located in their close

surroundings and have opposite absolute and relative spatial phase (relative to the interneuron).

Excitatory local connections are biased towards the iso-orientation domain. However, excitatory long-range horizontal connections target all orientation domains in a balanced manner, thus there is a strong crosstalk between all orientation domains. Note however that some of the targets of the long-range horizontal connections are excitatory cells, whereas some are inhibitory simple cells, since the network is correlation-based.

The excitatory long-range horizontal connections are mildly elongated along the orientation axis, most likely as a result of the stimulus configuration. During the learning mode the stimuli are contrast edges. In contradiction to the layer 2/3, there has not been any report on axial specificity of the layer 4 long-range horizontal connections.

Nevertheless, we believe that the network behavior supports the existence of elongated summation pools in visual cortex, and gives a simple explanation for how it might be carried out within area 17.

This paper was presented at the Annual Computational Neuroscience Meeting 2004, Baltimore.

5.4.4 Paper IV

A quantitative assessment of the layer 4 and layer 2/3 local and long-range horizontal connections based on two separate models is presented. The results show that layer 4 long-range horizontal connections target all orientation domains in a balanced manner, whereas layer 4 local connections are biased towards the iso-orientation domain.

The layer 2/3 network is significantly different. Both local and long-range horizontal connections of the layer 2/3 network are biased towards the iso-orientation domains. We hypothesize that the patchy layout of the long-range connections is a consequence of excitatory long-range connections targeting mainly other excitatory cells located in distal iso-orientation domains.

Furthermore, the fall-off with distance results in dense local and sparse distal connectivity for both networks. Preliminary results indicate that the layer 2/3 network, like the layer 4 network, can detect low contrast stimulus.

This paper was presented at the special session on ‘Biologically Inspired Computer Vision’, at 2nd CIRAS – Computational Intelligence, Robotics and Autonomous Systems in Singapore, December 2003.

5.4.5 Paper V

In this paper a laminar V1 model consisting of layers 4 and 2/3 is presented. The model is based on the BCPNN architecture, and hence is in line with the modular

structure of the neocortex. The model addresses development as well as functional roles of the horizontal connections that are found in these two cortical layers.

Long-range horizontal connections in the layer 4 network are equally distributed between orientation domains, whereas in the layer 2/3 network these connections prefer the iso-orientation domains. Layer 2/3 patchy connections are a result of lack of anti-correlated activity in this layer. In both layers local connections are biased towards the iso-orientation domain though. Anti-correlation between anti-phase unit pairs induces strongest inhibition in the layer 4, thus iso-orientation inhibition is stronger than cross-orientation inhibition.

Layer 4 network exhibits sharp orientation selectivity despite poorly tuned LGN input. Sharp orientation selectivity is achieved through (i) control of the total activity of the modeled hypercolumns by normalization inhibition, and (ii) providing layer 4 units with information from a larger region, through excitatory long-range connections. The role of inhibition, which operates locally, is to control excitation. This laminar V1 model addresses configuration-specific facilitation phenomena as well. Elongated layer 2/3 summation pools demonstrate that collinearly configured stimuli are easier to detect than orthogonally (or circularly) configured stimuli.

This paper is a technical report.

6 General Conclusions

This thesis work presents a canonical model of neocortical area V1. The intention with this model is to address computations that are carried out within this structure. The V1 of cat and other species, such as monkey and rodent, is relatively well documented, and hence have been the principal model for studying structure as well as function of cortical systems. The structural similarities between various cortical areas, which are primarily manifested by the modular and laminar organization of the neocortex, suggest that studies of V1 might contribute to a general understanding of other cortical systems as well.

To organize the enormous material that is available on this structure a top-down view has been taken. However, such an approach does not necessarily imply that the developed models are biologically plausible. Since the intention of this thesis work is to uncover the computations that are carried out within the V1; the developed models need to be faithful to the relevant aspects of known physiology and anatomy. Thus, a top-down view is combined with a bottom-up manner of implementing the models. This has helped to construct biologically plausible models, which are also simple enough to allow conceptual modeling and reasoning.

The main contribution of this thesis work is the mapping of the hypercolumn-module (Paper II) to local circuitry of layers 4 and 2/3 (Papers III–V). The intention was to construct these two cortical layers by simply tiling these modules to cover a two-dimensional space, and address the development of the horizontal connections. The quantitative assessments of the horizontal connections within these modeled layers have been presented in Papers IV and V. These results reveal that the distributions of the connections within these two modeled cortical layers are similar to those in V1.

Local horizontal connections are dense indicating high degree of correlation (or anti-correlation), in contrast to their long-range counterparts. Layer 4 local horizontal connections target mainly the iso-orientation domain, whereas long-range horizontal connections target all orientation domains in a balanced manner. However, both local and long-range horizontal connections of layer 2/3 are biased towards the iso-orientation domains. In this layer connections are axially specific

along the orientation axis of the units. Furthermore, in both layers inhibition operates within a hypercolumn-module. This is in line with what is found in the V1, i.e. inhibition is mainly local, whereas excitation extends far beyond the inhibitory network. Observe also that neither excitation nor inhibition dominates the network.

The simulations demonstrate that this connectivity pattern can address several response properties of the neurons, such as orientation selectivity, response saturation (followed by normalization), contrast-invariance of orientation tuning, and cross-orientation inhibition (Paper II–V). The proposed model is unique in that it addresses emergence of these phenomena within the framework of a conceptual model, which is in line with the known anatomy and physiology of the neocortex.

The function of the long-range horizontal connections has been investigated by addressing the configuration-specific facilitation phenomena (Papers III and V). Simulation results suggest that the visibility of Gabor patch stimuli is improved due to their elongation (along one direction). Not surprisingly the degree of facilitation, and hence improved visibility, is closely related to the direction of elongation, since summation pools found in the layer 2/3 network are axially specific along the orientation axis of the units. Observe that anisotropic inputs from this network are sufficient for explaining configuration-specific facilitation phenomena. Note further that layer 4 units receive input from a circular region, and hence cannot take part in this process.

Response facilitation requires robust communication between neurons located several millimeters from each other. Spike and burst synchronization might be responsible for this. In Paper I it is shown that groups of neurons (organized into orientation minicolumns) could indeed facilitate each other, through spike and burst synchronization, despite the fact that they are located several millimeters from each other. Furthermore, the simulations showed that these results are possible to achieve with low connectivity.

During this thesis work several additional issues have emerged. These issues are closely related to the thesis subject. One example is on the development of the thalamocortical circuitry. It would be interesting to see if this circuitry can develop simultaneously with the horizontal connections, within the framework provided by the BCPNN. One of the fundamental questions here is if the final network will resemble the properties of the orientation map, or if top-down control mechanisms are need, e.g. to achieve the repetitive pattern of the orientation map. Yet another interesting issue is related to the variety of RF types that exists within layer 4. Quantitative assessments of such complex networks might give further valuable insight to the distribution of connections within this layer.

Taken together, this thesis work has shown that network models consisting of abstract hypercolumn models can explain several fundamental response properties of neurons. When simplicity is combined with biological plausibility the network models can give valuable insight into the structure as well as function of cortical circuitry.

Bibliography

Adorján P, Levitt JB, Lund JS, Obermayer K (1999) A model for the intracorticla origin of orientation preference and tuning in macaque striate cortex. Vis. Neurosci. **16**:303–318.

Ahmet B, Anderson JC, Douglas RJ, Martin KA, Nelson JC (1994) Polyneural innervation of spiny stellate neurons in cat visual cortex. J. Comp. Neurol. **341**:39–49.

Albrecht DG, Hamilton DB (1982) Striate cortex of monkey and cat: contrast response function. J. Neurophysiol. **48**:217–237.

Albrecht DG, Geisler WS (1991) Motion selectivity and the contrast-response function of simple cells in the visual cortex. Visual Neurosci. **7**:531–546.

Albrecht DG, Geisler WS, Frazor RA, Crane AM (2001) Visual cortex neurons of monkeys and cats: temporal dynamics of the contrast response function. J. Neurophysiol. **88**:888–913.

Alonso J-M, Martinez LM (1998) Functional connectivity between simple cells and complex cells in cat striate cortex. Nat. Neurosci. **1**:395–403.

Alonso J-M, Usrey WM, Reid RC (1996) Precisely correlated firing in cells of the lateral geniculate nucleus. Nature **383**:815–819.

Amir Y, Harel M, Malach R (1993) Cortical hierarchy reflected in the organization of intrinsic connections in macaque monkey visual cortex. J. Comp. Neurol. **334**:19–46.

Baxter WT, Dow BM (1989) Horizontal organization of orientation-sensitive cells in primate visual cortex. Biol. Cybern. **61**:171–182.

Bayes T (1958) An essay towards solving a problem in the doctrine of changes. Biometrica **45**:296–315 (reprint of original article in Phil. Trans. R. Soc. **53**:370–418, 1763).

Ben-Yishai R, Bar-Or RL, Sompolinsky H (1995) Theory of orientation tuning in visual cortex. Proc. Natl. Acad. Sci. USA **92**:3844–3848.

Ben-Yishai R, Hansel D, Sompolinsky H (1997) Traveling waves and the processing of weakly tuned inputs in a cortical network module. J. Comput. Neurosci. **4**:57–77.

Blasdel GG (1992) Orientation selectivity, preference, and continuity in monkey striate cortex. J. Neurosci. **12**:3139–3161.

Blasdel GG, Fitzpatrick D. 1984. Physiological organization of layer 4 in macaque striate cortex. J. Neurosci. **4**:880–895.

Blasdel GG, Salama G (1986) Voltage-sensitive dye reveal a modular organization in monkey striate cortex. Nature **321**:579–585.

Bonds AB (1989) The role of inhibition in the specification of orientation selectivity of cells in the cat striate cortex. Visual Neurosci. **2**:41–55.

Bosking WH, Zhang Y, Schofield B, Fitzpatrick D (1997) Orientation selectivity and the arrangement of horizontal connections in tree shrew striate cortex. J. Neurosci. **17**:2112–2127.

Boycott BB, Wässle H (1974) The morphological types of ganglion cells of the domestic cat's retina. J. Physiol. **240**:397–419.

Braitenberg V, Braitenberg C (1979) Geometry of orientation columns in the visual cortex. Biol. Cybern. **33**:179–186.

Braitenberg V, Schüz A (1998) Cortex: statistics and geometry of neuronal connectivity. Springer.

Buxhoeveden DP, Casanova MF (2002) The minicolumn hypothesis in neuroscience. Brain **125**:935–951.

Campbell FW, Cooper GF, Enroth-Cyrell C (1969) The spatial selectivity of the visual cells of the cat J. Physiol. **203**:223–235.

Carandini M, Heeger DJ (1994) Summation and division by neurons in primate visual cortex. Science **264**:1333–1336.

Carandini M, Heeger DJ, Movshon JA (1997) Linearity and normalization in simple cells of the macaque primary visual cortex. J. Neurosci. **17**:8621–8644.

Chapman B, Stryker MP (1993) Development of orientation selectivity in ferret visual cortex and effects of deprivation. J. Neurosci. **13**:5251–5262.

Chisum HJ, Mooser F, Fitzpatrick D (2003) Emergent properties of layer 2/3 neurons reflect the collinear arrangement of horizontal connections in tree shrew visual cortex. J. Neurosci. **23**:2947–2960.

Chung S, Ferster D (1998) Strength and orientation tuning of the thalamic input to simple cells revealed by electrically evoked cortical suppression. Neuron **20**:1177–1189.

Coenen AML, Vendrik AJH (1972) Determination of the transfer ratio of cat's geniculate neurons through quasi-intracellular recordings and the relation with the level of alertness. Exp. Brain Res. **14**:227–242.

Connors BW, Bear MF, Paradiso MA (2002) Neuroscience: exploring the brain. Lippincott Williams and Wilkins Publishers.

Das A (1996) Orientation in visual cortex: a simple mechanism emerges. Neuron **16**:447–480.

Dean AF (1981) The relationship between response amplitude and contrast for cat striate cortical neurons. J. Physiol. **318**:413–427.

DeAngelis GC, Geoffrey MG, Ohwaza I, Freeman RD (1999) Functional micro-organization of primary visual cortex: receptive field analysis of nearby neurons. J. Neurosci. **19**:4046–4064.

Derrington AM, Fuchs AF (1979) Spatial and temporal properties of X and Y cells in the cat lateral geniculate nucleus. J. Physiol. **293**:347–364.

Derrington AM, Lennie P (1984) Spatial and temporal contrast sensivities of neurons in lateral geniculate nucleus of macaque. J. Physiol. (Lond) **357**:219–240.

Dow BM (2002) Orientation and color columns in monkey visual cortex. Cerebral Cortex **12**:1005–1015.

Dreher B, Fukada Y, Rodieck RW (1976) Identification, classification and anatomical segregation of cells with X-like and Y-like properties in the lateral geniculate nucleus of old-world primates. J. Physiol. (Lond) **258**:433–452.

Durack JC, Katz LC (1996) Development of horizontal projections in layer 2/3 of ferret visual cortex. Cerebral Cortex **6**:178–183.

Engel AK, König P, Kreiter AK, Singer W (1991) Inter-hemispheric synchronization of oscillatory neuronal responses in cat visual cortex. Science **252**:1177–1179.

Engel AK, Roelfsema PR, Fries P, Brecht M, Singer W (1997) Role of the temporal domain for response selection and perceptual binding. Cerebral Cortex **7**:571–582.

Ernst UA, Mandon S, Pawelzik KR, Kreiter AK (2004) How ideal do macaque monkeys integrate contours? Neurocomp. **58–60**:971–977.

Erwin E, Obermayer K, Schulten K (1995) Models of orientation and ocular dominance columns in the visual cortex: a critical comparison. Neural Comput. **7**:425–468.

Everson RM, Prashanth AK, Gabbay M, Knight BW, Sirovich L, Kaplan E (1998) Representation of spatial frequency and orientation in the visual cortex. Vision Res. **11**:251–259.

Favorov OV, Diamond ME (1990) Demonstration of discrete place-defined columns-segregates-in the cat SI. J. Comp. Neurol. **298**:97–112.

Ferster D (1988) Spatially opponent excitation and inhibition in simple cells of the cat visual cortex. J. Neurosci. **8**:1172–1180.

Ferster D, Chung S, Wheat H (1996) Orientation selectivity of thalamic input to simple cells of cat visual cortex. Nature **380**:249–252.

Ferster D, Miller KD (2000) Neural mechanisms of orientation selectivity in the visual cortex. Annual Reviews of Neurosci. **23**:441–471.

Fitzpatrick D (1996) The functional organization of local circuits in visual cortex: insights from the study of tree shrew striate cortex. Cerebral Cortex **6**:329–341.

Friedman-Hill S, Maldonado PE, Gray CM (2000) Dynamics of striate cortical activity in the alert macaque: I. incidence and stimulus-dependence of gamma-band neuronal oscillations. Cerebral Cortex **10**:1105–1116.

Gabbott PLA, Somogyi P (1986) Quantitative distribution of GABA-immunoreactive neurons in the visual cortex (area 17) of the cat. Exp. Brain Res. **61**:323–331.

Gil Z, Connors BW, Amitai Y (1999) Efficacy of thalamocortical and intracortical synaptic connections: quanta, innervation, and reliability. Neuron **23**:385–397.

Gilbert CD, Wiesel TN (1983) Clustered intrinsic connections in cat visual cortex. J. Neurosci. **3**:1116–1133.

Gilbert CD, Wiesel TN (1989) Columnar specificity of intrinsic horizontal connections and corticocortical connections in cat visual cortex. J. Neurosci. **9**:2432–2442.

Good IJ (1950) Probability and the weighing of evidence. London: Charles Griffin.

Gotz KG (1987) Do "d-blob" and "l-blob" hypercolumns tessellate the monkey visual cortex? Biol. Cybern. **56**:107–109.

Gotz KG (1988) Cortical templates for the self-organization of orientation-specific d- and l-hypercolumns in monkey and cats. Biol. Cybern. **58**:213–223.

Gray CM, Koenig P, Engel AK, Singer W (1989) Oscillatory responses in cat visual cortex exhibit inter-columnar synchronization which reflects global stimulus properties. Nature **338**:334–337.

Gray CM, Singer W (1989) Stimulus-specific neuronal oscillations in orientation columns of cat visual cortex. **86**:1698–1702.

Grossberg S, Raizada RDS (2000) Contrast-sensitive perceptual grouping and object-based attention in the laminar circuits of primary visual cortex. Vision Res. **40**:1413–1432.

Haig AR, Gordon E, Wright JJ, Meares RA, Bahramali H (2000) Synchronous cortical gamma-band activity in task-relevant cognition. Neuroreport **11**:669–675.

Hansel D, Sompolinsky H (1996) Chaos and synchrony in a model of a hypercolumn in visual cortex. J. Comput. Neurosci. **3**:7–34.

Hawken M, Parker AJ (1984) Contrast sensitivity and orientation selectivity in lamina IV of the striate cortex of old world monkeys. Exp. Brain Res. **54**:367–372.

Hebb DO (1949) The organization of behavior. New York: Wiley.

Heeger DJ (1992) Normalization of cell responses in cat striate cortex. Visual Neuroscience **9**:181–197.

Heeger DJ, Simoncelli EP, Movshon JA (1996) Computational models of cortical visual processing. Proc. Natl. Acad. Sci. USA **93**:623–627.

Hellwig B (2000) A quantitative analysis of the local connectivity between pyramidal neurons in layer 2/3 of the rat visual cortex. Biol. Cybern. **82**:111–121.

Hendrickson AE, Hunt SP, Wu J-Y (1981) Immunocytochemical localization of glutamic acid decarboxylase in monkey striate cortex. Nature **292**:605–607.

Hirch JA, Alonso J-M, Pillai C, Pierre C (2000) Simple and complex inhibitory cells in layer 4 of cat visual cortex. Soc. Neurosci. Abstr. **26**:1083.

Holst A (1997) The use of a Bayesian neural network model for classification tasks. PhD Thesis Department of Numerical Analysis and Computing Science, Royal Institute of Science, Stockholm, Sweden, TRITA-NA-P9708.

Horton JC (1984) Cytochrome oxidase patches: a new cytoarchitectonic feature of monkey visual cortex. Phil. Trans. R. Soc. Lond. B **304**:199–253.

Horton JC, Hubel DH (1981) Regular patchy distribution of cytochrome oxidase staining in primary visual cortex of macaque monkey. Nature **292**:762–764.

Hubel DH (1988) Eye, brain, and vision. New York: WH Freeman.

Hubel DH, Wiesel TN (1962) Receptive fields, binocular interaction and functional architecture in the cat's visual cortex. J. Physiol. **160**:106–154.

Hubel DH, Wiesel TN (1972) Laminar and columnar distribution of geniculo-cortical fibers in the macaque monkey. J. Comp. Neurol. **146**:421–450.

Hubel DH, Wiesel TN (1977) The functional architecture of the macaque visual cortex. The Ferrier lecture. Proc. Royal. Soc. B **198**:1–59.

Hübener M, Schulze S, Bonhoeffer T (1996) Cytochrome-oxidase blobs in cat visual cortex coincide with low spatial frequency columns. Soc. Neurosci. Abstr. **22**:951.

Humphrey AL, Norton TT (1980) Topographic organization of the orientation column system in the striate cortex of the tree shrew (Tupaia glis). I. Microelectrode recording. J. Comp. Neurol. **192**:531–47.

Issa NP, Trepel C, Stryker MP (2000) Spatial frequency maps in cat visual cortex. J. Neurosci. **20**:8504–8514.

Kandel ER, Schwartz JH, Jessell TM (eds.) (2000) Principals of neural science. Graham-Hill.

Kastner S, Nothdurft H-C, Pigarev IN (1997) Neuronal correlates of pop-out in cat striate cortex. Vision Res. **37**:371–376.

Katz LC (1987) Local circuitry of identified projection neurons in cat visual cortex. J. Neurosci. **7**:1223–1249.

Kayser AS, Miller KD (2002) Opponent inhibition: a development model of layer 4 of the neocortical circuit. Neuron **33**:131–142.

Kisvárday ZF, Martin KAC, Freund TF, Magloczky Z, Whitteridge D, Somogyi P (1986) Synaptic targets of HRP-filled layer III pyramidal cells in the cat striate cortex. Exp. Brain Res. **64**:541–552.

Kisvárday ZF, Martin KAC, Friedlander MJ, Somogyi P (1987) Evidence for interlaminar inhibitory circuits in the striate cortex of cat J. Comp. Neurol. **260**:1–19.

Kisvárday ZF, Tóth E, Rausch M, Eysel UT (1997) Orientation-specific relationship between populations of excitatory and inhibitory lateral connections in the visual cortex of the cat. Cerebral Cortex **7**:605–618.

Koffka K (1935) Principals of Gestalt psychology. New York: Harcourt, Brace and World.

Köhler W (1930) Gestalt psychology. London: Bell and Sons.

König P, Engel AK, Löwel S, Singer W (1993) Squint affects synchronization of oscillatory responses in cat visual cortex. Eur. J. Neurosci. **5**:501–508.

Kreiter AK, Singer W (1996) Stimulus-dependent synchronization of beuronal responses in the visual cortex of awake macaque monkey. J. Neurosci. **16**:2381–2396.

Krimer LS, Goldman-Rakic PS (2001) Prefrontal mirocircuits: membrane properties and excitatory input of local, medium, wide arbour interneurons. J. Neurosci. **21**:3788–3796.

Kuffler SW (1953) Discharge patterns and functional organization of mammalian retina. J. Neurophysiol **16**:37–68.

Lansner A, Ekeberg Ö (1987) An associative network solving the “4-bit adder problem”. In: Caudill M, Butler C (editors). IEEE First International Conference on Neural Networks. Pp II–549.

Lansner A, Ekeberg Ö (1989) A one-layer feedback artificial neural network with a bayesian learning rule. Int. J. Neural Syst. **1**:77–78.

Lansner A, Holst A (1996) A higher order bayesian neural network with spiking units. Int. J. Neural Syst. **7**:115–128.

Li Z (1998) A neural model of contour integration in the primary visual cortex. Neural Computation. **10**:903–940.

Löwel S, Singer W (1992) Selection of intrinsic horizontal connections in the visual cortex by correlated neuronal activity. Science **255**:209–212.

McLaughin D, Shapley R, Shelley M, Wielaard DJ (2000) A neuronal network model of macaque primary visual cortex (V1): orientation selectivity and dynamics in the input layer 4Cα. Proc. Natl. Acad. Sci. USA **97**:8087–8092.

Maffei L, Fiorentini A (1973) The visual cortex as a spatial frequency analyser. Vis. Res. **13**:1255–1267.

Maffei L, Fiorentini A, Bisti S (1973) Neural correlate of perceptual adaptation to gratings. Science **182**:1036–1038.

Malach R, Amir Y, Harel M, Grinvald A (1993) Relationship between intrinsic connections and functional architecture revealed by optical imagining and in vivo targeted biocytin injections in primate striate cortex. Proc. Natl. Acad. Sci. USA **90**:10496–10473.

Maldonado PE, Friedman-Hill S, Gray CM (2000) Dynamics of striate cortical activity in the alert macaque: II. Fast time scale synchronization. Cerebral Cortex **10**:1117–1131.

Martin KAC (2002) Microcircuits in visual cortex. Current Opinion in Neurobiology **12**:418–425.

Meyer G (1983) Axonal patterns and topography of short-axon neurons in visual areas 17, 18 and 19 of the cat. J. Comp. Neurol. **220**:405–438.

Meyer G (1987) Forms and spatial arrangement of neurons in the primary motor cortex of man. J. Comp. Neurosci. **262**:402–428.

Morrone MC, Burr DC, Maffei L (1982) Functional implications of cross-orientation inhibition of cortical visual cells. I. Neurophysiological evidence. Proc. R. Soc London Ser. B **216**:335–354.

Mountcastle VB (1957) Modality and topographic properties of single neurons of cat's somatic sensory cortex. J. Neurophysiol. **20**:408–438.

Mountcastle VB (1978) An organizing principle for cerebral function. In: Edelman GM, Mountcastle VB (editors). The mindful brain. MIT Press 7–50.

Mountcastle VB (1997) The columnar organization of the neocortex. Brain **120**:701–722.

Movshon JA, Hawken MJ, Kiorpes L, Skoczenski AM, Tang C, O'Keefe LP (1994) Visual noise masking in macaque LGN neurons. Invest. Ophthalmol. Vis. Sci. [Suppl] **35**:1662.

Murphy PC, Sillito AM (1986) Continuity of orientation columns between superficial and deep laminea of cat primary visual cortex. J. Physiol. **381**:95–110.

Obermayer K, Blasdel GG (1993) Geometry of orientation and ocular dominance columns in monkey striate cortex. J. Neurosci. **13**:4114–4129.

O'Leary JL (1941) The structure of area striata of cat. J. Comp. Neurol. **75**:131–164.

Palmer SE (1999) Vision science. MIT Press. pp 726.

Payne BR, Peters A (2002) The concept of cat primary visual cortex. in: BR Payne, A Peters (ed.). the cat primary visual cortex. Academic Press.

Pei X, Vidyasagar TR, Volgushev M, Creutzfeldt OD (1994) Receptive field analysis and orientation selectivity of postsynaptic potentials of simple cells in cat visual cortex. J. Neurosci. **14**:7130–140.

Peters A, Sethares C (1996) Myelinated axons and the pyramidal cell modules in monkey visual cortex. J. Comp. Neurol. **365**:232–255.

Peters A, Yilmaz E (1993) Neuronal organization of area 17 of cat visual cortex. Cerebral Cortex **3**:49–68.

Polat U, Norcia AM (1996) Neurophysiological evidence for contrast dependent long-range facilitation and suppression in the human visual cortex. Vision Res. **36**:2099–2109.

Polat U, Norcia AM (1998) Elongated physiological summation pools in the human visual cortex. Vision Research **38**:3735–3741.

Polat U, Sagi D (1993) Lateral interactions between spatial channels: Suppression and facilitation revealed by masking experiments. Vision Res. **33**:993–999.

Powell TPS, Mountcastle VB (1959) Some aspects of the functional organization of the cortex of the postcentral gyrus of the monkey: a correlation of findings obtained in a single unit analysis with cytoarchitecture. Bull Johns Hopkins Hosp. **105**:133–162.

Purves D, Augustine GJ, Fitzpatrick D, Katz LC, LaMantia A-S, McNamara JO (eds.) (1997) Neuroscience. Sunauer Associates Inc. pp 1–34.

Reid RC, Alonso JM (1995) Specificity of monosynaptic connections from thalamus to visual cortex. Nature **378**:281–284.

Rockland KS (1985) Anatomical organization of primary visual cortex (area 17) in the ferret. J. Comp. Neurol. **241**:225–236.

Rockland KS, Lund JS (1982) Widespread periodic intrinsic connections in the tree shrew visual cortex. Science **215**:1532–1534.

Rockland KS, Lund JS (1983) Intrinsic laminar lattice connections in primate visual cortex. J. Comp. Neurol. **216**:303–318.

Sandberg A (2003) Bayesian attractor neural networks of memory. PhD Thesis Department of Numerical Analysis and Computing Science, Royal Institute of Science, Stockholm, Sweden, TRITA-NA-0310.

Sandberg A, Lansner A, Petersson FM, Ekeberg Ö (2002) A Bayesian attractor network with incremental learning. Network: Computing in Neural Systems. **13**:179–194.

Schmidt KE, Kim D-S, Singer W, Bonhoeffer T, Löwel S (1997) Functional specificity of long-range intrinsic and interhemisphic connections in the visual cortex of strabismic Cats. J. Neurosci. **17**:5480–5492.

Schmidt KE, Löwel S (2002) Long-range intristic connections in cat primary visual cortex. in: Payne BR, Peters A (ed.). The cat primary visual cortex. Academic Press.

Sclar G, Freeman RD (1982) Orientation selectivity in the cat's striate cortex is invariant with stimulus contrast. Exp. Brain Res. **46**:457–461.

Shandlen MN, Movshon JA (1999) Synchrony unbound: a critical evaluation of the temporal binding hypothesis. Neuron **24**:67–77.

Sherman SM, Schumer RA, Movshon JA (1984) Functional cell classes in the macaque's LGN. Soc. Neurosci. Abstr. **10**:296.

Shoham D, Hübener M, Schulze S, Grinvald A, Bonhoeffer T (1997) Spatio-temporal frequency domains and their relation to cytochrome oxidase staining in cat visual cortex. Nature **385**:529–533.

Singer W (1993) Synchronization of cortical activity and its putative role in information processing and learning. Annu. Rev. Physiol. **55:**349–374.

Singer W (1999) Neuronal synchrony: a versatile code for the definition of relations? Neuron **24**:49–65.

Singer W, Gray CM (1995) Visual feature integration and the temporal correlation hypothesis. Annual Review of Neurosci. **18**:555–586.

Skottun BC, Bradley A, Sclar G, Ohzawa I, Freeman RD (1987) The effects of contrast on visual orientation and spatial frequency discrimination: a comparison of single cells and behaviour. J. Neurophysiology **57**:773–786.

Solomon JA, Watson AB, Morgan MJ (1999) Transducer model produces facilitation from opposite-sign flanks. Vision Res. **39**:987–992.

Solomon JA, Morgan MJ (2000) Facilitation from collinear flanks is cancelled by non-collinear flanks. Vision Res. **40**:279–286.

Somers D, Dragoi V, Sur M (2002) Orientation selectivity and its modulation by local and long-range connections in visual cortex. in: Payne BR, Peters A (ed.). The cat primary visual cortex. Academic Press.

Somers D, Nelson SB, Sur M (1995) An emergent model of orientation selectivity in cat visual cortical simple cells. J. Neurosci. **15**:5448–5465.

Somers D, Todorov EV, Siapas AG, Toth LJ, Kim D-S, Sru M (1998) A local circuit approach to understand integration of long-range inputs in primary visual cortex. Cerebral Cortex **8**:204–217.

Sompolinsky H, Shapley R (1997) New percpectives on the mechanisms for orientation selectivity. Current Opinion in Neurobiology **7**:514–522.

Steriade M, McCormic DA, Sejnowski TJ (1993) Thalamocortical oscilation in the sleeping and aroused brain. Science **262**:679–685.

Stevens CF, Zador AM (1998) Input synchrony and the irregular firing of cortical neurons. Nat. Neurosci. **1**:210–217.

Swindale NV (1982) A model for the formation of orientation columns. Proc R Soc Lond B **215**:211–230.

Tootell RBH, Silverman MS, De Valois RL (1981) Spatial frequency columns in primary visual cortex. Science **214**:813–815.

Troyer TW, Krukowski AE, Miller KD (1998) Contrast-invariant orientation tuning in cat visual cortex: thalamocortical input tuning and correlation-based intracortical connectivity. J. Neurosci. **18**:5908–5927.

Troyer TW, Krukowski AE, Miller KD (2002) LGN input to simple cells and contrast-invariant orientation tuning: an analysis. J. Neurophysiol. **87**:2741–2752.

Tömböl T (1978) Comparative data on the Golgi architecture of interneurons of different cortical areas in cat and rabbit. in: Brazier MAB, Petsche H (eds.) Architectonics of the Cerebral Cortex. pp. 59–76. New York. Raven Press.

Usrey WM, Reid RC (1999) Synchronous activity in the visual system. Annu. Rev. Physiol. **61**:435–456.

Wielaard DJ, Shelley M, McLaughin D, Shapley R (2001) How simple cells are made in a nonlinear network model of the visual cortex. J. Neurosci. **21**:5203–5211.

Williams LR, Thornber KK (2001) Orientation, scale, and discontinuity as emergent properties of illusory contour shape. Neural Computing. **13**:1683–1711.

Wong-Riley MTT (1979) Changes in the visual system of monocularity sutured or enucleated kittens demonstrable with cytochrome oxidase histochemistry. Brain Res. **171**:11–28.

Wässle H, Levick WR, Cleland BG (1975) The distribution of the alpha type of ganglion cells in the cat's retina. J Comp. Neurol. **159**:419–438.

Woolsey CN, Waltz EM (1942) Topical projection of nerve fibres from local regions of the cochlea to the cerebral cortex of the cat. Bull Johns Hopkins Hosp. **71**:315–344.

Yen S-C, Finkel LH (1998) Extraction of perceptually salient contours by striate cortical networks. Vision Res. **38**:719–741.

Yousef T, Bonhoeffer T, Kim D-S, Eysel UT, Tóth E, Kisvárday ZF (1999) Orientation topography of layer 4 lateral networks revealed by optical imagining in cat visual cortex (area 18). E. J. Neurosci. **11**:4291–4308.

Yu C, Klein SA, Levi DM (2002) Facilitation of contrast detection by cross-oriented surround stimuli and its psychophysical mechanisms. J. Vision. **2**:243–255.

7 Paper I – Spike and Burst Synchronization in a Detailed Cortical Network Model with I-F Neurons

Baran Çürüklü[1] and Anders Lansner[2]

[1]Department of Computer Science and Engineering, Mälardalen University, Västerås, SE-72123, Sweden
[2]Department of Numerical Analysis and Computer Science, Royal Institute of Technology, SE-10044 Stockholm, Sweden

In Proceedings of the International Conference on Artificial Neural Networks, pages 1095-1102, Vienna, August 2001, Springer-Verlag.

Abstract

Previous studies have suggested that synchronized firing is a prominent feature of cortical processing. Simplified network models have replicated such phenomena. Here we study to what extent these results are robust when more biological detail is introduced. A biologically plausible network model of layer II/III of tree shrew primary visual cortex with a columnar architecture and realistic values on unit adaptation, connectivity patterns, axonal delays and synaptic strengths was investigated. A drifting grating stimulus provided afferent noisy input. It is demonstrated that under certain conditions, spike and burst synchronized activity between neurons, situated in different minicolumns, may occur.

7.1 Introduction

The synchronized activity of the neurons in visual cortex is believed to contribute to perceptual grouping [14,20,21,22,24,28], see also [23]. It is also assumed that neurons in primary visual cortex have small and overlapping receptive field [8]. We assume also that local cortical connectivity (<300 μm) is dense [7]. Dense local connectivity should help neurons to synchronize their activities. This should mean that neurons with same or contiguous receptive fields are active in presence of stimulus.

Studies have shown evidence for long-range horizontal connections in primary visual cortex [10,13]. Recently Bosking et al. also showed evidence for modular and axial specificity of long-range horizontal connections in layer II/III, and suggested that these connections could help neurons respond to a stimulus, in part because they receive input from other layer II/III neurons [11].

We suggest that long-range horizontal connections that exist in layer II/III together with local connections can be used by the neurons for synchronization of their activities over distances of several millimeters on cortex surface.

This follows the same ideas as earlier network model simulations where horizontal connections [16,17,19,25, 27] and synchronization [15,18,26] play an important role.

7.2 Network Model

We have built a biologically plausible, but sub-sampled, network model. The network consists of neurons situated in six cortical minicolumns (orientation columns), having the same orientation preference. The minicolumns were lined up with a distance of 0.5 mm between two successive ones. We assume that minicolumns are co-linearly positioned in adjacent hyper-columns [8]. The cylinder shaped minicolumns had a height of 300 μm [7] and diameter of 50 μm [8].

Each of the six minicolumns was composed of 12 layer II/III pyramid cells. The neurons were positioned stochastically to fill up the volume of a minicolumn. Connection probability between two neurons was a function of the distance between them [7]. This resulted in a very spread connection probability of 15-80% for neuron pairs, and led to a connectivity of 50-60% between neurons inside a minicolumn [8].

Long-range horizontal connections were defined as connection between two neurons situated in different minicolumns. We computed the connection probability between such pairs of neurons by extrapolating the reported connection probabilities (<500 μm) by Hellwig [7] so that they fitted the findings by Bosking et al. [11]. This resulted in a smooth transition between local and long-range connection probabilities. In average a neuron received 6.2 intra-columnar inputs and 2.1 inter-columnar inputs.

We implemented a leaky Integrate-and-Fire model neuron with noise [1,2]. It was modified to allow adaptation of the membrane time constant [3]. Adaptation is very crucial for the dynamics because of the fact that our network, as many others, does not have inhibitory interneurons. The neuron population was heterogeneous with all values sampled from a uniform distribution with a deviation of 10%.

An axonal diameter of 0.3 μm [8] resulted in a spike propagation velocity of 0.85 m/s [5]. This value together with distances between neurons, and the synaptic delay, resulted in maximum delay inside a minicolumn of approximately 1.36 ms. Maximum delay between neurons situated in two minicolumns was approximately 3.96 ms. This delay corresponds to a distance of approximately 2.52 mm. Maximum values of EPSP:s were in the range of 0.5-2.2 mV for intra-columnar connections and three times those values for inter-columnar connections [4]. The simulation time step was 0.5 ms.

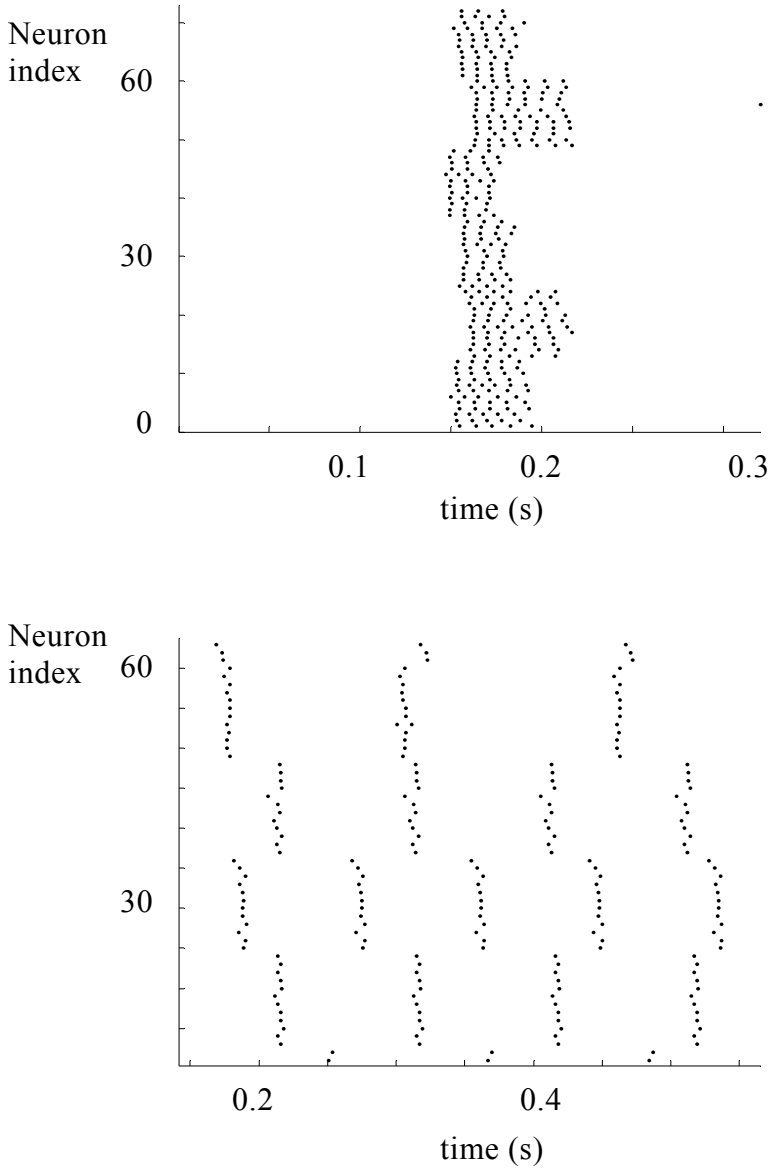

Figure 7.1. Population activity in the absent of long-range horizontal connections. Poisson spike train input (*above*), Constant current input (*below*).

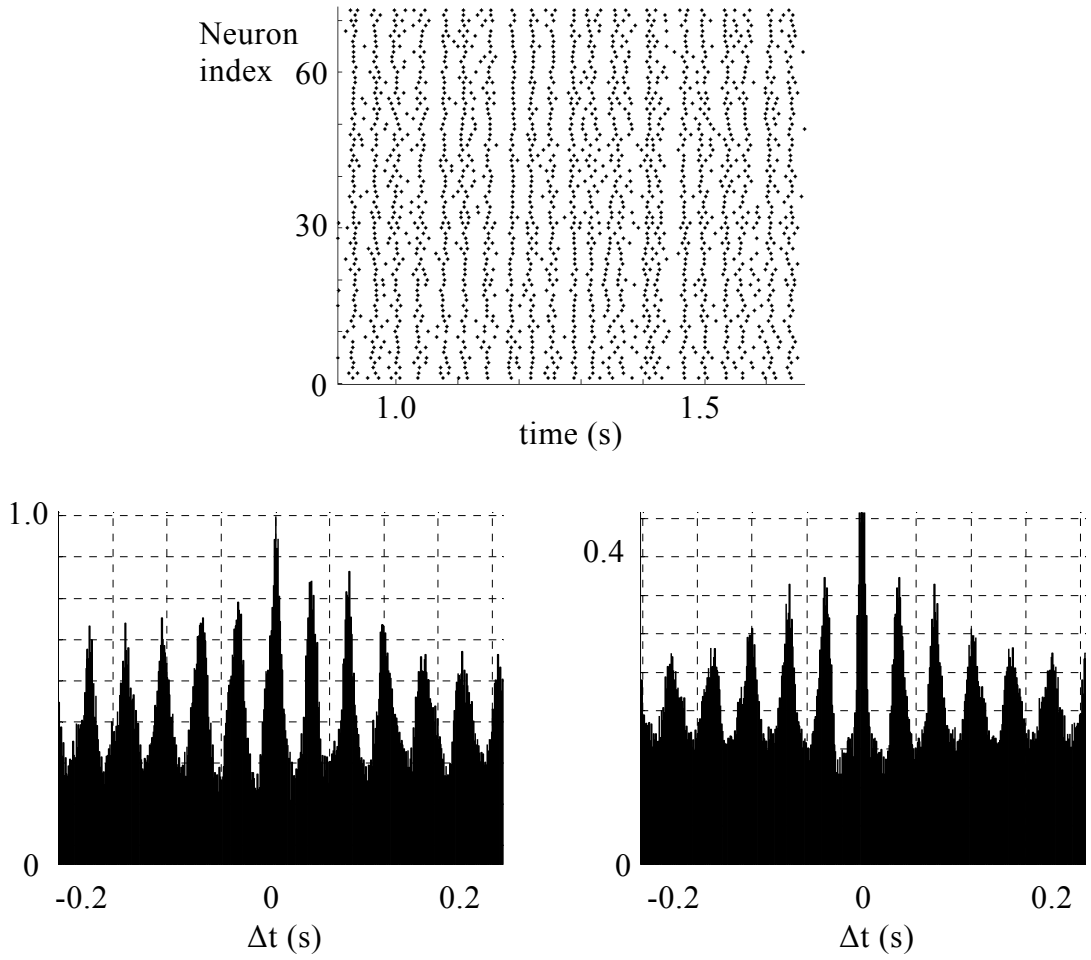

Figure 7.2. Population activity (*top*), and cross-correlation (*bottom left*) between minicolumn one (neurons 1-12) and six (neurons 61-72). Auto-correlation on minicolumn six (*bottom right*).

7.3 Simulation Results

We did three simulations series to demonstrate the influence of long-range horizontal connections on spike and burst synchronization. The initial simulation was done to show that, for our network, synchronization between neurons situated in different minicolumns is not possible, in the absent of the long-range horizontal connections. The network was tested on two different types of inputs. A drifting grating stimulus, modeled as a constant current [6], and a moving bar stimulus, modeled as a Poisson spike train with maximum frequency defined in a Gaussian manner [6]. We saw that in the absence of long-range horizontal connections, the neurons in different minicolumns were not synchronized with each other (Fig. 7.1). Although the response of the network to the two inputs was different, spike

synchronization between neurons inside a minicolumn was present in both cases, especially for constant current input.

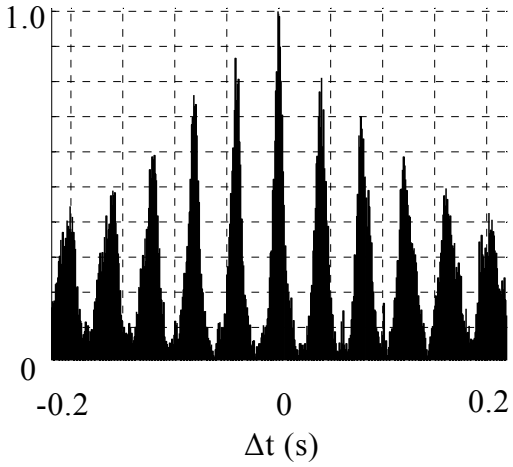

Figure 7.3. Cross-correlation between minicolumn one and six. Neurons in the two middle minicolumns were not receiving current input, and were not spiking throughout the simulation. Oscillation frequency is 25 Hz.

The following two simulations were done with the same two input types as described above, and in the presence of long-range horizontal connections. A drifting grating stimulus (constant current) resulted in both spike and burst synchronization for different values on input currents. In the first part of this simulation all the neurons received constant current. Some of the cells displayed repetitive bursting, for higher values of input current, synaptic weights or more dense connections. Spike synchronization as well as burst synchronization could be seen (Fig. 7.2). It is assume that the repetitive bursting behavior contributes to synchronous oscillation of the population [12]. But this behavior destroyed high precision spike synchronization (Fig. 7.2). In the second part of this simulation we fed only neurons in minicolumns one, two, five and six with constant current to see if neurons in minicolumns one and six still were correlated with each other. Observe that there were no direct connections between minicolumns one and six during this particular simulation, and neurons in the two middle minicolumns were not spiking (not shown here). Spike synchronization between neurons in minicolumn one and six was however present (Fig. 7.3). There was a tendency for a lag of a couple of milliseconds if synaptic weights were low or connections were sparse (not shown here). Observe that the shortest possible delay between two neurons situated in minicolumn one and six was 2.75 ms. Gamma-band oscillation (20-70Hz) could be generated with different values on current input, and we assumed that oscillation was a property of the network.

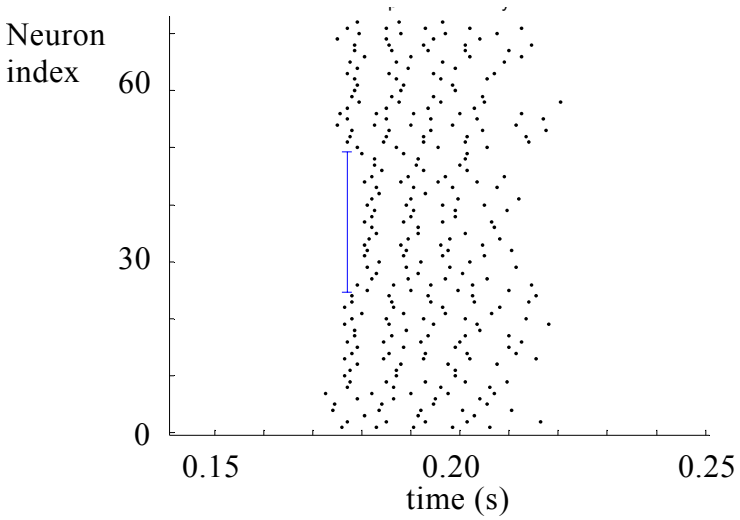

Figure 7.4. Population activity. Notice how minicolumns three and four lagged behind.

The intention of the moving *one* bar-stimulus simulation was to show that, it is possible for neurons to respond to a stimulus that they are not receiving directly. In this simulation all neurons received constant current input. However this input was not sufficient for generating a spike, and corresponded to lowering of the thresholds. Neurons in minicolumns one, two, five and six received uncorrelated Poisson spike trains for a short period of time (80-100 ms) as described above. Poisson spike EPSP:s were in the range of 0.05mV. On average neurons received 65 of these spikes. We saw that neurons in minicolumns three and four were activated by other neurons, with a lag of approximately 4 ms (Figs. 7.4 and 7.5).

High precision spike synchronization was present only during the first two spikes (Fig. 7.4). With lower values on Poisson spike EPSP:s or larger deviation for the Gaussian distribution high precision spike synchronization could be achieved for longer durations (not shown here). However we could see that burst synchronization and oscillation was present (Fig. 7.6).

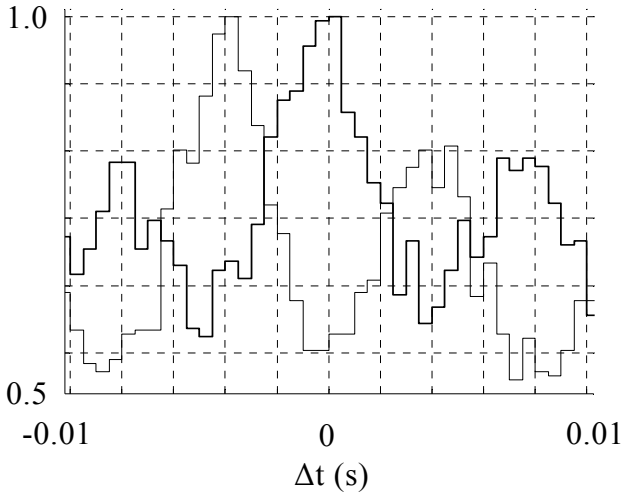

Figure 7.5. Cross-correlation between neurons 1-24 and 49-72 (*thick line*). Cross-correlation between neurons 1-24 and 25-48 (*thin line*) for the trial shown in Fig. 7.3.

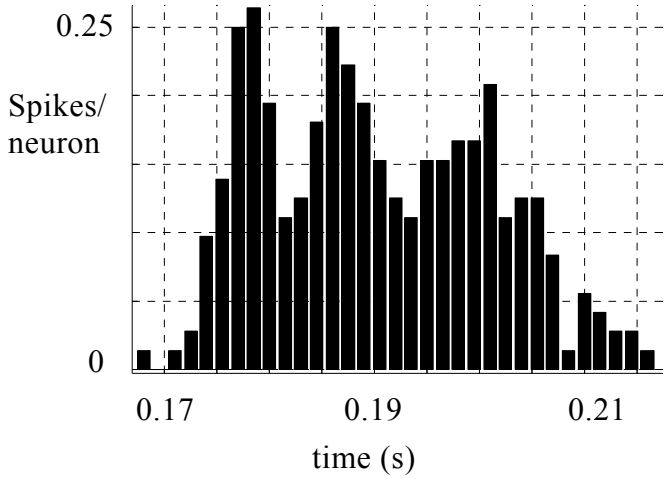

Figure 7.6. Average PSTH of six trials.

7.4 Conclusion

We have shown that phenomena like spike and burst synchronization is possible to simulate with a biologically detailed network of I-F neurons. High precision spike synchronization (<10 ms) was possible to achieve with a constant current input. With increased input some of the neurons displayed repetitive bursting, which helped population oscillation but destroyed high precision spike synchronization.

We saw also that the network behavior was rather independent of the input type. We assume that more pronounced spike synchronization could be achieved for the one bar stimulus simulation, if the stimulus configuration was different, as stated before.

The long-range horizontal connections played an important role for synchronization. Even with very few connections it was possible to spike synchronize neurons situated in minicolumns 2.5 mm from each other. We would like to stress the fact that, on average, there were at maximum two connections between neurons in minicolumn one and six during the simulations. Spike synchronization was tighter between neurons spatially closer to each other and decreased with distance.

Direction of our future research is to make the network model even more realistic. We are currently testing the network model with Poisson neurons. Cortical neurons are known for their irregularity of the interspike interval [3,9]. Preliminary results have shown that oscillation is possible to achieve with our network using Poisson neurons. Our intention is to expand the model with inhibitory neurons as well. We believe that inhibition will contribute to synchronized activity [4].

References

[1] W. Gerstner, Spiking Neurons, in: W. Maass, C. M. Bishop, Pulsed Neural Networks, The MIT Press, 1998.

[2] W. Kistler, W. Gerstner, J.L. van Hemmen, Reduction of Hodgkin-Huxley equations to a threshold model, Neural Comp. 9 (1997) 1069-1100.

[3] C. Koch, Biophysics of Computation: Information Processing in Single Neurons, Oxford University Press, 1999.

[4] E. Fransén, A. Lansner, A model of cortical associative memory based on a horizontal network of connected columns, Network: Comput. Neural Syst. 9 (1998) 235-264.

[5] C. Koch, Ö. Bernander, Axonal Modeling, in: M.A. Arbib (Ed.), The Handbook of Brain Theory and Neural Networks, The MIT Press, 1998.

[6] R.L. De Valois, N.P. Cottaris, L.E. Mahon, S.D. Elfar, J.A. Wilson, Spatial and temporal fields of geniculate and cortical cells and directional selectivity, Vision Research, 40 (2000) 3685-3702.

[7] B. Hellwig, A quantitative analysis of the local connectivity between pyramidal neurons in layer 2/3 of the rat visual cortex, Biol. Cybern. 82 (2000) 111-121.

[8] V. Braitenberg, A. Schüz, CORTEX: Statistics and Geometry of Neuronal Connectivity, Springer, 1998.

[9] M.N. Shadlen, W.T. Newsome, The Variable Discharge of Cortical Neurons: Implications for Connectivity, Computation, and Information Coding, J. of Neuroscience, 18(10):3870–3896, 1998.

[10] C. Lyon, N. Jain, J.H. Kaas, Cortical Connections of Striate and Extrastriate Visual Areas in Tree Shrews, J of Comparative Neurology 401 (1998) 109-128.

[11] H. Bosking, Y. Zhang, B. Schofield, D.Fitzpatrick, Orientation Selectivity and the Arrangement of Horizontal Connections in Tree Shrew Striate Cortex, J of Neuroscience, 17(6):2112-2127, 1997.

[12] C.M. Gray D.A. McCormick, Chattering cells: superficial pyramidal neurons contributing to the generation of synchronous oscillations in the visual cortex. Science 274 (1996) 109-113.

[13] M. Stetter, K. Obermayer, Biology and theory of early vision in mammals, in: H. H. Szu (Ed.), Brains and Biological Networks, INNS Press, 2000.

[14] W. Singer, C.M. Gray, Visual feature integration and the temporal correlation hypothesis, Annual Review of Neuroscience, 18 (1995) 555-586.

[15] K.E. Martin, J.A. Marshall, Unsmearing Visual Motion: Development of Long-Range Horizontal Intristic Connections, in: S.J. Hanson, J.D. Cowan, C.L. Giles (Eds.) Adv. in Neural Inf. Pro. Sys. 5 (1993) 417-424.

[16] S.C. Yen, L.H. Finkel, Extraction of Perceptually Salient Contours by Striate Cortical Networks, Vision Research 38(5):719-741, 1998.

[17] S.C. Yen, E.D. Menschik, L.H. Finkel, Perceptual grouping in striate cortical networks mediated by synchronization and desynchronization, Neurocomp. 26-27 (1999) 609-616.

[18] J.J. Wright, P.D. Bourke, C.L. Chapman, Synchronous oscillation in the cerebral cortex and object coherence: simulation of basic electrophysiological findings. Bio. Cyber. 83 (2000) 341-353.

[19] S.C.Yen, E.D. Menschik, L.H. Finkel, Cortical Synchronization and Perceptual Salience, Neurocomp. 125-130, 1998.

[20] S. Friedman-Hill, P.E. Maldonado, C.M. Gray, Dynamics of Striate Cortical Activity in the Alert Macaque: I. Incidence and Stimulus-dependence of Gamma-band Neuronal Oscillations, Cerebral Cortex, 10 (2000) 1105-1116.

[21] P.E. Maldonado, S. Friedman-Hill, C.M. Gray, Dynamics of Striate Cortical Activity in the Alert Macaque: II. Fast Time Scale Synchronization, Cerebral Cortex, 10 (2000) 1117-1131.

[22] A.R. Haig, E. Gordon, J.J. Wright, R.A. Meares, H Bahramali, Synchronous cortical gamma-band activity in task-relevant cognition, 11 (2000) 669-675.

[23] M.N. Shandlen, J.A. Movshon, Synchrony Unbound: A Critical Evaluation of the Temporal Binding Hypothesis, Neuron, 24 (1999) 67-77.

[24] W.M. Usrey, R.C. Reid, Synchronous Activity in the Visual System, Annu. Rev. Physiol. 61 (1999) 435–56.

[25] S. Grossberg, R. Williamson, A Neural Model of how Horizontal and Interlaminal Connections of Visual Cortex Develop into Adult Circuits that Carry Out Perceptual Grouping and Learning, Cerebral Cortex, 11 (2001) 37-58.

[26] T. Wennekers, G. Palm. How imprecise is neuronal synchorization?, Neurocomp. 26-27 (1999) 579-585.

[27] T. Hansen, H. Neumann, A model of V1 visual contrast processing utilizing long-range connections and recurrent interactions, ICANN, 61-66, 1999.

[28] A.K. Engel, P.R. Roelfsema, P. Fries, M. Brecht, W. Singer, Role of the Temporal Domain for Response Selection and Perceptual Binding, Cerebral Cortex, 7 (1997) 571-582.

8 Paper II – An Abstract Model of a Cortical Hypercolumn

Baran Çürüklü[1] and Anders Lansner[2]

[1]Department of Computer Science and Engineering, Mälardalen University, Västerås, SE-72123, Sweden
[2]Department of Numerical Analysis and Computer Science, Royal Institute of Technology, SE-10044 Stockholm, Sweden

In Proceedings of the 9th International Conference on Neural Information Processing, pages 80-85, Singapore, November 2002, IEEE.

Abstract

An abstract model of a cortical hypercolumn is presented. This model could replicate experimental findings relating to the orientation tuning mechanism in the primary visual cortex. Properties of the orientation selective cells in the primary visual cortex like, contrast-invariance and response saturation were demonstrated in simulations. We hypothesize that broadly tuned inhibition and local excitatory connections are sufficient for achieving this behavior. We have shown that the local intracortical connectivity of the model is to some extent biologically plausible.

8.1 Introduction

Most neurons in the primary visual cortex (V1) respond to specific orientations even though relay cells in the lateral geniculate nucleus (LGN), that carries the information from retina to V1, does not show evidence of orientation selectivity. It is not known in detail how orientation selectivity of the cells in V1 emerges and the issue is hotly debated (for a recent review see Ferster et al., [9]). Hubel and Wiesel [10] proposed that orientation selectivity of simple cells in V1 was a consequence of synaptic input from LGN. Still today the Hubel and Wiesel feedforward model serves as a model of thalamic input to cortex. However many of the properties of orientation selective cells in V1 cannot be predicted by such a feedforward model. Contrast-invariance of orientation tuning seen by simple and complex cells is perhaps the most striking example. As contrast increases the height of the response curve increases while the width remains almost constant [11,12,13].

It was also shown that response to contrast stimulus increases over approximately 50-60% of the response range and this behavior is followed by a rapid saturation and normalization of the cells activity [13]. The saturation level seems to be determined by stimulus property (orientation, spatial frequency) and not by electrical properties of the cells. Maximum response to non-preferred stimulus was reported to be lower than to preferred stimulus.

According to the findings by Hubel and Wiesel [16] the primary visual cortex has a modular structure. It is composed of orientation minicolumns each one comprising some hundreds of pyramidal cells and a smaller number of inhibitory

interneurons of different kinds. Contrast edge orientation is coded such that the cells in each orientation minicolumn respond selectively to a quite broad interval of orientations. Further, the orientation hypercolumn contains orientation minicolumns with response properties distributed over all angles, and thus represents the local edge orientation pertinent to a given point in visual space. A similar modular arrangement is found in many other cortical areas, e.g. rodent whisker barrels [15].

The Bayesian Confidence Propagation Neural Network model (BCPNN) has been developed in analogy with this possibly generic cortical structure [14]. This is an abstract neural network model in which each unit corresponds to a cortical minicolumn. The network is partitioned into hypercolumn-like modules and the summed activity within each hypercolumn is normalized to one.

The above network model relates to the so-called normalization models of V1 proposed by Albrecht et al. [20] and Heeger [21] that address properties of simple cells mentioned above. These assume that input from the LGN grows linearly with contrast stimulus. This input is divided by a linearly growing inhibitory input. The effect is division of the input from the LGN and that the summed activity of the cells in a hypercolumn is normalized. This would correspond to saturation of a cells activity. Later Carandini et al. [22,23] proposed that a pool of cells with different preferred orientations and spatial frequencies drives the shunting inhibition.

Cross-orientation inhibition is yet another feature of cortical simple and complex cells. Response to superposition of two gratings is less than sum of each response alone [8,25]. Morrone et al. [8] suggested that this inhibition arises from a pool of cells with different orientations. The cross-inhibition effect could be explained by a shunting inhibition proposed by the normalization models [22,23].

Here we present an abstract model of a cortical hypercolumn derived from the above-mentioned BCPNN architecture. Our main intention has been to address response saturation and contrast-invariance of orientation tuning behaviors of cortical cells. Initial tests were showing that cross-orientation inhibition was also prominent. All these behaviors could be achieved by a very simple network architecture (Figs. 8.1–8.3).

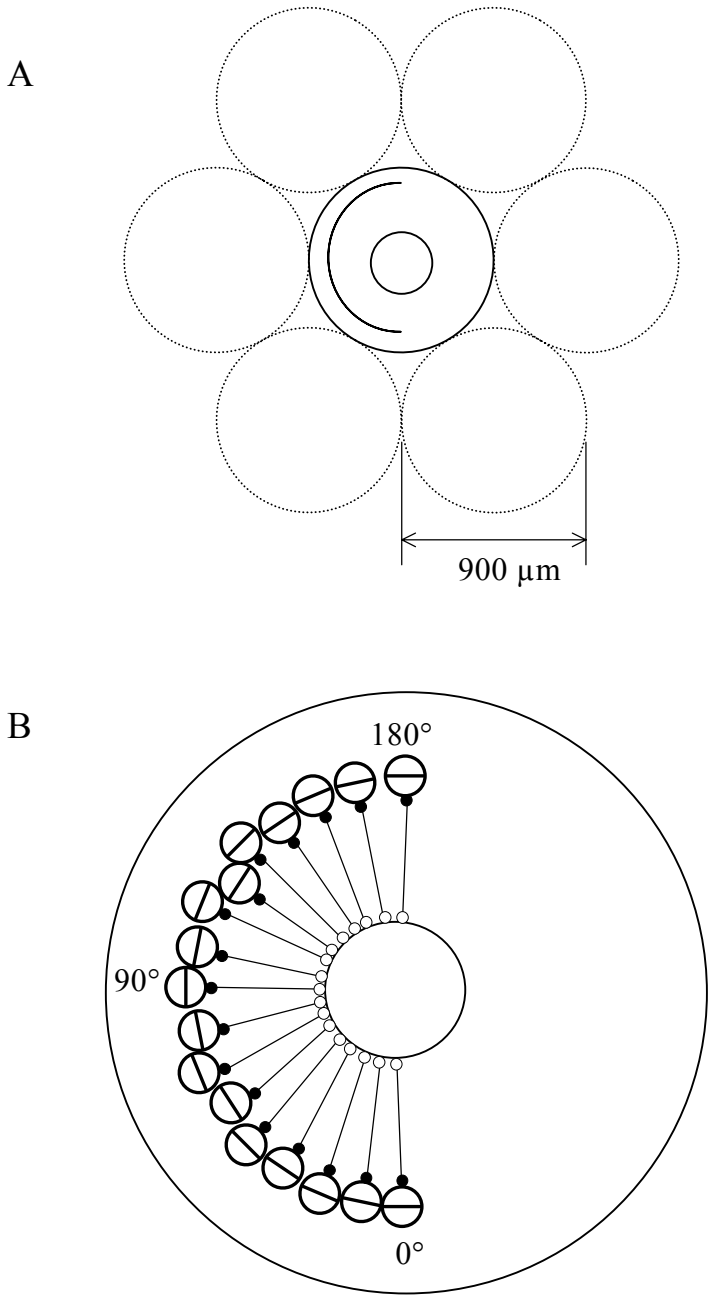

Figure 8.1. *A*, The hypothesized repetitive layout of the cat V1 demonstrated by 7 hypercolumns. *B,* The partial hypercolumn model used during the simulations consisted of 17 minicolumns.

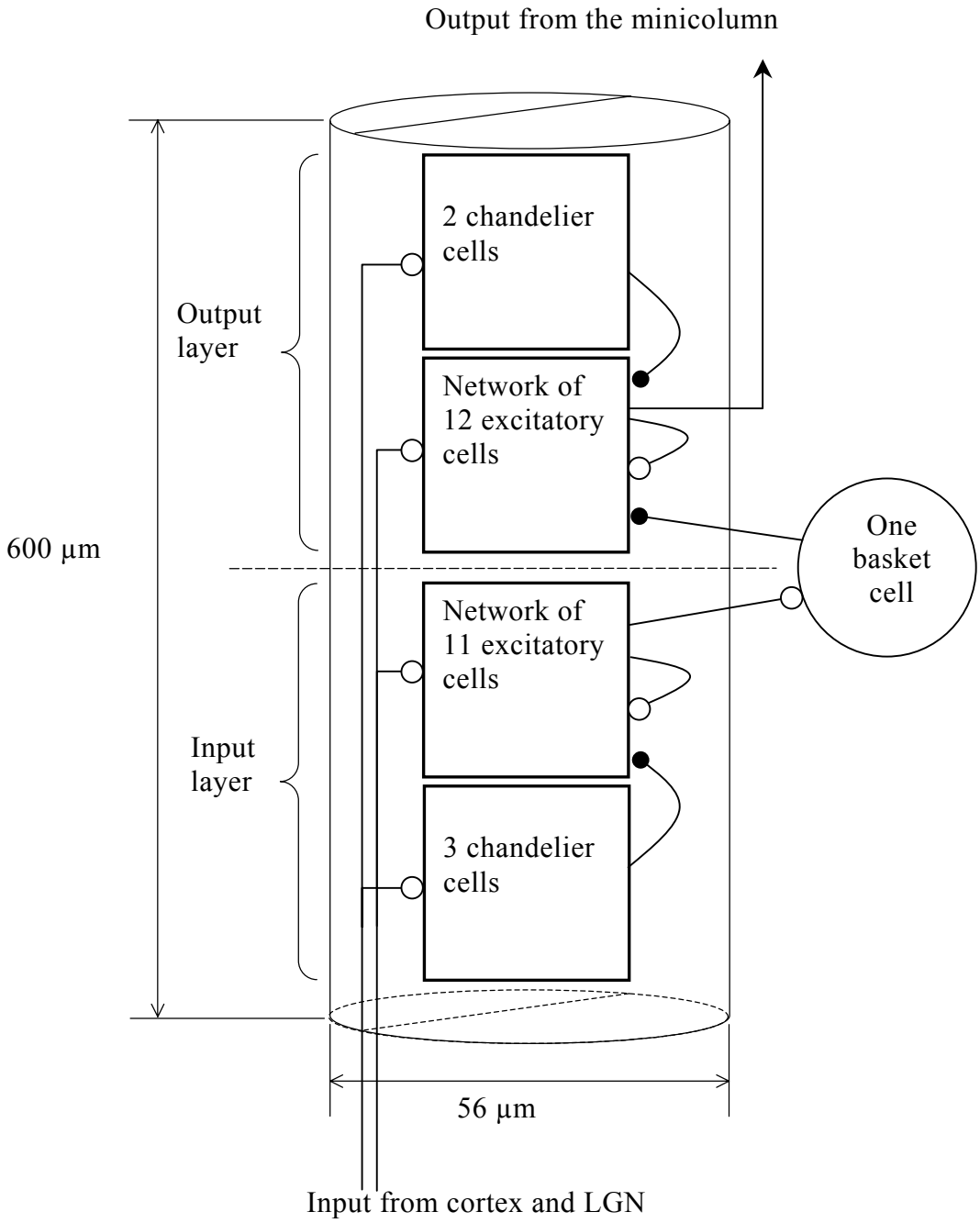

Figure 8.2. A scheme showing one of the subsampled orientation minicolumns and the basket cell representing the pool of inhibitory cells. Excitatory cells in the input layer are connected to the basket cell, and the basket cell inhibits the excitatory cells in the output layer.

8.2 Network Model

The foundation of our network model is the columnar organization seen in V1 and elsewhere in the cortex [16]. We assume that V1 is composed of repetitive structures, so-called minicolumns, and that these minicolumns rotate around hypothetical centers [18], and form hypercolumns (Fig. 8.1*A*). In our model a hypercolumn is represented by a finite number of minicolumns, each representing a particular orientation (Fig. 8.1*B*). For sake of simplicity we decided to use a partial hypercolumn model composed of 17 subsampled orientation minicolumns, ranging from 0° to 180°, with the angular distance of 11.25° between two successive ones (Fig. 8.1*B*). The diameter of the cylinder shaped minicolumns was 56 μm, as a consequence of the study done by Peters et al. [17] on cat V1. In that study, it was reported that apical dendrites of layer V pyramid cells formed clusters with a center-to-center spacing of about 56 μm, which provides an estimate of the mean distance between two successive minicolumns. The circular arrangement of the minicolumns gives the biologically plausible hypercolumn diameter of 900 μm for cat V1. The minicolumns has a height of 600 μm, and are abstractions of the layer II-IV of cat V1 [17]. Each of the subsampled minicolumns is composed of 28 neurons (Fig. 8.2) and the neuron population is heterogeneous with all values sampled from a uniform distribution with a standard deviation of 10%.

The hypercolumn model consists of two separate layers with two different tasks in order to achieve normalization behavior proposed by the BCPNN model (Fig. 8.2). It will be shown later that the excitatory neurons in the output layer replicate experimental findings relating to the orientation tuning mechanism in V1.

There were no connections between these two layers, and thus the interaction between them was through one basket cell, representing a pool of inhibitory cells (Figs. 8.1*B* and 8.2). This layout resulted in feedforward connectivity inside the hypercolumn model. Every input layer excitatory cell was connected to the basket cell, and thus could drive it. The basket cell was connected to every excitatory cell in the output layer. There were no connections between excitatory cells situated in different orientation minicolumns. Connection probability between two excitatory neurons inside a minicolumn layer was a function of the distance between them [6].

The implication of this scheme for the output layer is that, the distribution (in terms of orientation) of the inhibitory input to an excitatory cell is broader than the excitatory input. This is because the basket cell represents a pool of orientation specific neurons inhibiting a pool of excitatory neurons with all possible preferred orientation. Even though the connectivity pattern seen in the output layer is very simple, it is still biologically plausible. Kisvárday et al. [27] reported that, in an area of the size of cat V1 hypercolumn, 56 % of the excitatory and 47 % of the inhibitory connections were at iso-orientation, while cross-inhibition was shown by 14 % of excitatory and 20 % of inhibitory connections respectively. This

indicates that, the inhibitory network is less orientation specific than the excitatory network. A study based on ferret prefrontal microcircuits is also pointing in the direction of the basket cells as responsible for gain control of the local cortical network [26].

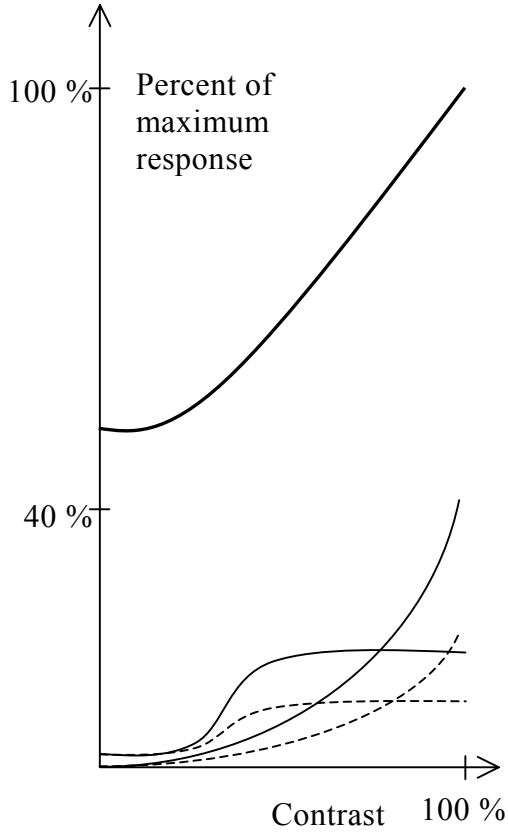

Figure 8.3. A scheme showing the activity of the excitatory cells in two minicolumns with preferred orientation (bottom solid lines) and non-preferred orientation (bottom dashed lines). Input layer excitatory cells (exponential curves) are driving the basket cell (thick top curve). The output layer excitatory cells (sigmoidal curves) are normalized when the basket cell's activity increases linearly.

Besides the basket cell, there were other inhibitory cells in the model. These cells were the local inhibitory chandelier cells [28] located inside the minicolumns, and hence inhibiting excitatory cells with the same orientation preference. In the input layer three chandelier cells inhibited an excitatory cell, while two chandelier cells inhibited the excitatory cells in the output layer.

Cortical neurons are known for their irregular spiking activity [3,4], and were thus modeled as Poisson processes. As the kernel of the Poisson process we used a leaky integrate-and-fire model [1,2]. The role of the leaky integrate-and-fire model was to sum the presynaptic inputs to generate the membrane potential of the cells. Maximum frequency of the excitatory and the inhibitory neurons were 100 Hz and 300 Hz respectively. Half-height of the IPSPs were 10 ms, and 15 ms for the EPSPs. Mean amplitudes of the EPSPs inside the minicolumns were 0.94 mV for the input layer, and 9.4 mV for the output layer. The strength of the synaptic connection between the input layer excitatory cells and the basket cell was set to give an EPSP of 3.5 mV. IPSPs generated by the chandelier cells had a mean of -3.2 mV, and that of the basket cell was -55.1 mV. Observe that the values are exaggerated, specially the IPSP generated by the basket cell, for compensating the small number of cells used in the network model. It is assumed that in cortex some 20 % of the cells are various inhibitory cells [31]. The PSP values and number of connections, especially inhibitory ones, were calculated to preserve this ratio between the inhibitory and the excitatory populations in V1. The PSP values were sampled from a uniform distribution with a standard deviation of 10%.

An axonal diameter of 0.3 μm [29] resulted in a spike propagation velocity of 0.85 m/s [30].

8.3 Simulation Results

One important assumption made was the linear response of the LGN cells to the contrast stimulus increase. This assumption was in line with the normalization models mentioned above. Results by Movshon et al. [24] indicate that the majority of LGN cells (namely P cells) have linear response functions and shows very little or no sign of saturation as a function of contrast stimulus increase. Our model does not have a LGN component, hence the LGN input is modeled as a constant current. During the simulations we defined the input to the modeled cells in the following way. The simulated LGN had two components, both constant currents. The first was a function of the contrast stimulus increase, and the second was, besides of contrast, also a function of the orientation of the postsynaptic cell. Tuning of this second component was 40° half-width at half-height [19] both for the excitatory and the chandelier cells. Observe that the basket cell did not receive any input from the LGN. The orientation dependent LGN input at 100 % contrast, for cells with the preferred orientation was 2.7 nA for excitatory cells, and 0.9 nA for chandelier cells. Orientation independent part of the LGN input was 0.9 nA for all excitatory cells, and 0.32 nA for all chandelier cells. Observe that input to cells having non-preferred orientation during high contrast might exceed input to cells having preferred orientation during low contrast as a results of the orientation independent part of the LGN input. As the background activity all excitatory cells

received additional current input. Excitatory cells in the output layer received 2 nA, while input layer excitatory cells received 1 nA. To guarantee that the inhibitory cells were active in their logarithmic range these cells received 3.5 nA throughout the simulation. The current values were sampled from a uniform distribution with a standard deviation of 10%.

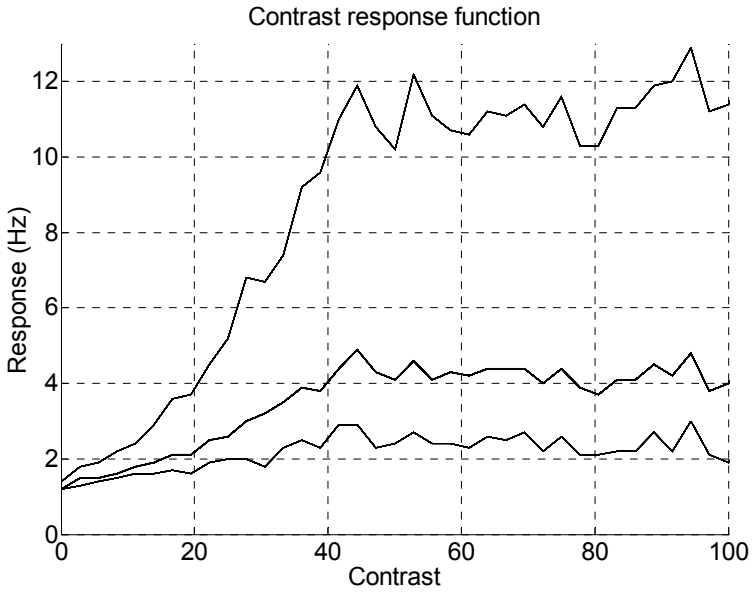

Figure 8.4. Contrast response function curves corresponding to mean activity of excitatory cells situated in the output layer. Top curve corresponds to cells situated in the minicolumn having the same orientation preference (90°) as the input to the hypercolumn. The thick curve in the middle corresponds to mean activity of cells in all 17 minicolumns. The bottom curve corresponds to activity of cells having a 45° orientation preference.

Experimental findings related to the orientation tuning mechanism in V1, and thus normalization in the BCPNN framework [14] is possible to achieve by assuming that excitatory and inhibitory cells are active in specific regions of their gain functions, and that these regions define their ranges. The sigmoidal gain function of the Poisson neuron could be divided roughly into two regions; the low activity region (<50 %) would correspond to the exponential function, and the high activity region (≥ 50%) to the logarithmic function. We assume here that the excitatory cells are in their low activity region and the inhibitory cells are in their high activity region.

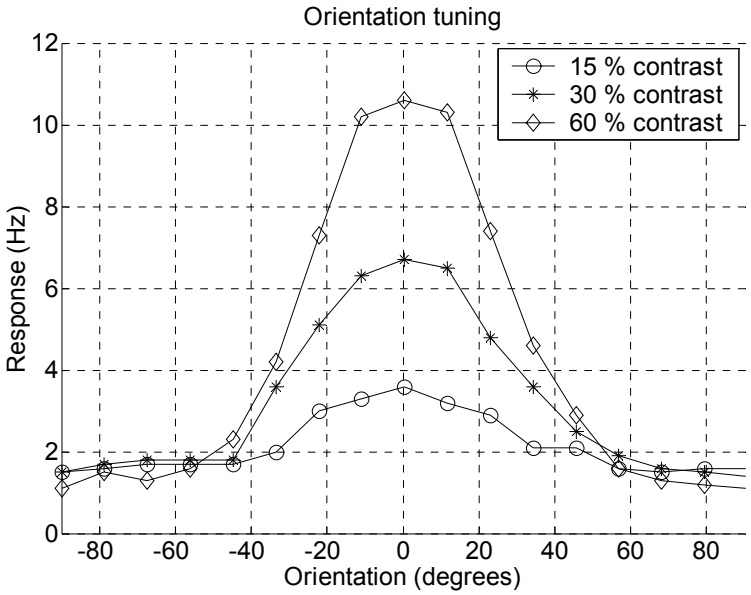

Figure 8.5. Contrast-invariance demonstrated by the network. Selectivity remains constant while the peak increases as a function of increasing contrast.

In order to analyze the network behavior we start with the input layer, and later continue with the output layer. Excitatory cells in the input layer of the hypercolumn model behaved like cells in a Hubel and Wiesel feedforward model [10]. This was not a surprise because orientation tuning of these cells was a function of the LGN input. Remember that the excitatory cells approximated the exponential function, and hence amplified their input. This resulted in the narrowing of the orientation tuning. Carandini et al. [19] reported that the half-width at half-height of the tuning of the spike responses was approx. 23° while membrane responses were approx. 38°. Their finding could motivate the narrowing of the half-width at half-height of the orientation tuning. At the same time, activity of the cells having non-preferred orientation was increased above resting activity levels as an effect of the increased contrast. This resulted in widening of the orientation tuning curve.

However, activity shown by the excitatory cells in the output layer (Fig. 8.4) corresponded well to the reported results of the nonlinear behavior of simple and complex cells [13]. The first region corresponded to the dynamic response range of the cortical cells. During this phase the activity of the cells increased monotonically as a function of increased contrast. This phase was followed by a rapid saturation. During the last phase the cells were normalized i.e. their activity was constant even though the contrast was increasing. It should be stressed that saturation of activity was evident in all cells independent of their orientation

preferences, and that, this level was not a function of the cells electrical properties as reported by [13].

It was shown by Albrecht et al. [13] that the contrast response function could be approximated by a hyperbolic function

$$\text{Response}(C) = R_{max} \cdot (C^n / (C^n + C_{50}{}^n))$$

where $C_{50}{}^n$ defined contrast value that was required to produce 50% of the cell's maximum response. R_{max} was the cell's maximum response rate. It was also reported in that study that contrast response curves were shifted vertically downward as the stimulus orientation diverged from the preferred orientation. This would mean that R_{max} changed while C_{50} and n remained relatively constant. This behavior was believed to be important for preserving the relative frequency response function independent of the contrast [12,13]. The excitatory cells in the output layer of the model hypercolumn had all these properties (Fig. 8.4). The R_{max} levels, <12 Hz, were below maximum frequency levels (≈100 Hz) governed by the electrical properties of the cells (Fig. 8.4). C_{50} levels (approx. 24%) of modeled cells were biologically plausible (Fig. 8.4).

Contrast dependent inhibition was reported by Sclar et al. [11]. According to their results, as the contrast increased activity of the cells having orientation preference that differed significantly from the stimulus orientation decreased below their spontaneous activity levels. This behavior was also demonstrated in our simulation, as seen when comparing the low and high contrast curves (Fig. 8.5). Cells having orientation preference that differed more than approximately 50° from the stimulus orientation were inhibited below their spontaneous activity levels. Contrast-invariance of orientation tuning in simple and complex cells could be seen as an effect of this contrast dependent inhibition.

Both contrast response function and contrast-invariance of orientation tuning could be explained by our network architecture. In order to explain interactions in detail we would like to focus on the connections from the excitatory cells in the input layer to the basket cell, and from the basket cell to the excitatory cells in the output layer. Remember that linear increase of the contrast results in exponentially increased activity of the input layer excitatory cells, and that these cells are driving the basket cell. The basket cell linearizes the input from these cells, because the response function of the basket cell is logarithmic. As a result, the basket cell responds to contrast in a linear fashion. Output from the basket cell is then fed into the output layer excitatory cells. The main part of the input received by these excitatory cells is from the LGN input and this intracortical inhibition. Observe that, in theory, both these inputs increase linearly with contrast. This means that these two inputs have constant and positive slopes. Consequently, the relative difference between them corresponds to a constant value, and hence defines a cells activity during the normalized phase.

Within the dynamic response range (contrast < 50%), net input to excitatory cells is increasing. The reason for this is that the excitatory cells in the input layer cannot drive the basket cell. When a certain threshold (contrast ≈ 40 %) is reached the input to the basket cell is strong enough (Fig. 8.4) to drive it.

The cross-inhibition effect was also tested during the simulations (not shown here). In the presence of one additional line stimulus the basket cell's activity increased resulting in a stronger inhibition of the excitatory cells than in case with a single line stimulus. It is also straightforward to see that activity of the basket cell is dependent of the contrast of the additional line stimulus.

8.4 Discussion

We have presented an abstract model of a cortical hypercolumn derived from the BCPNN architecture. This model could replicate important experimental findings relating to the orientation tuning mechanism in the primary visual cortex. Properties of the orientation selective cells in the primary visual cortex like, contrast-invariance and response saturation were demonstrated. One important assumption made was the linear response of the LGN cells to the contrast stimulus increase. As a result of this assumption, we showed that the normalization of the cells in the output layer could be explained by the local connections inside the hypercolumn.

Narrowing of the orientation tuning was possible through the reinforcement of the LGN input by the excitatory cells. As a side effect, cells having non-preferred orientations were excited above their resting activity levels, and this affected their orientation tuning negatively. The divisive inhibition of the excitatory cells in the output layer by the basket cell resulted in sharpening of the orientation tuning curves and normalization of their activity. The basket cell represented a pool of inhibitory cells with a mixture of preferred orientations. The activity of the basket cell was a function of the excitatory cells in the input layer, and thus represented the total activity inside the hypercolumn. This network configuration is supported by studies made on cat V1.

It is well known that the long-range horizontal intracortical connections play an important role in V1. The impact of such connections to the orientation tuning mechanism of the cortical cells will be addressed in the near future. One experiment will be to simulate cortical plasticity in the framework of the BCPNN incremental learning algorithm. In these experiments, stimuli defined as lines with random orientations moving across the model cortex will provide the activity patterns required for the learning algorithm to form assemblies of connected minicolumns. Our intention is to look into how well these resemble cortical connectivity patterns seen in V1 and how they influence the response dynamics of the network.

References

[1] W. Gerstner, *Pulsed Neural Networks*, The MIT Press, Chapter 1, 1998.

[2] W. Kistler, W. Gerstner, and J.L. van Hemmen, "Reduction of Hodgkin-Huxley equations to a threshold model", *Neural Comput.*, 9:1069-1100, 1997.

[3] C. Koch, *Biophysics of Computation: Information Processing in Single Neurons*, Oxford University Press, Chapter 15, 1999.

[4] M.N. Shadlen, W.T. Newsome, "The Variable Discharge of Cortical Neurons: Implications for Connectivity, Computation, and Information Coding", *J. of Neurosci.*, 18(10):3870–3896, 1998.

[5] V. Braitenberg, A. Schüz, *CORTEX: Statistics and Geometry of Neuronal Connectivity*, Chapter 36, Springer, 1998.

[6] B. Hellwig, "A quantitative analysis of the local connectivity between pyramidal neurons in layer 2/3 of the rat visual cortex", *Biol. Cybern*., 82:111-121, 2000.

[7] T.W. Troyer, A.E. Krukowski, N.J. Priebe, and K.D. Miller, "Contrast-invariant orientation tuning in cat visual cortex: thalamocortical input tuning and correlation-based intracortical connectivity", *J. of Neurosci*., 18:5908–27, 1998.

[8] M.C. Morrone, D.C. Burr, and L Maffei, "Functional implications of cross-orientation inhibition of cortical visual cells. I. Neurophysiological evidence", *Proc. R. Soc London Ser. B* 216:335–54, 1982.

[9] D. Ferster, K.D. Miller, "Neural Mechanisms of Orientation Selectivity in the Visual Cortex", *Annual Reviews of Neuroscience*, 23:441-471, 2000.

[10] D.H. Hubel, T.N. Wiesel, "Receptive fields, binocular interaction and functional architecture in the cat's visual cortex", *J. Physiol*., 160:106-154, 1962.

[11] G. Sclar, R.D. Freeman, "Orientation selectivity in the cat's striate cortex is invariant with stimulus contrast", *Exp. Brain Res*., 46:457–61, 1982.

[12] B.C. Skottun, A. Bradley, G. Sclar, I. Ohzawa, and R. Freeman, "The effects of contrast on visual orientation and spatial frequency discrimination: a comparison of single cells and behaviour", *J. of Neurophysiology*, 57:773–86, 1987.

[13] D.G. Albrecht, D.B. Hamilton, "Striate cortex of monkey and cat: contrast response function", *J. of Neurophysiology,* 48:217–37, 1982.

[14] A. Sandberg, A. Lansner, F.M. Petersson, and Ö. Ekeberg, "A Bayesian attractor network with incremental learning" *Network: Computing in Neural Systems, in press,* 2002.

[15] D. Purves, D.R. Riddle, A-S LaMantia, "Iterated patterns of brain circuitry (or how the cortex gets its spots)", *TINS,* 15 362–8, 1992.

[16] D. Hubel, T.N. Wiesel, "The functional architecture of the macaque visual cortex. *The Ferrier lecture." Proc. Royal. Soc. B* 198: 1-59, 1977.

[17] A. Peters, E. Yilmaz, "Neuronal organization of area 17 of cat cortex", *Cerebral Cortex*, 3:49-68, 1993.

[18] V. Braitenberg, C. Braitenberg, "Geometry of the orientation columns in the visual cortex", *Biol. Cyber.*, 33:179-186, 1979.

[19] M. Carandini, D. Ferster, "Membrane potential and firing rate in cat primary visual cortex", *J. of Neurosci.*, 20(1):470-484, 2000.

[20] D.G. Albrecht, W.S. Geisler, "Motion selectivity and the contrast-response function of simple cells in the visual cortex", *Visual Neuroscience*, 7:531–46, 1991.

[21] D.J. Heeger, "Normalization of cell responses in cat striate cortex", *Visual Neuroscience*, 9:181–97, 1992.

[22] M. Carandini, D.J. Heeger, "Summation and division by neurons in primate visual cortex", *Science,* 264:1333–36, 1994.

[23] M. Carandini, D.J. Heeger, and J.A. Movshon, "Linearity and normalization in simple cells of the macaque primary visual cortex", *J. of Neurosci.*, 17:8621–44, 1997.

[24] J.A. Movshon, M.J. Hawken, L. Kiorpes, A.M. Skoczenski, C. Tang, and L.P. O'Keefe, "Visual noise masking in macaque LGN neurons", *Invest. Ophthalmol. Vis. Sci.* [Suppl] 35:1662, 1994.

[25] A.B. Bonds, "The role of inhibition in the specification of orientation selectivity of cells in the cat striate cortex", *Visual Neuroscience*, 2:41–55, 1989.

[26] L.S. Krimer, P.S. Goldman-Rakic, "Prefrontal Microcircuits: Membrane properties and excitatory input of local, medium, wide arbour interneurons", *J. of Neurosci.*, 21(11):3788-3796, 2001.

[27] Z.F. Kisvárday, É. Tóth, M. Rausch, and U.T. Eysel, "Orientation-specific relationship between population of excitatory and inhibitory lateral connections in the visual cortex of the cat", *Cerebral Cortex*, 7:605-618, 1997.

[28] I. Farinas, J. DeFelipe, "Patterns of synaptic input on corticortical and cortithalamic cells in the cat visual cortex. II The axon initial segment", *J. Comp. Neurol.*, 304, 70-77, 1991.

[29] V. Braitenberg, A. Schüz, *CORTEX: Statistics and Geometry of Neuronal Connectivity*, Springer, 1998.

[30] C. Koch, Ö. Bernander, Axonal Modeling, in: M.A. Arbib (Ed.), *The Handbook of Brain Theory and Neural Networks*, 129-134, The MIT Press, 1998.

[31] C.D. Gilbert, J.A. Hirsch, and T.N. Wiesel, "Lateral interactions in cat visual cortex *Cold Spring Harbor Symp. On Quantitative Biology* vol LV", *Cold Spring Harbor Press*, 663-76, 1990.

9 Paper III – A Model of the Summation Pools within the Layer 4 (Area 17)

Baran Çürüklü[1] and Anders Lansner[2]

[1]Department of Computer Science and Engineering, Mälardalen University, Västerås, SE-72123, Sweden
[2]Department of Numerical Analysis and Computer Science, Royal Institute of Technology, SE-10044 Stockholm, Sweden

The Annual Computational Neuroscience Meeting 2004, Baltimore, USA.

Abstract

We propose a developmental model of the summation pools within the layer 4. The model is based on the modular structure of the neocortex and captures some of the known properties of layer 4. Connections between the orientation minicolumns are developed during exposure to visual input. Excitatory local connections are dense and biased towards the iso-orientation domain. Excitatory long-range connections are sparse and target all orientation domains equally. Inhibition is local. The summation pools are elongated along the orientation axis. These summation pools can facilitate weak and poorly tuned LGN input and explain improved visibility as an effect of enlargement of a stimulus.

9.1 Introduction

Studies examining long-range spatial interactions in visual cortex show that cortical circuit plays a major role in altering the responses of the neurons. As demonstrated by Polat and Norcia [8] enlargement of a Gabor patch stimulus results in increased visibility of the stimulus. Furthermore, elongation of the stimulus along the orientation axis of the neurons results in more prominent visibility than elongation that is orthogonal to the orientation axis. Consequently, summation pools, which are hypothesized to be elongated, have been proposed [8]. However, response properties, such as orientation selectivity, spatial phase and frequency, etc., of the neurons that are found within a neuron's summation pool are not entirely known. It is neither clear in which cortical layers these pools might be located.

In layer 4 of cat primary visual cortex the excitatory connections target the distal (>0.74 mm) iso- (±30º), oblique- (±30–60º) and cross-orientation (±60–90º) domains equally [12]. Local projections are, however, biased towards the iso-orientation domain [12]. Results by Yousef et al. [12] indicate that the hypothesized summation pools within the visual cortex [8] might be composed of neurons situated in all orientation domains.

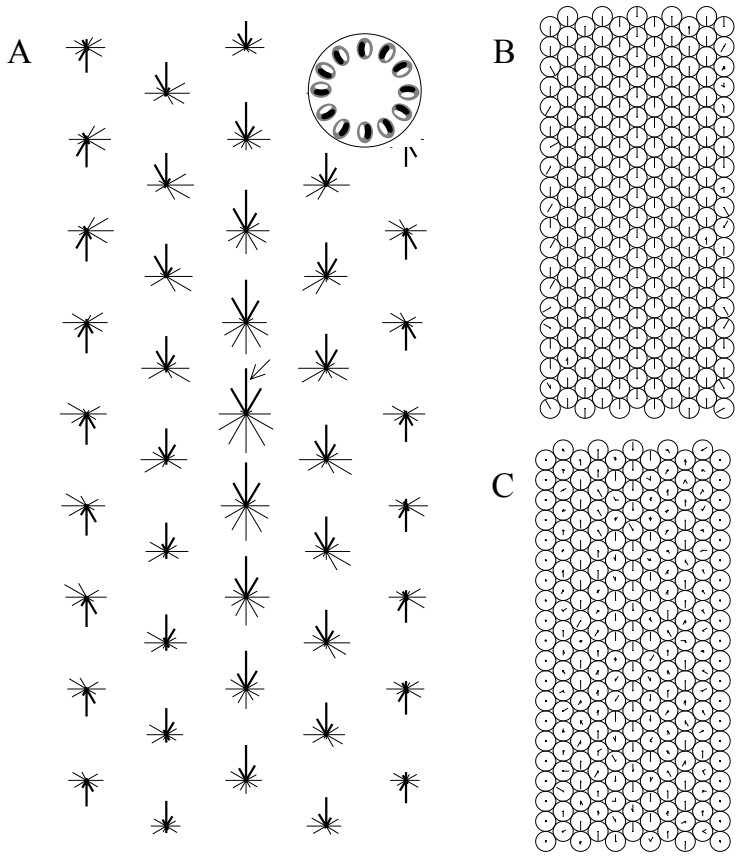

Figure 9.1. *A*, Polar-plots organized as the network model, each one representing a hypercolumn. The legend in *A* shows the orientation and the relative spatial phase of the units in each hypercolumn. *A,* Central part of the reference unit's summation pool is shown. This unit (marked with an arrow) is located in the hypercolumn that is in the middle of the network. Thick lines represent excitatory connections, thin lines correspond to inhibitory connections. Distance from the origin is proportional to the strength of the connection. *B*, Normalized activities after 50 ms. Distance from the origin is proportional to the activity level of a unit. Units receive input from the LGN and the network. *C*, Units receive solely LGN input. Note that only hypercolumns receiving maximum LGN input can converge after 50 ms.

According to the findings by Hubel and Wiesel [6,7] the primary visual cortex has a modular structure. It is composed of orientation minicolumns each one comprising some hundreds of excitatory cells and a smaller number of inhibitory interneurons of different kinds. Contrast edge orientation is coded such that the neurons in each orientation minicolumn respond selectively to a broad range of orientations.

The Bayesian Confidence Propagation Neural Network model (BCPNN) [9] has been developed in analogy with the modular structure of the primary visual cortex [6,7]. This is an abstract neural network model in which each unit corresponds to an orientation minicolumn. The network is partitioned into hypercolumn-like modules (referred to as hypercolumns in the text). Summed activity within these hypercolumns is normalized to one. Earlier a biologically plausible implementation of normalization has been proposed [2].

A developmental model of the summation pools within the layer 4 (area 17) based on cat data is proposed. This model is in line with the modular structure of the neocortex and captures some of the known properties of the layer 4. Excitatory local connections are dense and biased towards the iso-orientation domain. Excitatory long-range connections are, however, sparse and target all orientation domains equally. Inhibition is local and is mediated by inhibitory simple cells. Proposed summation pools are mildly elongated along the orientation axis. Simulations show that the proposed summation pools can facilitate weak and poorly tuned LGN input, and hence explain improved visibility as an effect of enlargement of the stimulus.

9.2 Network Model

The network model used during the simulations consists of 220 (11x20) hypercolumns arranged to form a hexagonal array (Fig. 9.1*A*). Each hypercolumn consists of 12 layer 4 (area 17) units. Their receptive fields (RF) are designed as contrast edge detectors (composed of two elongated subregions with opposite sign). Difference in orientation preference between two successive units inside a hypercolumn is 30°. Note that every orientation is represented twice with two units, which have opposite absolute spatial phase (their subfields with opposite sign overlap). Absolute spatial phase refers to the position of the ON- and OFF-subregions with respect to the visual field.

The RF centers of the units belonging to a hypercolumn are positioned in the center of their host hypercolumn. The distance between the centers of two adjacent hypercolumns is constant throughout the network model and corresponds to 0.2º of visual angle (at 2º of eccentricity [4]). The visual world covered by the model is 2.4x5.4º. The RF width is 1º [4] and the height is ~1.5º indicating strong overlap between units positioned in neighboring hypercolumns. Orientation tuning of the LGN input is ~40º at half-width at half-height [1]. The LGN input is computed using a model developed by Troyer et al. [11]. All units are tuned for the same spatial frequency of 1 cycle/degree [4].

9.3 Simulation Results

The simulations are divided into two parts. During the first part, BCPNN incremental learning algorithm is used to develop hypothesized layer 4 summation pools. Later we address the question of whether or not these summation pools can facilitate weak and poorly tuned LGN input, and hence improve visibility as reported in [8].

The BCPNN learning algorithm is correlation based, thus if two units are correlated during a time step the connection between them strengthens. Anticorrelation results in an inhibitory connection via a local inhibitory interneuron. Excitatory connections are reciprocal, since the weight matrix is symmetric. For this network configuration training of the fully connected network lasts for 1000 simulation steps, where every step corresponds to 1 second. The learning rate, which defines the degree of weight modification, is 0.005 [9]. At every time step, the activity levels of the units are initiated using a new contrast edge stimulus, whose position and orientation are sampled from a uniform distribution. Its width is 1º, and spatial frequency is 1 cycle/degree.

Noise is added to the activity levels through several steps. First, a normally distributed noise with a standard deviation of 10% of the so-called bias value is added. The bias value is defined as the activity level of units inside a hypercolumn in absence of stimulus. Later, the activity levels are rectified so that all negative activity levels are set to zero, and a 5-10% uniform distribution noise is added to all units to simulate the background activity. The activity levels are normalized so that the sum of activities in each hypercolumn is equal to one. The contrast of the stimulus is 100%, though the effect of high noise in combination with the BCPNN normalization procedure lowers this level considerably.

Central part of the reference unit's summation pool is visualized in Figure 9.1*A*. Units that are correlated with the reference unit are connected to it through reciprocal excitatory connections (Fig. 9.1*A*, thick lines). The result of anticorrelation is inhibitory connection through a local inhibitory simple cell (Fig. 9.1*A*, thin lines). Ferster [5] has shown that inhibitory simple cells inhibit excitatory simple cells that are located in their close surroundings if they have opposite absolute spatial phase. Based on the proposed scheme [5] it is hypothesized that anticorrelated units can inhibit each other by local or long-range excitation of the inhibitory simple cells.

Strength of the excitatory connections between the reference unit and the units, which have the same orientation preference and absolute spatial phase as the reference unit, tends to decrease along the axis that corresponds to the preferred orientation of the reference unit (Fig. 9.1*A*). Along the orthogonal axis the connection type switches from excitatory to inhibitory (Fig. 9.1*A*). Thus, along this axis the reference unit becomes correlated with the units that have opposite relative spatial phase, but similar absolute spatial phase. Relative spatial phase

refers to the position of the ON- and OFF-subregions with respect to the center of a RF.

Local connections have higher amplitude than long-range horizontal connections (Fig. 9.1*A*). This indicates strong local and sparse distal connectivity within the summation pool. As reported earlier, based on a similar network model [3], the excitatory long-range horizontal connections target all three distal orientation domains equally, whereas local connections are biased towards the iso-orientation domain (see also [12]). Thus, based on the connections made by the reference unit we hypothesize that the summation pools are highly heterogeneous with respect to orientation preference. Finally, the area covered by the connections emerging from the reference unit is mildly elongated along the orientation axis (This property is not shown in Fig. 9.1*A*). This effect is due to the stimulus used during the training.

We assume that the proposed summation pools can facilitate weak and poorly tuned LGN input, and hence improve visibility as reported in [8]. We show this through computer simulations that consist of two parts. During the simulations the stimulus is a vertical contrast edge, positioned in the center of the network model (see the legend in Fig. 9.1*A*. The RF at 12 o'clock represents the unit that is tuned to this stimulus). This stimulus is identical to the stimuli used during the training of the network. During the simulations 46% of the total excitatory input of a unit is from the LGN, whereas the rest is intracortical input [1]. The simulation time step is 10 ms, and the 'membrane time constant' of the units is 50 ms [9]. A hypercolumn has converged when the activity of its units is below <1% of a unit's maximum activity level. Maximum activity of a unit is 1.0 (all other units in its host hypercolumn are silent). The second requirement for convergence is that a unit dominates the hypercolumn, i.e. its activity is >0.9. This will occur after a number of simulation steps, since the model is a recurrent attractor network.

During the first simulation, units receive input from both the LGN and the other units within the network model (Fig. 9.1*B*). During this simulation the LGN input is amplified and sharpened by the connections between the units. As a result almost all hypercolumns converge after 50 ms. Note that in the middle three columns of hypercolumns the lines from the origin point upwards (Fig. 9.1*B*). This illustrates that the hypercolumns located in these three columns converge to the unit, which prefers the stimulus. During the second simulation, connections between the units are removed and compensated by stronger LGN input. As shown in Figure 9.1*C*, LGN input alone is not sufficient for the majority of the hypercolumns to converge. Note that only those hypercolumns that receive maximum LGN input converge. This is due to the attractor properties of the network.

Reported results on convergence pattern and relative speed (Figs. 9.1*B*-*C*) are rather independent of the parameter choices. Qualitatively similar results have been achieved with different values on simulation time step, membrane time constant, network size and shape, RF size, RF overlap between units located in

adjacent hypercolumns, stimulus contrast used during training and retrieval, orientation tuning, contrast gain, etc.

9.4 Conclusions

We propose a developmental model of the summation pools within the layer 4 (area 17) based on cat data. The model is in line with the modular structure of the neocortex and captures some of the known properties of the layer 4. Excitatory local connections are dense and biased towards the iso-orientation domain. Excitatory long-range connections are, however, sparse and target all orientation domains equally. Inhibition is local and is mediated by inhibitory simple cells. Proposed summation pools are mildly elongated along the orientation axis.

Simulations show that the proposed summation pools can facilitate input from the weak and poorly tuned LGN, and hence explain improved visibility as an effect of enlargement of the stimulus. During the simulations the effect of the elongated shape of the proposed summation pools on network performance has not been addressed. It is reasonable to assume that elongated summation pools can explain reported differences in degree of improved visibility, which seems to be related to stimulus configuration [8]. Our intention is to investigate this effect in the near future in the framework of a laminar model, since elongated summations pools are more likely to be found in the superficial layers [10].

References

[1] Hubel, D.H. & Wiesel, T.N. (1962) Receptive fields, binocular interaction and functional architecture in the cat's visual cortex. *J. Physiol*., 160:106–154.

[2] Reid, R.C. & Alonso, J.M. (1995) Specificity of monosynaptic connections from thalamus to visual cortex. *Nature*, 378:281–284.

[3] Ferster, D. & Miller, K.D. (2000) Neural Mechanisms of Orientation Selectivity in the Visual Cortex. *Annual Reviews of Neurosci.*, 23:441–471.

[4] Polat, U. & Norcia, A.M. (1996) Neuropsychological Evidence for Contrast Dependent Long-range Facilitation and Suppression in Human Visual Cortex. *Vision Res.*, 36, 2099–2109.

[5] Polat, U. & Norcia, A.M. (1998) Elongated physiological summation pools in the human visual cortex. *Vision Res.*, 38, 3735–3741.

[6] Adini, Y., Sagi, D. & Tsodyks, M. (1997) Excitatory-inhibitory network in the visual cortex: psychophysical evidence. *Proc. of the National Academy of Sciences USA*, 94, 10426–10431.

[7] Solomon J.A. & Morgan M.J. (2000) Facilitation from collinear flanks is cancelled by non-collinear flanks. *Vision Research*, 40:279–286.

[8] Solomon, J. A., Watson, A. B. & Morgan, M. J. (1999). Transducer model produces facilitation from opposite-sign flanks. *Vision Research*, 39, 987–992.

[9] Gilbert, C.D. & Wiesel, T.N. (1989) Columnar specificity of intrinsic horizontal connections and corticocortical connections in cat visual cortex. *J. Neurosci.*, 9:2432–2442.

[10] Kisvárday, Z.F., Tóth, E., Rausch, M. & Eysel, U.T. (1997) Orientation-specific Relationship Between Populations of Excitatory and Inhibitory Lateral Connections in the Visual Cortex of the Cat. *Cerebral Cortex*, 7, 605–618.

[11] Yousef, T., Bonhoeffer, T., Kim, D.-S., Eysel, U.T., Tóth, E. & Kisvárday, Z.F. (1999) Orientation topography of layer 4 lateral networks revealed by optical imagining in cat visual cortex (area 18). *E. J. of Neurosci.*, 11:4291–4308.

[12] Bosking, W.H., Zhang, Y., Schofield, B. & Fitzpatrick, D. (1997) Orientation Selectivity and the Arrangement of Horizontal Connections in Tree Shrew Striate Cortex. *J. Neurosci.*, 17(6):2112–2127.

[13] Rockland, K.S. & Lund, J.S. (1982) Widespread periodic intrinsic connections in the tree shrew visual cortex. *Science*, 215, 1532–1534.

[14] Schmidt, K.E. & Löwel, S. (2002) Long-range Intristic Connections in Cat Primary Visual Cortex. In B.R. Payne, A. Peters (eds.). *The Cat Primary Visual Cortex*, Chapter 10. Ac. Press.

[15] Hubel, D., Wiesel, T.N. (1977) The functional architecture of the macaque visual cortex. *The Ferrier lecture. Proc. Royal. Soc. B.* 198:1–59.

[16] Mountcastle, V.B. (1997) The columnar organization of the neocortex, *Brain*, 120, 701–722.

[17] DeAngelis G.C., Geoffrey, M.G., Ohwaza, I. & Freeman, R.D. (1999) Functional Micro-Organization of Primary Visual Cortex: Receptive Field Analysis of Nearby Neurons. *J. Neurosci.*, 19(9):4046–4064.

[18] Braitenberg, V. & Braitenberg, C. (1979) Geometry of the orientation columns in the visual cortex. *Biological Cybernetics*, 33:179–186.

[19] De Valois, R.L. & De Valois, K.K. (1990) Striate Cortex. *Spatial Vision*. Oxford Sci. Pub.

[20] Chung, S. & Ferster, D. (1998) Strength and Orientation Tuning of the Thalamic Input to Simple Cells Revealed by Electrical Evoked Cortical Suppression. *Neuron*, 20, 1177–1189.

[21] Albrecht, D.G., Geisler, W.S., Frazor, R.A. & Crane, A.M. (2001) Visual Cortex Neurons of Monkeys and Cats: Temporal Dynamics of the Contrast Response Function. *J. Neurophysiol.*, 88:888–913.

[22] Kayser, A.S. & Miller, K.D. (2002) Opponent Inhibition: A Developmental Model of Layer 4 of the Neocortical Circuit. *Neuron*, 33, 131–142.

[23] Troyer, T.W., Krukowski, A.E. & Miller, K.D. (2002) LGN Input to Simple Cells and Contrast-Invariant Orientation Tuning: An Analysis. *J. Neurophysiol.*, 87:2741–2752.

[24] Grossberg, S. & Raizada, R.D.S. (2000) Contrast-sensitive perceptual grouping and object-based attention in the laminar circuits of primary visual cortex. *Vision Science*, 40, 1413–1432.

[25] Sandberg, A., Lansner, A., Petersson, F.M. & Ekeberg, Ö. (2002) A Bayesian attractor network with incremental learning. *Network: Computing in Neural Systems*, 13, 179–194.

[26] Hirch, J.A., Alonso, J-M, Pillai, C. & Pierre, C. (2000) Simple and complex inhibitory cells in layer 4 of cat visual cortex. *Soc. Neurosci. Abstr.*, 26, 1083.

10 Paper IV – Quantitative Assessment of the Local and Long-Range Horizontal Connections within the Striate Cortex

Baran Çürüklü[1] and Anders Lansner[2]

[1]Department of Computer Science and Engineering, Mälardalen University, Västerås, SE-72123, Sweden
[2]Department of Numerical Analysis and Computer Science, Royal Institute of Technology, SE-10044 Stockholm, Sweden

In Proceedings of the special session on 'Biologically Inspired Computer Vision', at the 2nd CIRAS – Computational Intelligence, Robotics and Autonomous Systems, Singapore, December 2003.

Abstract

We present a quantitative assessment of the local and long-range horizontal connections within two separate models of layer 4 and layer 2/3 of the striate cortex. Connections between the orientation minicolumns, building the models, are developed during exposure to visual input. Layer 4 long-range horizontal connections target all orientation domains in a balanced manner, whereas local connections are biased towards the iso-orientation domain. However, both local and long-range horizontal connections of the layer 2/3 network are biased towards the iso-orientation domains. We hypothesize that the patchy layout of the layer 2/3 long-range connections is a consequence of excitatory cells targeting mainly other excitatory cells located in distal iso-orientation domains. Furthermore, both networks demonstrate dense local and sparse distal connectivity.

10.1 Introduction

The columnar organization of the neocortex [6,15] is one of the most influential findings in neuroscience [16]. Hubel and Wiesel [15] found that the striate cortex (primary visual cortex) is composed of orientation minicolumns each one comprising some hundreds of excitatory cells and a smaller number of inhibitory interneurons of different kinds. Vertical penetration of the cortex showed that contrast edge orientation is coded such that the cells in each orientation minicolumn respond selectively to a broad range of orientations. Furthermore, orientation selectivity was shifted smoothly during horizontal penetration. One decade earlier, Hubel and Wiesel [1] addressed the fundamental question of the orientation selectivity of the cortical cells. The proposed model of orientation selectivity, which is known as the 'feedforward' model, relies heavily on the arrangement of the thalamic afferents. According to this arrangement, the ON-center LGN cells converge on the ON-subregions of a simple cell's receptive field (RF). The OFF-subregions of a simple cell were constructed in the same way by the OFF-center LGN cells (see also [2]). Still today the Hubel and Wiesel feedforward model serves as a model of the thalamocortical circuitry. However, some of the orientation selectivity properties are not possible to predict by the feedforward model [3]. Contrast invariance of orientation tuning is one such example. As contrast increases the height of the response curve increases while the width remains almost constant [21]. Furthermore, the psychophysical studies examining the long-range spatial interactions within the visual cortex clearly

demonstrate that the cortical circuitry plays a major role in cortical cell responses. Polat and Norcia [5] demonstrated that elongation of a Gabor patch along the orientation axis results in facilitation of the responses of the cells in visual cortex, probably as an effect of summation fields.

Since the discovery of the patchy layout of the layer 2/3 long-range horizontal connections [13], the layout and the function of intracortical connections have started to drawn more attention. It is now widely accepted that the long-range horizontal connections of the superficial layers are a prominent feature of the visual cortex [7–14]. More recent studies on a variety of species have confirmed the patchy, iso-orientation biased, layout of these connections [7,8,10,12]. A study by Kisvárday et al. [10] shows that 56.2% of the excitatory local connections target the iso-orientation (±30º) domain. Oblique- (±30–60º) and cross-orientation (±60–90º) domains receive 28.4 and 15.3 per cent of the connections respectively. Long-range connections show a similar pattern, i.e. 40.0% of them descending from the injection site are targeting the iso-orientation domains, 36.9% the oblique-, and 23.1% the cross-orientation domains. Same study reveals also that only 30% of the excitatory connections from an injection site, in area 17 of cat, are defined as distal (>0.5 mm), and thus the majority of the connections target nearby cells. A recent study by Chisum et al. [8] reveals the fall-off in bouton distribution as a function of distance from an injection site. Number of boutons along the preferred axis is down to 15% of the maximum only 0.7 mm from the injection site. At 1.4 mm the number of boutons is roughly 5% of the maximum. The decrease along the orthogonal axis is even more dramatically. Thus, axial specificity of the layer 2/3 long-range connections is prominent. Chisum et al. [8] show that the dramatic fall-off with distance implies that most long-range connections are between neurons for which the RFs overlap by at least 50%. Furthermore, the long-range horizontal connections are to be responsible for the summation field of the neurons. Chisum et al. [8] observe also the similarity between the elongated RF and axial specificity of the long-range connections.

Surprisingly, the long-range horizontal connections found in the layer 4 have drawn much less attention. Layer 4 is the main recipient of the thalamic input, and the simple cells found in the cat layer 4 are well tuned for orientation [1,2]. Thus, the interplay between the orientation map and the layout of long-range connections is essential for understand the origins of orientation selectivity. The findings suggest that the layout of the layer 4 long-range horizontal connections is different from those found in the superficial layers [8,10,11,14]. Their extent is only 50% of the long-range connections of the superficial layers [10]. Furthermore, Yousef et al. [11] found that layer 4 long-range connections (of area 18) are hardly biased towards iso-orientation domains. 35.4% of the connections (>740 μm) targeted the iso-orientation domain. Oblique- and cross-orientation domains received 33.7% and 30.9% of the connections respectively. The pattern shown by the local connections (<740 μm) is different. The local iso-orientation domain receive

60.0% of the connections, while 22.0% of the connections are targeting the oblique- and 18.0% the cross-orientation domains. Note that as much as 40% of the local connections are targeting oblique- and cross-orientation domains. Inhibitory long-range horizontal connections extent only one third to one half of the excitatory network, and the excitatory ones outnumber them. Thus, majority of the long-range connections are considered to be excitatory in both layer 4 and layer 2/3 [10]. It seems that independent of the layer, the excitatory long-range horizontal connections are neither random nor restricted to iso-orientation domains. Consequently cross-talk between different orientation domains is a prominent feature of both the layer 4 and the superficial layers.

The Bayesian Confidence Propagation Neural Network (BCPNN) has been developed in analogy with the known generic cortical structure [24]. This is an abstract neural network architecture in which each unit corresponds to a cortical minicolumn. The learning rule is based on Hebb's ideas on synaptic plasticity and emergence of cell assemblies [26]. Thus, correlated activity reinforces the connections between the units. Anti-correlated activity results in weakening of a connection, and emergence of an inhibitory one. The network is partitioned into hypercolumn-like modules and the summed activity within each hypercolumn is normalized to one. A biologically plausible model of a hypercolumn module based on the BCPNN was presented recently [28].

A quantitative assessment of the local and long-range horizontal connections within two separate models, of layer 4 and superficial layers, of the striate cortex is presented. Long-range horizontal connections of the layer 4 network target all orientation domains in a balanced manner, whereas local connections are biased towards the iso-orientation domain. The pattern shown by the layer 2/3 network is different. Both local and long-range horizontal connections are biased towards the iso-orientation domains. We hypothesize that the patchy layout of the layer 2/3 long-range connections is a consequence of excitatory cells targeting mainly other excitatory cells located in distal iso-orientation domains. Both networks demonstrate dense local and sparse distal connectivity as a result of fall-off with distance. Furthermore, tests with contrast edges indicate that both layer 4 and layer 2/3 networks can detect contrast edges, which have low contrast. However, these tests need to be verified quantitatively.

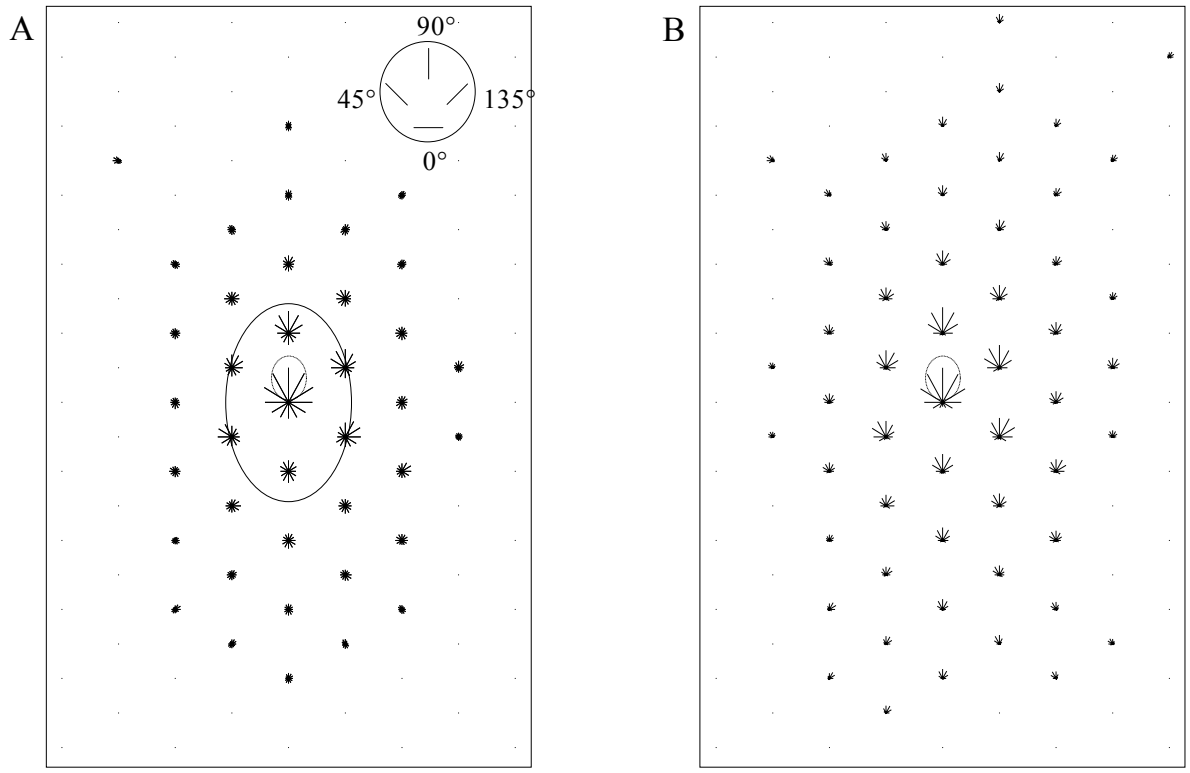

Figure 10.1. *A*, Layer 4 network connections, which originate from the abstract injection positioned at 90º (illustrated with the dotted oval in the middle), visualized by 9x11 polar-plots organized as the network model. Each polar-plot represents a hypercolumn module. The legend (top right) shows the orientation of the units in each polar-plot, consequently the relative spatial phases are ignored. Distance from the origin is proportional to the strength of the connection. The oval marks the RFs of units detecting vertical lines inside the host hypercolumn. We see that these units' RF overlap with many other hypercolumns, and hence indicate strong overlap between RF of units situated in neighboring hypercolumns. Note the elongated shape of the long-range connections. *B*, Same as *A* but for the layer 2/3 network connections.

10.2 Network Model

As stated before the columnar organization of the striate cortex [15] is the main influence of our network model. We hypothesize that V1 is composed of repetitive structures, i.e. orientation minicolumns. We assume further that the orientation minicolumns can be grouped around hypothetical centers, the so-called pinwheels [18], to form modules we refer to as hypercolumns. We hypothesize that a

hypercolumn can be built from a finite number of orientation minicolumns each one representing a unique orientation. The network model used during the simulations consists of 99 (9x11) hypercolumns arranged to form a hexagonal array. The diameter of the circular hypercolumns, and thus the distance between two adjacent hypercolumns is 0.7 mm [19]. The size of the network model in cortical dimensions is 5.6x8.1 mm. The distance between the RF centers of two adjacent hypercolumns corresponds to 0.5º of visual angle (at 5º of eccentricity [19]). The visual field covered by the model is 4.5x7.3º. Note that the modeled cortical patch, and hence the visual field covered by the network model is elongated. This shape was chosen after observing the axial specificity of the long-range horizontal connections, and having the computational limitations in mind. However no artifacts related to corner effects due to the elongated shape of the network model was observed during the simulations.

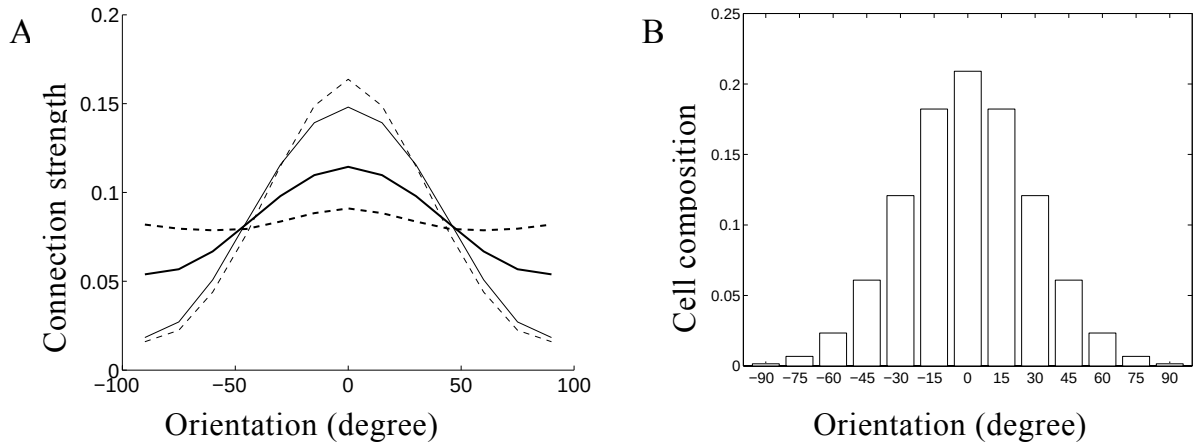

Figure 10.2. *A*, Fraction of the layer 4 local (solid thick line) and long-range (dashed thick line) connections as a function of the deviation from the mean orientation selectivity at the abstract injection site. Long-range connections are equally distributed, whereas local connections are biased towards the iso-orientation domain. Furthermore, both layer 2/3 local (solid thin line) and long-range (dashed thin line) connections are biased towards the iso-orientation domains. *B*, Composition of the abstract injection sites for layer 4 and layer 2/3 networks. Spread of orientations inside these regions correspond roughly to that of an iso-orientation domain and is less than those in *A*.

Each layer 4 hypercolumn consists of 24 units, representing 12 orientations. The difference in orientation selectivity between two successive units inside a model hypercolumn is 15°. Observe that having this configuration, we represent every orientation twice with two so-called anti-correlation units. These anti-correlation units represent the same orientation. But they have opposite relative and absolute

spatial phases, so that the units' subfields with opposite sign overlap. The RF centers of the units belonging to a model hypercolumn are positioned in the center of their host hypercolumn. As a consequence of this arrangement, the units belonging to a hypercolumn analyze the same spot of the visual field. Furthermore, as shown by the oval, which represents RFs of units detecting vertical lines, there is a strong overlap between the RF of units situated in neighboring hypercolumns (Fig. 10.1A). The RFs of the units are designed as contrast edge detectors, and hence are composed of two subregions with opposite sign. Orientation tuning of the LGN input is 40º at half-width at half-height [20], suggesting a subfield aspect ratio of 3:1. The RF width is 1º [19], and hence the RF height is 1.5º. All units are tuned for the same spatial frequency of 1 cycle/degree [19]. The thalamic input of the units is computed using a model developed by Troyer et al. [23].

The inhibition is mediated by local interneurons. Recently, Hirch et al. [4] reported inhibitory simple cells, which have good orientation tuning, and complex inhibitory cells that are untuned for orientation. We assume that the inhibitory simple cells can mediate local inhibition to excitatory simple cells. We hypothesize further that the opponent inhibition theory proposed by Ferster [22] can explain the local circuitry of inhibitory and excitatory simple cells. Opponent inhibition implies that the presynaptic inhibitory simple cell has opposite absolute spatial phase as the postsynaptic excitatory cell. Furthermore, the cells' subfields with opposite sign overlap, i.e. they have opposite relative spatial phase. We hypothesize that the inhibitory complex cells reported by Hirch et al. [4] can regulate the total activity of the excitatory cells in a region, which corresponds to a hypercolumn.

10.3 Simulation Results

The simulations are divided into two phases. During the first phase, we intent to show that the incremental BCPNN learning rule can develop a network that quantitatively resembles layer 4 local and long-range connectivity. During the second phase, the objective is to show that layer 2/3 local and long-range connectivity can be derived based on the results from the first phase and additional simulations.

The incremental BCPNN learning rule [24] develops the fully connected recurrent network of units. The result is a weight matrix, which contains information on the degree of correlation between pairs of units located in the different regions of the network. Briefly, the incremental BCPNN learning rule behaves in the following way. If two units are correlated during a time step, the connection between them strengthens. This corresponds to the creation of an excitatory connection. However, anti-correlation between two units will result in an inhibitory connection (via a local inhibitory interneuron [4,22]). We assume

that the excitatory long-range connections can mediate long-range inhibition through local inhibitory interneurons. We hypothesize that interneurons can inhibit excitatory simple cells in their close surroundings as proposed by the opponent inhibition theory [22]. If units are uncorrelated, the weight will fluctuate around zero value. Thus, the weight between two units is a measure of the correlation between them during the training sequence. The weight matrix is symmetric, and hence can be interpreted both as connections from one unit to all units in the network, and connections from all units into one. Training of the fully connected network lasts for 1000 simulation steps. The time step is defined as 1 second, and hence the simulation duration corresponds to 1000 seconds. The learning rate, which defines the degree of weight modification, is 0.005 [15]. At every time step, the activity levels of the units are initiated with a new arbitrary contrast edge stimulus. The position and the orientation of the stimulus are sampled from a uniform distribution. The stimulus width is 1º, and its spatial frequency is 1 cycle/degree. Observe that for convenience, the width and the spatial frequency of the stimulus is the same as that of the RFs. Noise is added to the activity levels through several steps. First a normally distributed noise with a standard deviation of 10% of the so-called bias value is added. The bias value is defined as the mean activity of an arbitrary unit inside a hypercolumn in absence of stimulus. The activity levels are rectified so that all negative activity levels are set to zero, and a 5-10% uniform distribution noise is added to all units to simulate the background activity. Later the activity levels are normalized so that the sum of activities in each hypercolumn is equal to one, as required by the incremental BCPNN learning rule. The contrast of the stimulus is 100%, though the effect of high noise in combination with the normalization procedure lowers this level considerably.

Recently we reported the behavior of a layer 4 network similar to the current network [25]. We saw that the long-range connections have facilitory effect on the units. This result was in line with the elongated summation pools proposed by Polat et al. [27]. The network could detect a noisy contrast edge much faster in presence of the intracortical connections. As revealed by the weight matrix, the modular specificity of the long-range connections targeting excitatory cells was prominent. Cross-orientation domains were inhibited through excitatory long-range connections targeting local inhibitory interneurons. However, quantitative values on corticocortical connections reported by Yousef et al. [11] and others are based on connections from cells located inside an injection site, which can be 200–400 μm across, i.e. roughly an iso-orientation domain. Inside such a patch we find cells with a broad range of orientation preferences. Note that the information available as the weight matrix is fundamentally different from the data on the connections from an injection site. As a consequence, an abstract injections site, which corresponds to a typical iso-orientation domain, is constructed (Fig. 10.2*B*). Spread of orientation preferences inside an orientation minicolumns is also an important factor while constructing an abstract injection site. Note that Murphy and Sillito [17] reported that orientation selectivity could vary 9–18º inside an

orientation minicolumn. To enable a quantitative assessment, the connections originating from the abstract injection site are divided into local connections, i.e. connections to the units inside the so-called host hypercolumn, and long-range connections, i.e. connections to units located in all other hypercolumns. The abstract injection site is located inside the host hypercolumn. Connection strengths from this abstract injection site is defined as the weighted sum of connections from each one of the units participating in the connection. The size of this weight corresponds to a fraction that defines the occurrence of neurons with a given orientation selectivity inside the injection site, which has the size of an iso-orientation domain (Fig. 10.2*B*). The strength of the connections is visualized as polar-plots (Fig. 10.1*A*). Connections to distal hypercolumns, which are >15% of the connections within the host hypercolumn are plotted and used during the quantitative assessment. Calculations show that 43.3% of the local connections target the iso-orientation domain (Fig. 10.2*A*). Oblique-orientation domain's share of the local connections is 33.1%, and the cross-orientation domain receives 23.6% of the local connections. However, the distribution of the excitatory long-range connections differs prominently. Only 35.5% are targeting the iso-orientation domains. The oblique- and cross-orientation domains receive, respectively, 32.4 and 32.1 per cent of the connections. These values are close to reported values of Yousef et al. [11]. To test the parameter dependencies, the abstract injection site was set to infinity, i.e. nearly the whole model. The distributions were almost equal for all three orientation domains, both for local and distal connection. Iso-orientation domains were targeted by 34.6% of the connections, while 33.7 and 31.7 per cent of the connections targeted oblique- and cross-orientation domains respectively.

The patchy layout of the layer 2/3 long-range connections is investigated by a series of simulations. The layer 2/3 network used during the simulations has similar set up as the previous networks, which were used to investigate the layer 4 connectivity. However, now the units have complex cell RFs, and hence only 12 units are needed in each hypercolumn instead of 24 as earlier. Input to a complex cell unit is defined as the sum of rectified inputs to the anti-correlation unit pairs, found in the layer 4 network, having the same orientation selectivity as the complex cell unit. Note that the anti-correlation pairs have same orientation selectivity but opposite relative spatial phase, i.e. they detect the same orientation but opposite phase. We hypothesize that the patchy layout of the layer 2/3 network is, at least partially, a consequence of excitatory cells targeting mainly other excitatory cells located in distal iso-orientation domains. To test this hypothesis the excitatory connections targeting the inhibitory interneurons are removed (Fig. 10.1*B*). The distribution of the long-range connections from the abstract injection site is 58.4% to iso-, 31.4% to oblique- and 10.2% to cross-orientation domains (Fig. 10.2*A*). Local connections show a similar pattern. The iso-orientation domain receives 54.3% of the connections. Oblique- and cross- orientation domains receive 33.4 and 12.3 per cent respectively. Kisvárday et al. [10] report a similar

distribution for the local connections, whereas the long-range connections reported by Kisvárday et al. [10] are less orientation specific.

The fall-off with distance for both layer 4 and layer 2/3 networks is less than the reported values by Chisum et al. [8]. We found that the degree of overlap between RFs of units situated in adjacent hypercolumns is one decisive factor that controls the degree of fall-off. When the distance between the RF centers of two adjacent hypercolumns increased, the extent of the long-range connections is reduced (not shown here). A consequence of the fall-off with distance is dense local and sparse distal connectivity demonstrated by both networks. Furthermore, the elongated shape of the long-range connections of both networks matches well the RF aspect ratio of the units. These findings are in line with the reported similarities between RF shape and the extent of the long-range connections by Chisum et al. [8]. Furthermore, preliminary results indicate that both networks can detect low contrast (15%) stimulus, defined as contrast edge. However, to confirm this observation and investigate the optimal extent of the long-range horizontal connections, in relation to the RF sizes and shapes, additional simulations must be carried out.

10.4 Discussion

We presented a quantitative assessment of the layer 4 and layer 2/3 local and long-range horizontal connections based on two separate models. Our results show that layer 4 long-range horizontal connections target all orientation domains in a balanced manner, whereas layer 4 local connections are biased towards the iso-orientation domain. However, the layer 2/3 network is significantly different. Both local and long-range horizontal connections of the layer 2/3 network are biased towards the iso-orientation domains. We hypothesize that the patchy layout of the long-range connections is a consequence of excitatory long-range connections targeting mainly other excitatory cells located in distal iso-orientation domains. Furthermore, the fall-off with distance results in dense local and sparse distal connectivity for both networks. Preliminary results indicate that the layer 2/3 network, like the layer 4 network, can detect low contrast stimulus. We intend to confirm this observation by further simulations in the near future. The optimal extent of the long-range horizontal connections, in relation to the RF sizes and shapes, needs also be investigated more carefully.

References

[1] D.H. Hubel & T.N. Wiesel, Receptive fields, binocular interaction and functional architecture in the cat's visual cortex. *J. Physiol.*, 160:106–154, 1962.

[2] R.C. Reid & J.M. Alonso, Specificity of monosynaptic connections from thalamus to visual cortex. *Nature*, 378:281–284, 1995.

[3] D. Ferster & K.D. Miller, Neural Mechanisms of Orientation Selectivity in the Visual Cortex. *Annual Reviews of Neurosci.*, 23:441–471, 2000.

[4] J.A. Hirch, J.-M., Alonso C. Pillai & C. Pierre, Simple and complex inhibitory cells in layer 4 of cat visual cortex. *Soc. Neurosci. Abstr.*, 26, 1083, 2000.

[5] U. Polat & A.M. Norcia, Elongated physiological summation pools in the human visual cortex. *Vision Res.*, 38, 3735–3741, 1998.

[6] V.B. Mounthcastle, Modality and topographic properties of single neurons of cat's somatic sensory cortex, *J. Neurophysiol.*, 20:408–434, 1957.

[7] K.E. Schmidt, D.-S. Kim, W. Singer, T. Bonhoeffer & S. Löwel, Functional Specificity of Long-Range Intrinsic and Interhemispheric Connections in the Visual Cortex of Strabismic Cats, *J. Neurosci.*, 17(14):5480–5492, 1997.

[8] H.J. Chisum, F. Mooser & D. Fitzpatrick, Emergent Properties of Layer 2/3 Neurons Reflect the Collinear Arrangement of Horizontal Connections in Tree Shrew Visual Cortex, *J. Neurosci.*, 23(7):2947–2960, 2003.

[9] C.D. Gilbert & T.N. Wiesel, Columnar specificity of intrinsic horizontal connections and corticocortical connections in cat visual cortex. *J. Neurosci.*, 9:2432–2442, 1989.

[10] Z.F. Kisvárday, E. Tóth, M. Rausch & U.T. Eysel, Orientation-specific Relationship Between Populations of Excitatory and Inhibitory Lateral Connections in the Visual Cortex of the Cat. *Cerebral Cortex*, 7, 605–618, 1997.

[11] T. Yousef, T. Bonhoeffer, D.-S. Kim, U.T. Eysel, E. Tóth & Z.F. Kisvárday, Orientation topography of layer 4 lateral networks revealed by optical imagining in cat visual cortex (area 18). *E. J. of Neurosci.*, 11:4291–4308, 1999.

[12] W.H. Bosking, Y. Zhang, B. Schofield & D. Fitzpatrick, Orientation Selectivity and the Arrangement of Horizontal Connections in Tree Shrew Striate Cortex. *J. Neurosci.*, 17(6):2112–2127, 1997.

[13] K.S. Rockland & J.S. Lund, Widespread periodic intrinsic connections in the tree shrew visual cortex. *Science*, 215, 1532–1534, 1982.

[14] K.E. Schmidt & S. Löwel, Long-range Intrinsic Connections in Cat Primary Visual Cortex. In B.R. Payne, A. Peters (eds.). *The Cat Primary Visual Cortex*, Chapter 10. Ac. Press, 2002.

[15] D. Hubel, T.N. Wiesel, The functional architecture of the macaque visual cortex. The Ferrier lecture. *Proc. Royal. Soc. B.*, 198:1–59, 1977.

[16] V.B. Mountcastle, The columnar organization of the neocortex, *Brain*, 120, 701–722, 1997.

[17] P.C. Murphy & A.M. Sillito, Continuity of orientation columns between superficial and deep laminea of cat primary visual cortex, *J. Physiol.*, 381, 95–110, 1986.

[18] V. Braitenberg & C. Braitenberg, Geometry of the orientation columns in the visual cortex. *Biological Cybernetics*, 33:179–186, 1979.

[19] R.L. De Valois & K.K. De Valois, *Spatial Vision*, Chapter 4, Oxford Sci. Pub, 1990.

[20] S. Chung & D. Ferster Strength and Orientation Tuning of the Thalamic Input to Simple Cells Revealed by Electrical Evoked Cortical Suppression. *Neuron*, 20, 1177–1189, 1998.

[21] G. Sclar & R.D. Freeman, Orientation selectivity in the cat's striate cortex is invariant with stimulus contrast, *Exp. Brain Res*., 46:457–461, 1982.

[22] D. Ferster, Spatially opponent excitation and inhibition in simple cells of the cat visual cortex, *J. Neurosci.*, 8, 1172–1180, 1988.

[23] T.W. Troyer, A.E. Krukowski & K.D. Miller, LGN Input to Simple Cells and Contrast-Invariant Orientation Tuning: An Analysis. *J. Neurophysiol.*, 87:2741–2752, 2002.

[24] A. Sandberg, A. Lansner, F.M. Petersson & Ö. Ekeberg, A Bayesian attractor network with incremental learning. *Network: Computing in Neural Systems*, 13(2):179–194, 2002.

[25] B. Çürüklü & A. Lansner, Layout and Function of the Distal Projections within the Striate Cortex, *submitted to NIPS*, 2003.

[26] D.O. Hebb, *The Organization of Behavior*, New York: Wiley, 1949.

[27] U. Polat & A.M. Norcia, Elongated physiological summation pools in the human visual cortex. *Vision Res.*, 38, 3735–3741, 1998.

[28] B. Çürüklü & A. Lansner, An Abstract Model of a Cortical Hypercolumn, *Proc. of Int. Conf. on Neural Information Processing*, 80–85, 2002.

11 Paper V – On the development and functional roles of the horizontal connections within the primary visual cortex (V1)

Baran Çürüklü[1] and Anders Lansner[2]

[1]Department of Computer Science and Engineering, Mälardalen University, Västerås, SE-72123, Sweden
[2]Department of Numerical Analysis and Computer Science, Royal Institute of Technology, SE-10044 Stockholm, Sweden

Technical Report, February 2005.

Abstract

A laminar V1 model consisting of layers 4 and 2/3 is presented. The model is in line with the modular structure of the neocortex and addresses development of the horizontal connections within V1. Later, the functional roles of the horizontal connections are addressed. The neurons populating the layer 4 model exhibit sharp orientation selectivity despite poorly tuned LGN input. Sharp orientation selectivity is achieved through (i) control of the total activity of the modeled hypercolumns by normalization inhibition, and (ii) providing layer 4 units with information from a larger region than their classical receptive fields. This laminar V1 model addresses configuration-specific facilitation phenomena as well. Elongated layer 2/3 summation pools demonstrate that collinearly configured stimuli are easier to detect than orthogonally (or circularly) configured stimuli.

11.1 Introduction

Neurons found in V1 respond selectively to the orientations of bar-like stimuli (Hubel and Wiesel, 1962), whereas retinal ganglion cells and neurons that populate the lateral geniculate nucleus (LGN) prefer small point-like stimuli (Kuffler, 1953; Kaplan and Shapley, 1982). Since its discovery, the orientation selectivity (OS) property of the V1 neurons has drawn much attention (Das, 1996; Sompolinsky and Shapley, 1997; Ferster and Miller 2000; Martin, 2002). It is hypothesized that emergence of this property demonstrates how the incoming sensory information is represented by the neocortex.

In cat V1, OS is evident already in the simple cell dominated layer 4, which is the main recipient of the thalamic input (Hubel and Wiesel, 1962). According to the Hubel-Wiesel model, which is the earliest model of the OS, the receptive fields (RF) of simple cells are composed of alternated ON (light preferring) and OFF (light preferring) subfields (Hubel and Wiesel, 1962). The Hubel-Wiesel model assumes that ON subregions of the simple cells emerge through projections of the ON-center LGN cells. OFF subregions of these neurons emerge similarly, i.e. through the projections that originate from the OFF-center LGN cells. This model assumes that the RF are strongly elongated along the axis that coincides with the simple cells' preferred orientations. According to this assumption an elongated region of the visual field is covered by the RF of the LGN cells that project to a simple cell's subfield. Thus, the anisotropy seen in the subfields is explained solely by the projections from the LGN. The Hubel-Wiesel model addresses

emergence of OS in layer 4 of cat V1 in a pure feedforward fashion without and involvement of the intracortical connections.

Recently, emergence of OS (and contrast-invariance of orientation tuning) has been addressed by a more complex feedforward model (Troyer et al., 1998; Kayser and Miller, 2002; Lauritzen and Miller, 2003), which assumes opponent inhibition (Ferster, 1988). Like the Hubel-Wiesel model the opponent inhibition model assumes that the LGN input is well tuned for orientation. It also assumes that the LGN input has an additional component, which depends solely on stimulus contrast (Troyer et al., 2002). According to the opponent inhibition model a network that comprises two functionally distinct (simple and complex) inhibitory sources (Ferster, 1988; Hirsch et al., 2000; 2003) explains sharpening of the (already well tuned) LGN input, and the silencing of the component of the LGN input, which depends solely on the stimulus contrast (Lauritzen and Miller, 2003).

A number of studies have shown that the subfields of the simple cells are indeed elongated in several species, e.g. cats (Jones and Palmer, 1987; Pei et al., 1994; Reid and Alonso, 1995), and ferrets (Chapman et al., 1991). Jones and Palmer (1987) report that mean width-to-length aspect ratio of a simple cell RF having two subfields is roughly 1:1.5. These results support the existence of a thalamocortical circuitry, which is assumed by the feedforward models. However, reported aspect ratio values of the full RF, and individual subfields cannot explain sharp tuning, which is demonstrated by the V1 neurons. Orban (1984) has shown that in average simple cells respond selectively to a narrow band of orientations, i.e. ~20º at half-width at half-height. This requires stronger anisotropy in the RF than the reported values.

An essential support for the feedforward models is the cooling experiment conducted by Ferster et al. (1996). In this work the activity of the V1 neurons is reduced by cooling down the cortex to ~9ºC. During the experiment LGN is intact, and hence is the main source of input of the V1 neurons. The authors show that despite the cooling procedure V1 neurons are orientation selective. However, this support is only qualitative, since as a result of the cooling procedure the V1 neurons respond selectively to an orientation band of ~45º (half-width at half-height), which is considerably broader than the reported values (Orban, 1984). Furthermore, as pointed out by Sompolinsky and Shapley (1997), in Ferster et al. (1996) only the first harmonic of the responses are used when the tuning curve is calculated, and hence responses that are untuned for orientation are ignored. Based on these findings, Sompolinsky and Shapley (1997) argue that the results of Ferster et al. (1996) indicate that the simple cell RF have low aspect ratios. Thus, it is plausible to assume that the emergence of OS cannot be explained solely by the thalamocortical circuitry.

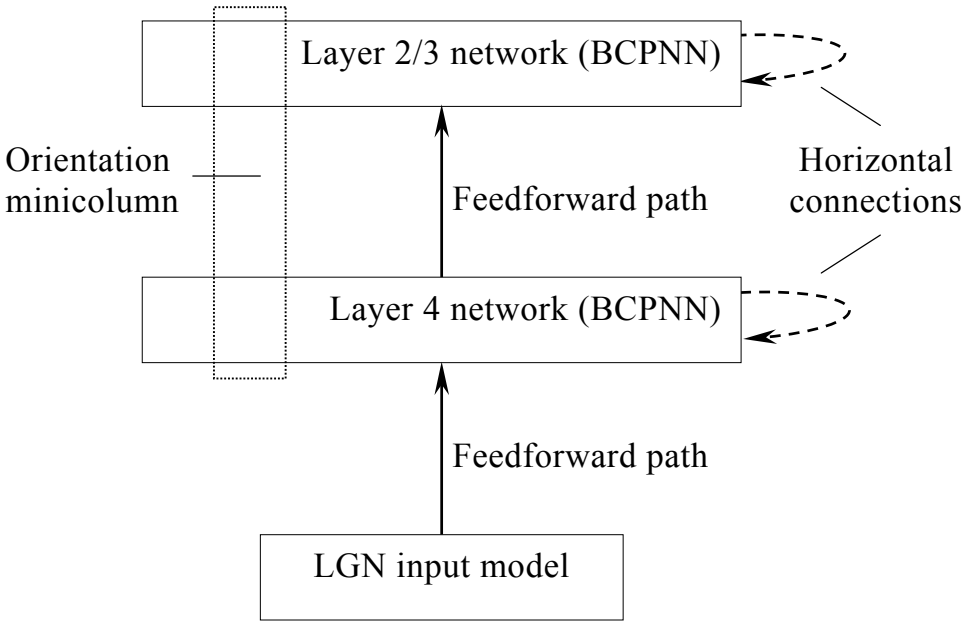

Figure 11.1. Illustration of the information flow within the V1 model. External input source of the layer 4 network is the LGN (solid line). Layer 2/3 units receive their external inputs from the layer 4 units (solid line). In both cortical layer models internal input is from other units in the same layer. This input is mediated by the horizontal connections (dashed lines). The feedforward path (solid lines), which consists of LGN → layer 4 → layer 2/3 is fixed, while the horizontal connections (see Figs. 11.2 and 11.6) are subject to change during the learning phase. Both the feedforward path and the horizontal connections are classified as excitatory. The horizontal connections target either other units directly (E→E), or through inhibitory interneurons (E→I), which are located in the near surrounding of the target units.

An alternative approach to address the emergence of OS is taken by the recurrent models (Ben-Yishai et al., 1995; 1997; Somers et al., 1995; 2002; McLaughin et al., 2000; Wielaard et al., 2001). In contrast to the feedforward models, these models assume that the LGN input is poorly tuned for orientation. This assumption is in line with results on mildly elongated RF. Based on this assumption the recurrent models demonstrate that sharp orientation tuning emergences mainly through lateral interactions mediated by the horizontal connections. Recurrent models assume that the result of the lateral interactions is the manifestation of the so-called Mexican Hat activity pattern, which guarantees that the neuron activities are considerably higher in the center of this active region than in the surroundings. However, the recurrent models achieve the Mexican Hat activity pattern either by an odd arrangement of the horizontal connections (Ben-Yishai et al., 1995; 1997; Somers et al., 1995; 2002) or by extremely strong inhibition (McLaughin et al., 2000; Wielaard et al., 2001) (see Martin (2002) for a critical review of feedforward and recurrent models of hypercolumns).

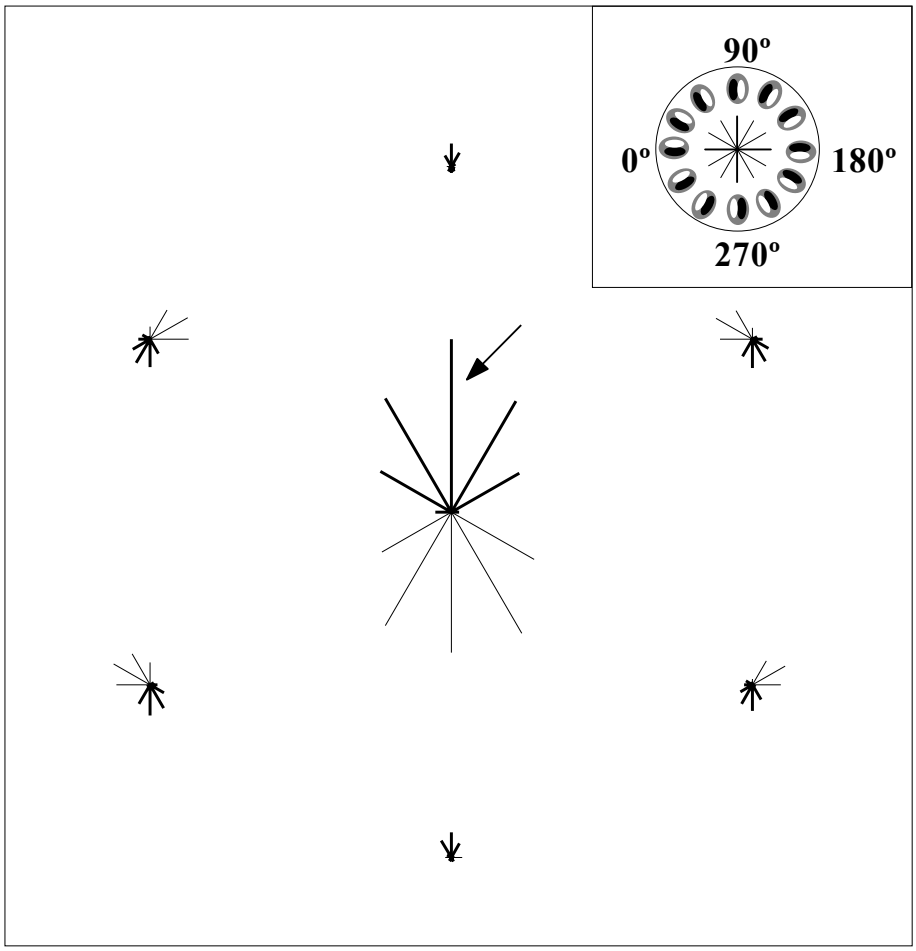

Figure 11.2. Illustration of the layer 4 reference unit's (marked with an arrow) isotropic summation pool consisting of seven hypercolumn-modules represented by as many polar graphs. The legend (top right) shows orientation preference as well as relative spatial phase of presynaptic units. Thick lines represent connections that target the reference unit directly (E→E), whereas thin lines correspond to projections to the inhibitory interneurons that are part of the reference unit (E→I). Since the connection matrix is symmetric polar graphs can be interpreted as projections of the reference unit as well. The length of the lines (in polar graphs) is proportional to the strength of the corresponding connections.

According to the connection pattern proposed in Ben-Yishai et al. (1995; 1997) and Somers et al. (1995; 2002) inhibitory connections extend longer than their excitatory counterparts. Narrowly tuned excitatory input in combination with broadly tuned inhibition generates effectively the desired Mexican Hat activity pattern. However, as also pointed out in Martin (2002), the connection pattern in

layers 4 and 2/3 of the V1 is the opposite (Ferster, 1988; Kritzer et al., 1992; McDonald CT and Burkhalter 1993; Kisvárday et al., 1997; Hirsch et al., 2000; 2003; Roerig and Chen, 2002). Kisvárday et al. (1997) report that the inhibitory network is <50% of the excitatory network.

The influence of the horizontal connections over the response properties of the neurons extends beyond emergence of fundamental response properties, such as OS. There are evidences on (facilitative and suppressive) surround effects, which cannot be explained by the classical receptive fields (CRF) (Allman et al., 1985). It has been reported that the visibility of a grating stimulus improves when its size increases (Howell and Hess, 1978; Robson and Graham, 1981). Later, is has been shown that this visibility is closely related to stimulus configuration as well (Polat and Sagi, 1993; 1994a; 1994b; Polat and Norcia, 1998; Polat and Tyler, 1999; Chisum et al., 2003).

Polat and Norcia (1998) have addressed configuration-specific facilitation phenomena in human vision in low-contrast conditions. Authors propose that these phenomena reveal the non-linear interactions (summation in this case) between CRF and their non-linear surrounds. Based on measurements of visually evoked potentials in human visual cortex, the authors have shown that elongation of a foveally viewed circular Gabor patch has a positive effect on its visibility. Furthermore, elongation along the orientation axis (collinear configuration) results in a more prominent improvement in visibility than orthogonal elongation of the stimuli. Polat and Norcia (1998) propose that elongated summation pools, which probably emerge through long-range interactions, can explain phenomena related to configuration-specific facilitation.

Long-range horizontal connections have been found in a variety of species including tree shrew (Rockland and Lund, 1982; Fitzpatrick, 1996; Bosking et al., 1997; Chisum et al., 2003), ferret (Rockland, 1985; Durack and Katz, 1996), cat (Gilbert and Wiesel, 1983; 1989; Kisvárday et al., 1997; Schmidt et al., 1997; Yousef et al., 1999), and monkey (Rockland and Lund, 1983; Amir, 1993; Malach et al., 1993). These connections, which mainly arise from layer 2/3 pyramidal and spiny stellate cells, travel up to 4 mm on (cat) cortex surface and target mainly distal iso-orientation domains (referred to as modular specificity). Since an iso-orientation domain represents roughly 1/3 of the orientations these projections become also patchy. Furthermore, these connections terminate in a region that is elongated along the orientation axis of the source neurons (referred to as axial specificity).

A recent study shows that neurons, in layer 2/3 of tree shrew V1, have elongated RF, and are sharply tuned for orientation (Chisum et al., 2003). In addition, they perform length summation, which indicates that these neurons can integrate information from remote locations. Chisum et al. (2003) have shown that along the orientation axis of the neurons the size of these summations pools coincides well with the region covered by the layer 2/3 long-range horizontal connections. Furthermore, responses to the collinearly positioned Gabor patches

are stronger than responses to noncollinear constellations of Gabor patches. This result is interpreted as an indication of the axial specificity of the layer 2/3 long-range horizontal connections. According to Chisum et al. (2003) anatomical differences between layer 4 and layer 2/3 horizontal connections is reflected in the response properties of the neurons that populate these two layers. Layer 4 neurons lack far-reaching horizontal connections, which are common in layer 2/3 (Chisum et al., 2003). These neurons are also poorly tuned for orientation (Humphrey and Norton, 1980; Chisum et al., 2003), and do not exhibit length summation (Chisum et al., 2003).

It is not clear how and when the orientation map and the horizontal connections develop and take their final form. However, there seems to be a consensus on that the neurons respond selectively to stimulus orientation already at eye opening. This finding has been demonstrated on newborn kittens (Hubel and Wiesel, 1962; 1963; Blakemore and Van Sluyters, 1975; Buisseret and Imbert, 1976; Frégnac and Imbert, 1978; Albus and Wolf, 1984; Gödecke et al., 1997; Crair et al., 1998), ferrets (Chapman and Stryker, 1993; Chapman et al., 1996), and monkeys (Wiesel and Hubel, 1974). However, as pointed out in Chapman and Stryker (1993), reported values on the degree of orientation selectivity at the eye opening vary, even within the same species (in this case the cat). According to Hubel and Wiesel (1963) all neurons are orientation selective already at eye opening, whereas others are more conservative and suggest that 25–30% of the neurons respond selectively to stimulus orientation (Blakemore and Van Sluyters, 1975; Buisseret and Imbert, 1976; Frégnac and Imbert, 1978; Albus and Wolf, 1984).

It has also been reported that the overall shape of the orientation map remains unchanged when the newly opened eyes are subject to normal visual experience (Chapman et al., 1996; Crair et al., 1998; White et al., 2001). Thus, it seems that the genetic factors play an important role in the emergence of the orientation map, whereas the impact of the visual experience on this process is unclear (Gödecke et al., 1997; Crair et al., 1998; Chapman et al., 1999; Miller et al., 1999). However, after eye opening the neurons' selectivity to orientations increases significantly (Blakemore and Van Sluyters, 1975; Frégnac and Imbert, 1978; Chapman and Stryker, 1993; Chapman et al., 1996; Gödecke et al., 1997; Crair et al., 1998; White et al. 2001). Furthermore, this period coincides with the maturation of the horizontal connections. Note also that dark rearing or binocular deprivation can alter normal development of the orientation map, as well as the horizontal connections (Imbert and Buisseret, 1975; Chapman and Stryker, 1993; Chapman et al., 1996; White et al., 2001). These studies indicate that the orientation map continues to develop after the eye opening, and takes its final form through the interactions mediated by the developing thalamocortical circuitry, and the horizontal connections.

It is hypothesized that the layout of the horizontal connections plays an important role in the emergence of OS, and the manifestation of configuration-

specific facilitation phenomena. To address these issues a laminar model of the V1 is proposed and examined here.

11.2 Methods

11.2.1 Model overview

The model consists of layers 4 and 2/3 of V1 as well as the thalamic input to V1. Each modeled cortical layer is a Bayesian Confidence Propagation Neural Network (BCPNN) (Lansner and Ekeberg, 1987; 1989; Lansner and Holst, 1996; Holst, 1997; Sandberg et al., 2002; Sandberg, 2003). Modeled cortical layers are connected to each other in a feedforward manner (see Fig. 11.1 and Section 11.5.2). Consequently, information flow between the components of the model is LGN → layer 4 (BCPNN) → layer 2/3 (BCPNN). Layer 2/3 does not receive direct LGN input (Fig. 11.1).

The LGN is not modeled explicitly. Instead, input to V1 is calculated based on a simplified but realistic model of the thalamic input to the cortical neurons. The LGN cell response model proposed by Troyer et al. (2002) has been modified and extended to fit the proposed model (see Section 11.5.1).

The experiments consist of two distinct studies. In the first study, emergence of OS within the layer 4 is addressed. Later, configuration-specific facilitation phenomena in layer 2/3 are addressed. These studies aim to illustrate the influence of the fully developed horizontal connections on the manifestation of these two phenomena. Each study starts with the learning phase, during which the horizontal connections are developed. Network behavior is investigated in the retrieval phase. For simplicity the feedforward path (LGN → layer 4 → layer 2/3) is assumed to be non-plastic. Note however that we do not rule out the putative influence of the postnatal development of the thalamocortical circuitry, and the interlaminar connections on the manifestation of these phenomena, especially emergence of OS.

11.2.2 LGN input to V1

Modeled LGN input has two components (Troyer et al., 2002). The first component is a function of both stimulus orientation and stimulus contrast (Eq. 11.2). The second component is untuned for stimulus orientation, i.e. it is solely a function of stimulus contrast.

Since the V1 model addresses interactions near fovea, it is assumed that the LGN X cells are the main source of sensory input (Ferster, 1990). These cells have roughly linear contrast gain functions (Derrington and Lennie, 1984).

Consequently, it is assumed that the LGN input is a linear function of the stimulus contrast (Eqs. 11.4–11.6).

In the model the LGN input is poorly tuned for orientation (Eq. 11.1). The half-width of the tuning curve at half-height is 47.2º. This value is in line with reported values on low RF aspect ratios. The LGN input is also considered to be weak, despite the indications that the LGN EPSPs have higher amplitudes than the intracortical EPSPs (Stratford et al., 1996). Weak LGN input is in line with the finding that most synapses in layer 4, which is the main recipient layer of the thalamic input to the cortex, are of cortical origin. Among the synapses that target a layer 4 neuron, between ~4% (Garey and Powell, 1971; Hornung and Garey, 1981; Winfield and Powell, 1983; LeVay, 1986; Peters and Payne, 1993; Ahmed et al., 1994), and ~24% (LeVay and Gilbert, 1976; Einstein et al., 1987) originate from the LGN. In the model it is assume that 2/3 of the excitatory drive originate from layer 4, whereas 1/3 originate from the LGN input ($\Psi_{L4} = 2/3$, see Section 11.5.2).

11.2.3 V1 model

The modular structure of the neocortex has been the primary influence of the BCPNN (Mountcastle, 1957; 1978; 1997; Powell and Mountcastle, 1959; Hubel and Wiesel, 1962; 1977; Buxhoeveden and Casanova, 2002). Thus, a BCPNN consists of modules that are abstractions of hypercolumns (referred to as 'hypercolumn-modules' in the text). These hypercolumn-modules consist of units that correspond to cortical minicolumns (orientation minicolumns in the context of this paper). Activity of a unit is the mean firing rate of the population of neurons that the unit represents.

Each BCPNN comprises 49 (7x7) hypercolumn-modules, arranged to form a hexagonal array. The diameter of a hypercolumn-module is 1 mm (Kisvárday et al., 1997). The center-to-center distance in visual angle between two adjacent hypercolumn-modules is 1/(√3)º (~0.58º). Along the horizontal axis the distance between two adjacent hypercolumn-modules is 0.5º. The center-to-center distance, and hence the cortical magnification factor, is fixed throughout the network model.

The layer 4 hypercolumn-modules consist of 12 units, whereas their layer 2/3 counterparts comprise six units. The RF centers of the units are positioned in the center of their so-called host hypercolumn-modules. The RF of the layer 4 units are modeled as contrast edge detectors (Section 11.5.1). These units are tuned for the spatial frequency of 1 c/deg. For the simplicity all RF widths are 1º. Thus, there is a substantial overlap between units positioned in adjacent hypercolumn-modules. The difference in orientation preference between two successive layer 4 units inside a hypercolumn-module is 30º. Note that two units represent one orientation when the signs of their RF subfields are ignored. The RF of these two units have opposite absolute spatial phase relative to each other. There are six such anti-phase unit pairs in each layer 4 hypercolumn-module. Each layer 2/3 unit

receives input from an anti-phase pair located in the layer 4 hypercolumn-module below (Eq. 11.7). As a result, complex cell like RF of layer 2/3 units are generated. Only 10% of the excitatory drive of a layer 2/3 unit is from the layer 4 anti-phase pairs ($\Psi_{L23} = 0.1$). This ratio is in line with the finding that in layer 2/3 the main part of the input is from other layer 2/3 neurons.

The total activity within a hypercolumn-module is normalized to one (Eq. 11.8). This procedure is supported by the studies on response saturation phenomena of the V1 neurons (Maffei et al., 1973; Dean, 1981; Albrecht and Hamilton, 1982). Albrecht and Hamilton (1982) have shown that, as stimulus contrast increases, the neurons increase their activities up to the level of ~50–60% of their maximum response levels (determined by their electrical properties). This behavior is followed by rapid saturation and normalization. In the normalization phase the neurons have roughly constant responses, i.e. they do not increase their activities due to increase in stimulus contrast. It is thus hypothesized that mechanisms behind the normalization phenomenon play an important role in keeping the total activity within a cortical patch under a certain level.

Similar to the cortex, in the BCPNN normalization aims to limit the maximum activity. In the V1 model normalization is carried out simply by dividing the activities of the units with the total activity of their host hypercolumn-modules (Eq. 11.8). Observe that this procedure is purely mathematical. The detailed neuronal mechanisms have been addressed earlier in the cortical hypercolumn model derived from the BCPNN architecture (Çürüklü and Lansner, 2002). One important assumption was made on the linear response of the LGN cells to contrast stimulus increase (Derrington and Lennie, 1984). Thus, rapid saturation followed by normalization was explained solely by interactions within the model. One inhibitory neuron integrated the activity of the input layer excitatory neurons, and inhibited excitatory neurons found in the output layer (referred to as the normalization inhibition). This single inhibitory neuron represented a population of inhibitory neurons evenly distributed in a cortical hypercolumn. Since this inhibition become mainly a function of the stimulus contrast, its tuning relative excitatory inputs become less significant then in other recurrent models (Ben-Yishai et al., 1995; 1997; Somers et al., 1995; 2002). Such an inhibition can be mediated by a combination of inhibitory complex and simple cells (Hirsch et al., 2000; 2003; Krimer and Goldman-Rakic, 2001; see Section 11.5.2 for the details).

The BCPNN learning algorithm is correlation based, and hence if two units are correlated in a time step the connection between them strengthens (Eqs. 11.9–11.13). Anti-correlation results in development of an inhibitory connection via local inhibitory interneurons (Ferster, 1988; Hirsch et al., 2000; 2003). As a consequence, horizontal connections in the V1 model run between two units, and represent groups of excitatory axons that originate from one orientation minicolumn and target either excitatory or inhibitory neurons in the target

orientation minicolumn (these connections are referred to as E→E and E→I connections, respectively).

In layer 4 of cat, inhibitory simple cells inhibit excitatory simple cells that are located in their close surroundings if they have opposite absolute spatial phase relative their excitatory targets, i.e. their subfields with opposite sign overlap (Ferster, 1988). Absolute spatial phase refers to the position of the ON- and OFF-subregions with respect to the visual field. Based on Ferster (1988) it is hypothesized that anti-correlated units can inhibit each other by local or long-range E→I connections. In the BCPNN model this inhibition is implemented by a non-plastic inhibitory connection. Strength of this non-plastic connection is one, and hence the strength of the inhibition is given by the E→I connections. In contradiction to the normalization inhibition, latter form of inhibition is highly selective and connects anti-correlated units to each other. Thus, these two forms of inhibition have both different connectivity patterns, and functional roles.

Learning phase corresponds to the period that follows eye opening and continues for roughly four weeks (Crair et al., 1998; White et al., 2001). During this critical period the development of the cortex can be altered by visual deprivation. The learning phase is 10000 simulation time steps long. During each time step a new contrast edge stimulus is generated. Since the learning phase corresponds to a rather vague time period the learning time step is dimensionless, and is set to one. The network's learning capacity depends on the dimensionless learning rate $\alpha = 0.05$, which is the inverse of the learning time constant τ_L (Eqs. 11.9–11.13).

Position, orientation ($0^\circ \le \theta_{st} < 360^\circ$), and contrast ($0 \le c \le 1$) of the contrast edge stimuli are sampled from a uniform distribution. Their spatial frequency is 1 c/deg, width is 1º, and they are infinitely long. It is assumed that these contrast edge stimuli correspond to small fractions of real images, and hence mimic natural visual images seen by a small patch of the V1. After adding Gaussian noise with standard deviation of 5% to the units' activity values, correlations between pairs of units in each layer are calculated. Based on the degree of correlation weights and biases are updated. Thus, the weight matrix reflects the degree of correlation between unit pairs.

Retrieval time step as well as the membrane time constant (τ_C) of the units are 2 ms. Gaussian noise with standard deviation of 2.5% is added to LGN input before it is fed into the units, whereas the intracortical input is modified with a Gaussian noise with standard deviation of 5%. In the OS study the model is tested on detection of contrast edges. In the second study the stimuli are sinusoidal gratings.

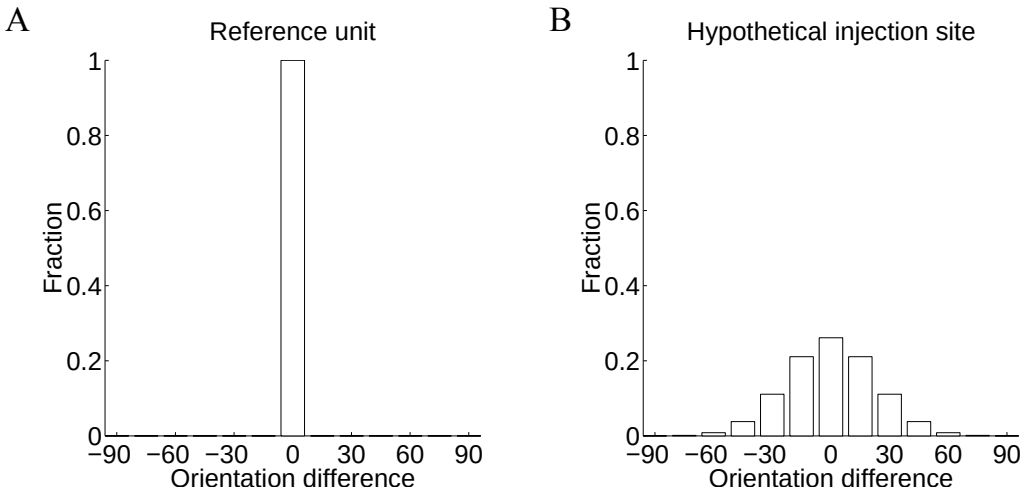

Figure 11.3. Distributions of the populations used in quantitative assessments. *A*. The population consists of the reference unit solely. *B*. The receiving population corresponds to an injection site, located at the reference unit.

	Iso-orientation (%)	Oblique-orientation (%)	Cross-orientation (%)
E→E (local)	49.2	34.0	16.8
(long-range)	50.4	32.8	16.8
E→I (local)	47.1	38.0	14.9
(long-range)	23.4	29.4	47.2
Total (local)	48.2	36.0	15.8
(long-range)	38.2	31.3	30.5

Table 11.1. Distribution of the horizontal connections that target the reference unit located in layer 4 (Fig. 11.3*A*). The projections are either direct, i.e. they target the reference unit though E→E connections, or indirect. In the latter case connections target the local interneurons through E→I connections. The distributions are calculated based on the sum of the log weights for each category. Local connections are within the same hypercolumn-module, whereas long-range connections travel between two hypercolumn-modules. The projections are classified as from iso-, oblique- and cross-orientation domains relative the reference unit.

	Iso-orientation (%)	Oblique-orientation (%)	Cross-orientation (%)
E→E (local)	40.8	33.3	25.9
(long-range)	40.6	33.2	26.2
E→I (local)	40.4	34.5	25.1
(long-range)	27.1	32.6	40.3
Total (local)	40.6	34.0	25.4
(long-range)	34.0	33.0	33.0

Table 11.2. Distribution of the horizontal connections that target the injection site located in layer 4 (Fig. 11.3*B*). These projections are either direct, i.e. they target the reference unit though E→E connections, or indirect. In the latter case connections target the local interneurons through E→I connections. The distributions are calculated based on the sum of the log weights for each category. Local connections are within the same hypercolumn-module, whereas long-range connections travel between two hypercolumn-modules. The projections are classified as from iso-, oblique- and cross-orientation domains relative the reference unit.

To see if the V1 model has detected the stimuli the units that are located in the center hypercolumn-modules are monitored (they are positioned in the center of the 7x7 network model (Fig. 11.2)). In the OS study center hypercolumn-module of the layer 4 is monitored, whereas in the second study its layer 2/3 counterpart is monitored. Since the BCPNNs are configured as attractor networks, the monitored center hypercolumn-module will converge to an orientation, which is represented by a unit (this applies to all other hypercolumn-modules as well). If the orientation preferences of that unit and the stimulus are same, it is assumed that the V1 model has detected the stimulus (in the text the unit, which represents the orientation of the stimulus, is referred to as the reference unit). However, if the center hypercolumn-module has converged towards another orientation the stimulus has not been detected.

A simulation continues until an orientation has been detected, or if this does not occur the simulation is terminated after 200 ms. This time period is considered to be sufficient for a convergence to occur. By definition, convergence occurs when the following three requirements are fulfilled simultaneously in the monitored center hypercolumn-module: (i) any unit's activity is >0.75 (recall that the total activity is 1 in a hypercolumn-module), (ii) between two consecutive time steps mean difference in activity for the units is <0.1, and (iii) requirements (i–ii) must be valid for a time period of 20 ms.

Simulation results are evaluated quantitatively by measuring confidence in convergence, and mean convergence times. Confidence is the number of correct detections divided by the number of trials for each simulation setting. High confidence means sharp tuning. The second measurement is the mean time for correct convergences, for each simulation setting. The 20 ms time period, which is required for testing convergence, is not included in the convergence time.

11.3 Results

11.3.1 Emergence of OS within layer 4

In this work it is hypothesized that there is a strong correlation between the lateral extent of the layer 4 network, and the degree of OS demonstrated by the V1 neurons. To investigate the validity of this hypothesis a V1 model has been trained. Later, with respect to the lateral extent of the layer 4 network two V1 models are configured. These two networks inherit the properties of the original layer 4 network as well as allow an examination of our hypothesis.

In the first of these two network configurations, solely horizontal connections within a hypercolumn-module are permitted, and hence this network is referred to as the 'local network'. In the second configuration connections between adjacent hypercolumn-modules are also allowed (Fig. 11.2). This network is referred to as the 'full network'. The lateral extent of the full network corresponds to the distance traveled by most excitatory axons, i.e. less than 2 mm (Yousef et al., 1999). The hypothesis is that the full network units are more orientation selective than their local network counterparts, since they have access to information from a larger region of the visual field. It is assumed that this hypothesis is in line with what is found in V1. In monkey, layer 4Cβ cells are not selective to orientation, in contrast to the layer 4Cα neurons (Hubel and Wiesel, 1977; Blasdel and Fitzpatrick, 1984; Hawken and Parker, 1984). One possible explanation for this finding might be that the lateral connections in layer 4Cα are more prominent than those found in layer 4Cβ (Martin, 2002). Cat layer 4 neurons are orientation selective (Hubel and Wiesel, 1962). These neurons have widespread lateral connections (Martin and Whitteridge, 1984; Yousef et al., 1999). Note also that layer 4 neurons in tree shrew (Humphrey and Norton, 1980; Chisum et al., 2003), and ferret (Chapman and Stryker, 1993) are poorly tuned for orientation, whereas their counterparts in layer 2/3 demonstrate sharp tuning. Since the LGN afferents rarely target layer 2/3 (Bullier and Henry, 1979; Ferster and Lindstrom, 1983; Martin and Whitteridge, 1984), it is plausible to assume that the layer 2/3 horizontal connections play an active role in the emergence of OS in these species.

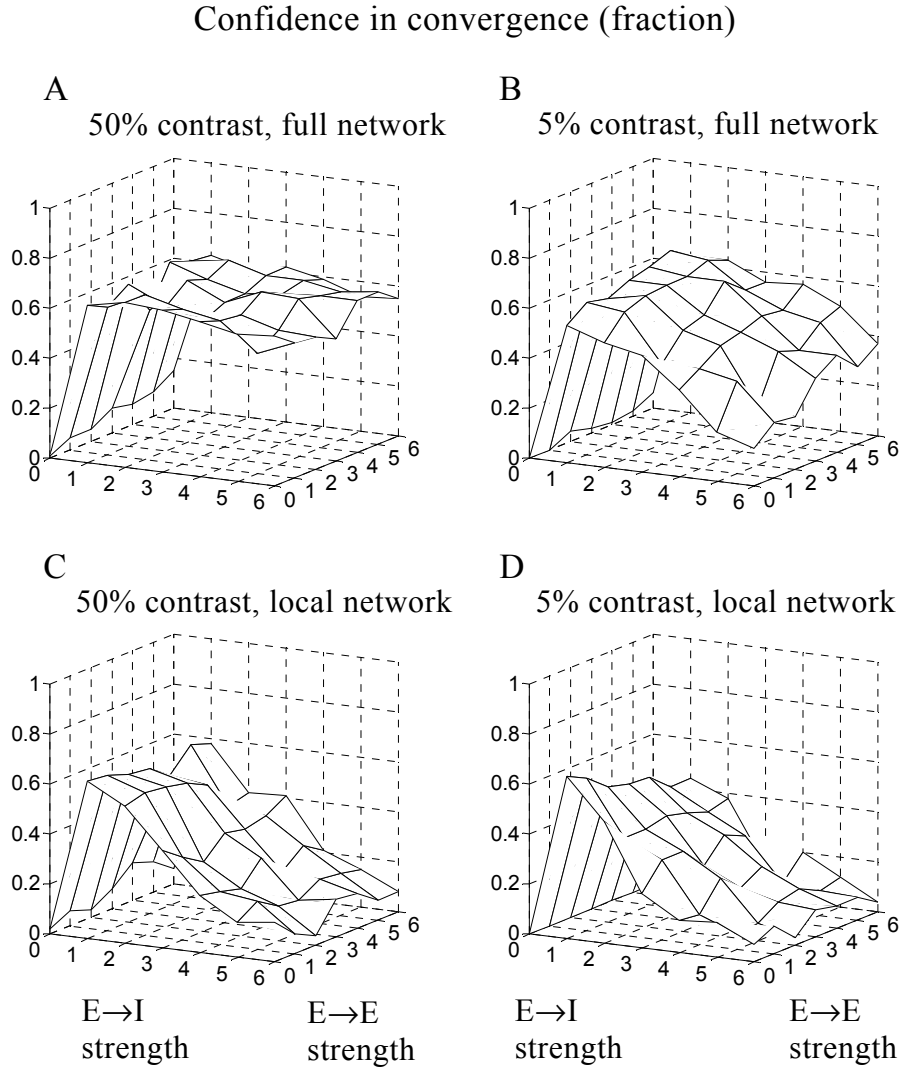

Figure 11.4. Confidence in convergence (defined as the number of correct detections divided by the number of trials) for the layer 4 reference unit (Fig. 11.2). *A–B*: Poor performance when E→E connections are absent, otherwise the full network can detect the contrast-edge. In low-contrast the network's performance decreases when excitation increases. This can be balanced by increase in inhibition though. Results are representative for the full network. *C–D*: The local network performs poorly independent of contrast. Inhibition does not seem to control excitation. Furthermore, ~25% of 200 trained layer 4 networks performed as this one, whereas in the rest OS was absent.

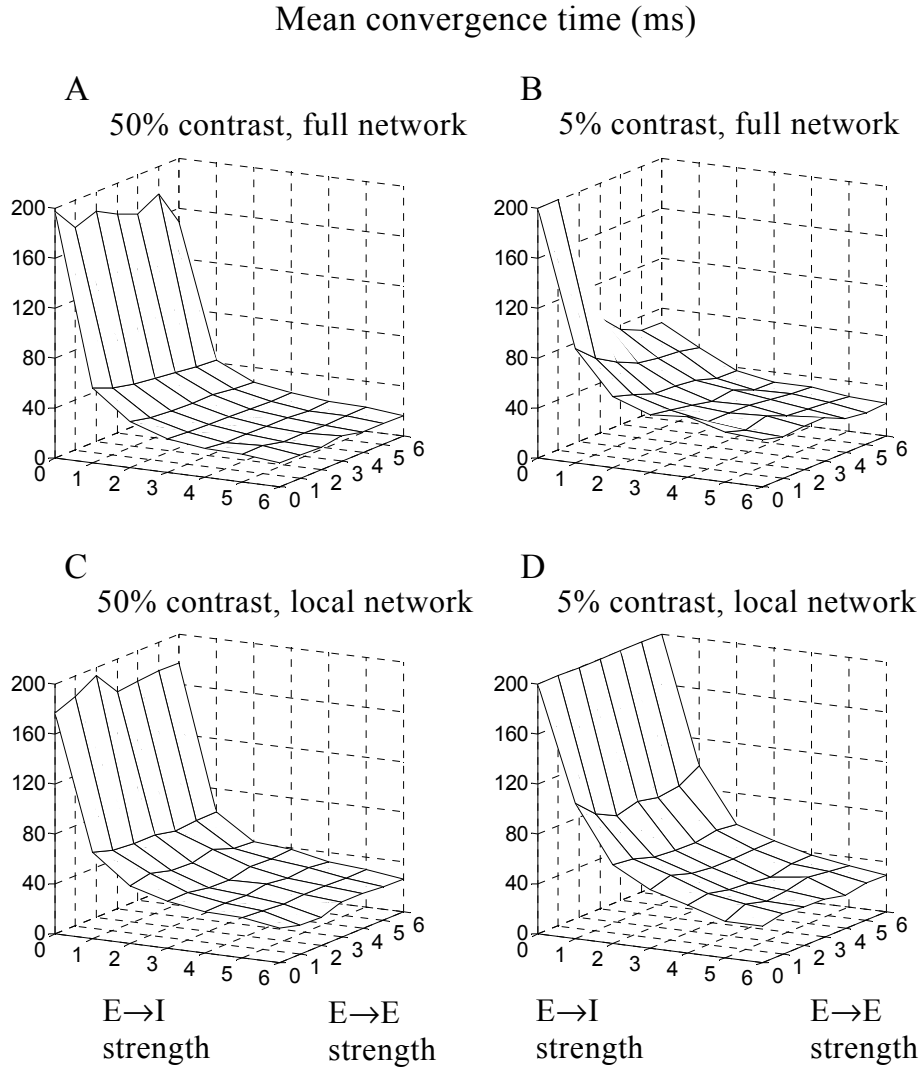

Figure 11.5. Mean convergence times of the reference unit calculated on correct detections (Fig. 11.4). In all cases both networks detect the stimulus faster when the excitatory strength is increased. Inhibitory strength does not influence convergence times. *A–B*: At E→E/I strengths = 1, convergence times are 53.5 ms (standard deviation = 9.3 ms) and 76.8 ms (standard deviation = 19.1 ms) for high- and low-contrast conditions, respectively, for the full network. Note that the network is somewhat slower in low-contrast. *C–D*: Similar results as in *A–B*, with convergence times 63.9 ms (standard deviation = 18.8 ms) and 93.2 ms (standard deviation = 23.7 ms). The local network converges slower than the full network.

For a valid comparison of the local and full networks all four sources of inputs (local and long-range excitatory/inhibitory) are modified to have the same amplitude. This is achieved by minor modifications of the original layer 4 weight

matrix. Now, by having different layer 4 internal gains, total strength of a unit's input can be controlled (independently of network configuration). In the local network configuration the internal gain is double that of full network to compensate the missing long-range connections (γ_h^{L4} in Section 11.5.2 is 90 and 45 respectively). The gain of the LGN input source is the same for both configurations: $\gamma_{ext}^{L4} = 90$. Layer 2/3 gains are 90 throughout the simulations. It is important to point out that despite weight modification and limiting the lateral extent of the horizontal connections quantitative properties as well as behavior of the original layer 4 network are preserved in the full network, since in the original network long-range inputs (excitatory and inhibitory) are as strong as the local inputs, and inhibition is roughly half of excitation.

Based on the full network quantitative assessments of the horizontal connections have been done (Tables 11.1 and 11.2). This helps to classify layer 4 connections in three groups; iso- (±30º), oblique- (±30–60º), and cross-orientation (±60–90º), and hence reveal the degree of correlation between these three orientation domains. First, projections that involve the reference unit are classified (Fig. 11.3*A*). Later, a population, with the reference unit in the core, has been put together. It is assumed that this population represents a small cortical patch, which corresponds to an injection site (Fig. 11.3*B*). Observe that the horizontal connections are reciprocal, and hence Tables 11.1 and 11.2 can be interpreted both as inputs and outputs of these two hypothetical patches.

It is evident that in the both cases local and long-range E→E connections prefer the iso-orientation domain (Tables 11.1 and 11.2). Still, ~50–60% of the E→E connections are between oblique- and cross-orientation domains. Local E→I connections show the same projection pattern as the E→E connections. Observe that strongest inhibition is between iso-orientation domains (Ferster, 1986; 1988). Furthermore, due to uncorrelated inputs direct cross-orientation inhibition is very weak. The model explains cross-orientation inhibition (Morrone et al., 1982; Bonds, 1989) by normalization inhibition, since this form of inhibition integrates total activity of a hypercolumn-module and inhibits all units equally strong (Çürüklü and Lansner, 2002). The result is net inhibition for those units that are not selective for the stimulus. Long-range E→I connections target mainly the cross-orientation domains (Tables 11.1 and 11.2). When two connection types are combined, the long-range connections become equally distributed between the three orientation domains.

These results are relatively independent of parameter settings. When the lateral extent increases long-range E→E as well as E→I connections become even less selective. Thus, the total effect is conserved. Due to increase in network size units see the stimuli more seldom. The result is reduced weight amplitudes. Connection patterns are not influencing though. The only parameter that has a major influence on the results is center-to-center distance in visual angle. When this parameter decreases the hypercolumn-modules start to collapse to one spot in the visual field.

As a result all distributions become as in the local connection case. Note that changing the center-to-center distance does also affect the pattern of long-range connections. Based on the degree of correlation between unit pairs these connections can be inhibitory or excitatory. This does not affect the numbers presented in quantitative assessments though. Furthermore, results in Tables 11.1 and 11.2 are representative for other orientations as well. Since the (hexagonal shaped) network is not symmetric in all directions (and to examine if corner effects influence the results) quantitative assessments for units with preferred orientations 0º, 30º, and 60º have been done. The results were similar to those presented in Tables 11.1 and 11.2. Taken together, the quantitative assessments of the full network suggest that local connections prefer the iso-orientation domain, whereas long-range connections are distributed equally between orientation domains. These results are in agreement with the quantitative assessment of the layer 4 (Yousef et al., 1999).

In the retrieval phase, mechanisms behind OS are investigated by analyzing network performance related to the detection of vertical contrast edge stimuli ($\theta_{st} = 90°$), in high- and low-contrast conditions (50 and 5%, respectively). The stimuli are positioned at the middle hypercolumn-module. Their spatial frequencies and widths are 1 c/deg and 1º, respectively. In order to investigate robustness of the results, and also demonstrate how the horizontal connections influence OS, excitatory (E→E) and inhibitory (E→I) strengths are varied (step length = 1) for each network configuration and contrast. For each such combination, simulations are repeated 100 times. Since the local network behavior is found to be highly unpredictable, and almost impossible to quantify (with respect to confidence as a function of connection strengths) 200 such simulation series have been done. One such simulation series is shown here (Figs. 11.4 and 11.5). Some 50 additional simulations have been done to verify that the results presented in Figs. 11.4 and 11.5 are representative for all orientations (as previously, these orientations were 0º, 30º, and 60º).

Roughly one fourth of the trained local networks behaved as in Figs. 11.4*C–D*, however, with considerably lower maximum confidence values in most of the cases (and never higher than their full network counterparts). OS was practically absence, i.e. <0.08, in the remaining local networks, independent of connection strengths and stimulus contrast. Observe that in absence of stimulus the monitored hypercolumn-module can converge to any of the 12 orientations, and hence the threshold of correct detection is ~0.08. Lower confidence values indicate no convergence within the 200 ms time period (Fig. 11.4). Increase of convergence time period to 500 ms does not change the results, and hence it is assumed that in general local network performance with respect to OS is poor and unpredictable.

	Iso-orientation (%)	Oblique-orientation (%)	Cross-orientation (%)
E→E (local)	55.0	30.0	15.0
(long-range)	53.5	30.5	16.0

Table 11.3. Distribution of the E→E connections that target the reference unit located in layer 2/3 (Fig. 11.3*A*). The distributions are calculated based on the sum of the log weights for each category. Local connections are within the same hypercolumn-module, whereas long-range connections travel between two hypercolumn-modules. The projections are classified as from iso-, oblique- and cross-orientation domains relative the reference unit.

	Iso-orientation (%)	Oblique-orientation (%)	Cross-orientation (%)
E→E (local)	51.3	32.7	16.0
(long-range)	50.0	33.3	16.7

Table 11.4. Distribution of the E→E connections that target the injection site located in layer 2/3 (Fig. 11.3*B*). The distributions are calculated based on the sum of the log weights for each category. Local connections are within the same hypercolumn-module, whereas long-range connections travel between two hypercolumn-modules. The projections are classified as from iso-, oblique- and cross-orientation domains relative the reference unit.

There are major differences between the behavior of the full and local networks. In both contrast conditions the full network can detect the stimuli (Figs. 11.4*A–B*), whereas the performance of the local network is considerably poorer, especially when excitation is increased (Figs. 11.4*C–D*). Remember also that this layer 4 network performs better than most of the trained layer 4 networks.

The full network confidence graphs reveal that the horizontal connections play an important role in the emergence of OS (Figs. 11.4*A–B*). When the E→E connections are absent the full network performs poorly. When inhibition is absent, i.e. both connection strengths are set to zero, converge within the given time period is not possible. Note that this case corresponds to the situation right at the beginning of the learning phase, since horizontal connections are absent. It is

thus assumed that for the proposed layer 4 model, i.e. the full network, poorly tuned LGN input is not sufficient for the emergence of OS (Fig. 11.4).

Independent of network configuration and contrast the highest confidence values yield when the excitatory connections are untouched (E→E strength = 1). This finding has been verified with additional simulation, during which the connection strength step length was 0.1 (instead of 1 as in 11.4). Thus, the E→E weights, which are the result of training with the BCPNN learning algorithm, yield highest degree of OS.

In general, increase in E→E strength decreases the confidence values, since the probability of converging to neighboring units increases, as a consequence of increased activity (Fig. 11.4*B*). Decrease in confidence can be compensated if the E→I strength is increased as well (Fig. 11.4*B*, see also Çürüklü and Lansner (2004)). A natural consequence of increase in total excitation is also faster convergence (Fig. 11.5). For the full network when the connection strengths are untouched mean convergence times are 53.5 ms (standard deviation = 9.3 ms), and 76.8 ms (standard deviation = 19.1 ms), respectively, in high- and low-contrast conditions. Mean convergence times for the local network are considerably longer: 63.9 ms (standard deviation = 18.8 ms), and 93.2 ms (standard deviation = 23.7 ms). Thus, even if the confidence of the local network matches that of the full network, which rarely happens, it converges slower. The variations in standard deviations between network configurations indicate that the local network is less reliable even in high-contrast conditions. Furthermore, in both configurations the networks converge slower when the stimulus contrast decreases. This so-called latency shift takes roughly the form of an exponential decay function (Albrecht et al. (2001) approximate latency shift by an inverted Naka-Rushton function).

A careful analysis of Figs. 11.4 and 11.5 reveals a possible functional role of inhibition. Assume that decrease in convergence time is desired. This can only be achieved by increasing excitation (Fig. 11.5). However, a consequence of increased excitation is also decrease in confidence. The only way of tackling this problem is to increase inhibition as well. Thus, a combined increase in excitation and inhibition does speed up the network without decreasing the confidence.

The units of the full network units have larger RF due to horizontal connections. In this context the center-to-center distance in visual angle between two adjacent hypercolumn-modules plays an important role, since performance of the full network worsens if this distance is decreased. Not surprisingly, when this distance is 0º, there are practically no differences between the full and local networks in convergence confidence (the full network is somewhat more consistent in its behavior due to averaging of the inputs). Consequently, the role of these connections is not only to smooth out noisy input. This is yet another indication of that there is a correlation between network performance and lateral extent of the horizontal connections.

	$1/\lambda_{st}$ (c/deg)	γ_x/σ_{st} (deg)	γ_y/σ_{st} (deg)
Circular	1	1/6	1/6
Orthogonal	1	∞^{-1}	1/6
Collinear	1	1/6	∞^{-1}

Table 11.5. Parameter settings for the Gabor stimuli used in the configuration-specific facilitation study (see Section 11.5.1). Circularly configured stimulus is isotropic. Orthogonal configuration is when the stimulus is elongated along the horizontal axis. Collinear configuration is equal to a vertical contrast-edge (similar to the stimuli used during the training). Note that spatial frequency and orientation of the stimuli are same in all three cases.

11.3.2 Configuration-specific facilitation in layer 2/3

In this study the learning phase is carried out as in the OS study. The layer 4 network is configured as a full network with connections strengths set to one, whereas the layer 2/3 network is untouched (Fig. 11.6). Input from the layer 4 anti-phase unit pairs generates a patchy, axially specific layer 2/3 network, which is similar to layer 2/3 of V1 (Kisvárday et al., 1997).

Presence of patches located at iso-orientation domains is an indication of correlated activity between units that are selective for similar orientations (Fig. 11.6; Tables 11.3 and 11.4). Apparently, the network does not develop E→I connections, which indicates absence of anti-correlated activity between unit pairs in layer 2/3 network. Recall that these connections are common in layer 4 network, especially between anti-phase unit pairs within a hypercolumn-module (Fig. 11.2). Quantitative assessments of the layer 2/3 reveal that 50–55% of the E→E connections are between iso-orientation domains, whereas 30–33% and 15–17% are between oblique- and cross-orientation domains, respectively (Tables 11.3 and 11.4; constellations of receiving populations correspond to those in the layer 4 cases, see Fig. 11.3). There are minor differences between local and long-range connection distributions. The former are somewhat more selective for the iso-orientation domain. These findings are further verified with quantitative assessments of units that prefer other orientations as well (0º, 30º, and 60º). These numbers are in line with what has been reported by Kisvárday et al. (1997).

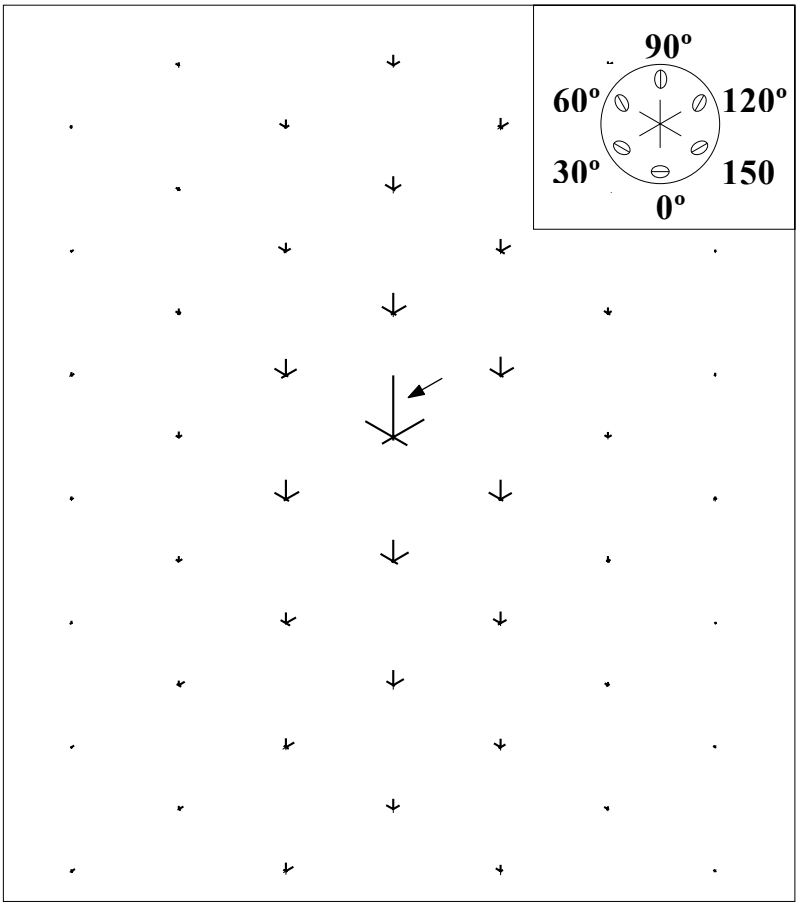

Figure 11.6. Illustration of the layer 2/3 reference unit's (marked with an arrow) elongated summation pool, which includes the whole layer 2/3 network. The legend (top right) shows the orientation preference of the presynaptic layer 2/3 units participating in the projections to the layer 2/3 reference unit. The summation pool is iso-orientation biased and antistrophic along the orientation axis of the layer 2/3 reference unit. Thick lines represent E→E connections. Note the absence of E→I connections. The length of the lines is proportional to the strength of the corresponding connection. Since the connection matrix is symmetric E→E connections are reciprocal, and hence the figure can be interpreted as the projections of the layer 2/3 reference unit.

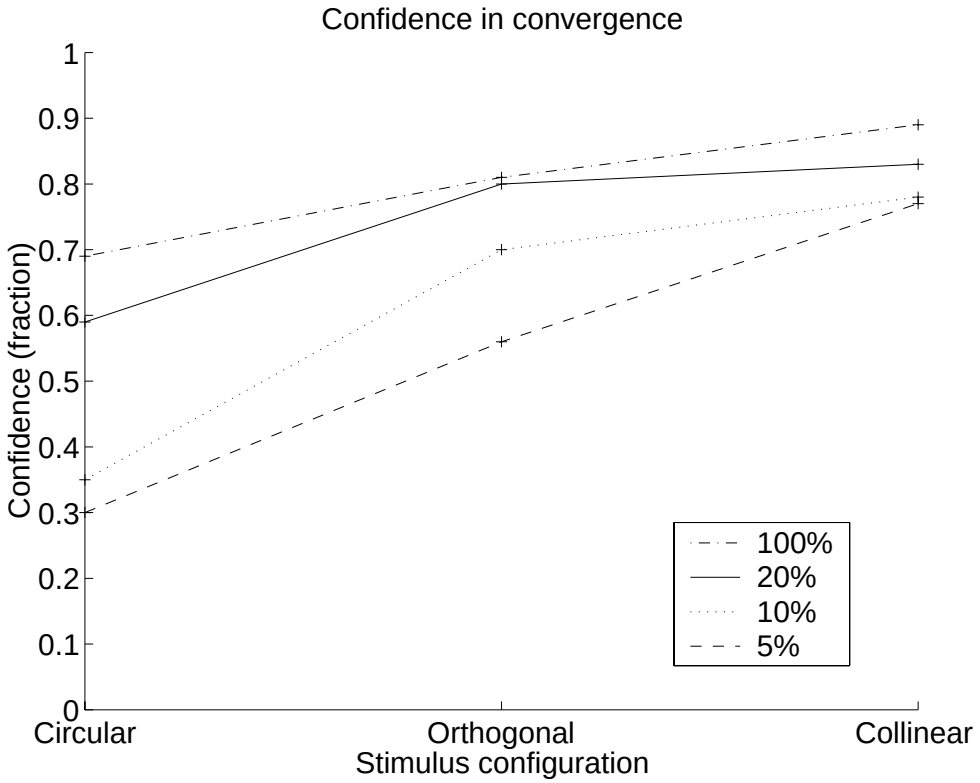

Figure 11.7. Confidence in convergence for the layer 2/3 reference unit (Fig. 11.6). The confidence is a function of both stimulus configuration and contrast. Network behavior is investigated on four contrast levels (5, 10, 20, and 100 %), and three stimulus configurations (circular, orthogonal and collinear configuration).

The region covered by the layer 2/3 long-range horizontal connections is elongated along the orientation axis of the units. This is due to the elongated shape of the contrast edge stimuli used in the learning phase. Consequently, when these stimuli are less elongated the layer 2/3 networks become less axially specific. Unit pairs that are close to each other in space are more correlated than those far away. The result is decrease in connection strengths with increased distance. Otherwise different parameter settings generate similar network layouts, and hence it is assumed the results are robust. Especially the modular specificity is evident in all trained layer 2/3 networks.

Configuration-specific facilitation has been investigated using three different vertically orientated ($\theta_{st} = 90°$) Gabor patch stimuli (Table 11.5) under various contrast conditions (5, 10, 20, and 100%). In the first case the retrieval stimulus is a circular Gabor patch. The remaining two stimuli are elongated along one axis: either along horizontal (orthogonal configuration) or vertical (collinear configuration). Layer 2/3 network is tested 100 times on each contrast and stimulus configuration. Only some 20 simulation series have been done since the

layer 2/3 network behavior is fairly deterministic. As in the OS study confidence values are calculated. One such simulation series is shown here (Fig. 11.7). In this context confidence values reflect the degree of facilitation as a function of stimulus configuration (and contrast). High confidence means sharp OS, and hence is an indication of strong facilitation.

The result of elongation of the stimulus is increase of stimulus area. The consequence is increase of confidence independent of stimulus contrast (Fig. 11.7). This improvement in confidence is further configuration-specific, since collinear configuration results in a more prominent increase of the confidence than orthogonal. These results are in line with experimental studies on configuration-specific facilitation phenomena (Polat and Norcia, 1998; Chisum et al., 2003).

Differences in facilitation effects are more prominent in low-contrast (5%), since in this case ratios between confidences for circular, orthogonal, and collinear configurations are 1.0:2.0:2.7 (Fig. 11.7). This shows that in low-contrast, collinearly configured stimuli are almost three times easier to detect that circularly configured stimuli. When stimulus contrast is high layer 2/3 network detects all three stimuli equally well (Fig. 11.7). In high-contrast (100%) the same ratios are 1.0:1.2:1.3. Apparently, the network is less dependent on stimulus configuration in high-contrast. Differences in facilitation between circular and collinear configurations are still evident even in high-contrast though. This result is in line with Chisum et al. (2003). Furthermore, independent of stimulus configuration, confidence increase is linear as a function of log contrast, as reported by Polat and Norcia (1998). This suggests fast improvement of confidence as a function of contrast increase in low-contrast conditions.

It is assumed that the layer 2/3 is responsible for configuration-specific facilitation phenomena. The layer 4 network is circular and mainly local (Fig. 11.2), thus behavior of this network is not likely to depend on stimulus configuration. In other words, the layer 4 network cannot detect the differences between these three stimuli. The situation is different for the layer 2/3 network, since in this case units receive input from an anisotropic region (Fig. 11.6), which is overlapped with the stimulus. As a consequence, input from collinearly positioned units (with similar orientation preferences, due to modular specificity) is stronger than from all other units in the layer 2/3 network. Recall also that horizontal connections are reciprocal, thus units along the line, which overlaps with the stimulus, excite each other in a positive feedback loop.

Since one anti-phase unit pair targets each layer 2/3 unit, low layer 4 RF ratios are preserved in layer 2/3. Thus, In the V1 model confidence-specific facilitation phenomena are not due to elongated CRF (Gilbert and Wiesel, 1985; DeAngelis et al., 1994). Neither is total amount of excitatory input is different due to stimulus configuration, since the hypercolumn-modules are normalized. Thus, in this study configuration-specific facilitation phenomena are explained solely by the axially specific layout of the long-range horizontal connections in layer 2/3.

Only one parameter influenced the simulation results considerably, i.e. center-to-center distance in visual angle between two adjacent hypercolumn-modules. When this parameter is decreased layer 4 units become less orientation specific, which has a negative effect on the confidence values in layer 2/3 as well. Nevertheless, differences in facilitation were still evident. The simulations have been done with other orientations as well (0º, 30º, and 60º) with similar results as in Fig. 11.7. Thus, it is assumed the precise layout of the long-range horizontal connections does not influence the results.

11.4 Conclusions

In this paper, a laminar model of the layers 4 and 2/3 of area V1 of mammals is presented. The model addresses development as well as functional roles of the horizontal connections found in these two cortical layers. It is assumed that both layers are subject to visual experience at the eye opening. It is further assumed that the LGN input is poorly tuned for orientations. These two assumptions are sufficient for modeling how correlation based networks of horizontal connections are developed simultaneously in layers 4 and 2/3 by the BCPNN learning rule. These assumptions are in line with reports on rapid improvement of OS during the first weeks after eye opening, when the eyes are subject to normal visual experience. This period coincides with the development of the horizontal connections as well. Thus, it seems that improvement of response properties of the neurons is closely related to normal development of these connections. This process is fragile though, since manipulation of the visual input, e.g. through dark rearing or binocular deprivation, alters normal development of these connections. One indication of this is the reduction of the lateral extent of these connections. Yet another consequence of manipulation of the visual input is poorly tuned neurons.

The resulting networks resemble some of the cortical layers' properties. In the layer 4 network, units that are correlated develop E→E connections, whereas anti-correlation results in the development of E→I connections. Both types of connections target mainly the local iso-orientation domain, thus iso-orientation inhibition dominates cross-orientation inhibition. The layout of the long-range connections is different though. These connections are distributed equally between orientation domains. Due to the elongated shape of the stimuli used in the learning phase the connections in layer 2/3 become axially specific. Modular specificity in layer 2/3 is explained by the finding that units in this layer are rarely anti-correlated. Patches are located at the iso-orientation domains. This indicates strong correlated activity between units that are selective for similar orientations. It remains to be shown if the same conditions are in fact valid during the development of V1 in reality.

In both layers normalization inhibition operates within a hypercolumn-module. In layer 4 there is an additional source of inhibition mediated by the (excitatory) E→I connections. These connections target local inhibitory interneurons, thus this form of inhibition is local as well. These assumptions are in line with what is found in V1, i.e. inhibition is mainly local, whereas excitation extends far beyond the inhibitory network. Observe also that neither excitation nor inhibition dominates the network.

The V1 model addresses phenomena that are related to the layout of the horizontal connections. In the first study it is shown that the presence of normally developed horizontal connections is responsible for emergence of OS. This is in line with rapid improvement of this response property after eye opening. Furthermore, the simulation results suggest that this property is dependent on the lateral extent of the horizontal connections. In the full network case the units are highly orientation selective, in contrast to units in the local network that are poorly tuned. Recall that in both cases the units receive roughly the same amount of excitation. When the horizontal connections are absent the network cannot even converge. This indicates absence of OS.

The proposed layer 4 network addresses OS by assuming (i) normalization inhibition for controlling the total activity of the hypercolumn-modules, and (ii) long-range E→E connections, which provide units with information from a larger region than their CRF. Increase in the strengths of the E→E connections decreases convergence times as well as confidence values. The E→I connections play a major role in stabilizing the activity of the units though. Increasing the strengths of these connections prevents the drop off in confidence values without affecting convergence times. Observe the layer 4 network addresses OS by assuming V1 like connectivity, i.e. the network is not dominated by extremely strong inhibition, and the excitatory network encloses its inhibitory equivalent.

It seems that the elongated summation pools in the layer 2/3 network can address configuration-specific facilitation phenomena. Simulation results suggest that the visibility of a stimulus is improved due to its elongation along one direction. Not surprisingly the degree of facilitation, and hence improved visibility, is related to the direction of elongation, since summation pools found in the layer 2/3 network are axially specific along the orientation axis of the units. Observe that anisotropic inputs from this network are sufficient for explaining configuration-specific facilitation phenomena. It seems also that differences in facilitation effects are more prominent in low-contrast conditions. Note further that the layer 4 network receives input from a circular region, and hence does not take part in this process.

Based on these results it is plausible to assume that the horizontal connections play an important role in the formation of the V1 neurons' response properties. Our intention is to examine further issues related to development as well as functional roles of these connections.

11.5 Appendix

11.5.1 LGN input equations

Tuning curve of the LGN input is defined by the following equation:

$$\Omega_{\sigma_{os}}(\delta\theta) = e^{\frac{-\delta\theta^2}{2\sigma_{os}^2}}, \qquad (1)$$

where $\delta\theta = \theta_{st} - \theta_{rf}$ is the orientation preference difference (in radians) between the orientation of the contrast edge stimulus (θ_{st}), and the orientation preference of a unit (θ_{rf}). Parameter σ_{os} defines the sharpness of the orientation tuning. In the simulations $\sigma_{os} = 0.7$, which yields poor tuning (half-width at half-height is 47.2º).

The LGN input has two components (Troyer et al., 2002):

$$i_{LGN}(x, y, c, \delta\theta) = DC(c) + F1(c) \cdot \Omega_{\sigma_{os}}(\delta\theta) \cdot f_{\gamma_x\gamma_y\lambda_{st}\sigma_{st}}(x, y)a, \qquad (2)$$

where

$$DC(c) = F1(c) = \frac{c}{2}, \quad 0 \le c \le 1 \qquad (3)$$

and

$$f_{\gamma_x\gamma_y\lambda_{st}\sigma_{st}}(x, y) = \cos\left(\frac{2\pi \cdot x}{\lambda_{st}}\right) \cdot e^{-\frac{x^2\gamma_x^2 + y^2\gamma_y^2}{2\sigma_{st}^2}}.$$

Parameters γ_x and γ_y (together with σ_{st}) define the extent of the stimulus in x- and y-axis respectively. Spatial frequency of the stimulus is given by $1/\lambda_{st}$. Before feeding into the layer 4 units the LGN input is rectified, since the mean LGN activity cannot fall below zero:

$$I_{LGN}(x, y, c, \delta\theta) = \max[i_{LGN}(x, y, c, \delta\theta), 0].$$

11.5.2 V1 model equations

Standard BCPNN framework, which consists of network architecture and learning rule (Sandberg et al., 2002), has been adapted to the simulations that are done with the proposed V1 model. Following equation defines the total input ($H_{jj'}^{\xi}$) of unit

jj'. This unit, whose orientation is represented by the index *j'*, is located in hypercolumn-module *j*, and cortical layer model ξ:

$$H_{jj'}^{\xi} = \Psi_{\xi}\gamma_{h}^{\xi}h_{jj'}^{\xi} + \left(1-\Psi_{\xi}\right)\gamma_{ext}^{\xi}ext_{jj'}^{\xi}, \quad \xi \in \{L4, L2/3\}, \tag{4}$$

where

$$0 \le \Psi_{\xi} \le 1, \tag{5}$$

and

$$\gamma_{h}^{\xi}\max\left(h_{jj'}^{\xi}\right) = \gamma_{ext}^{\xi}\max\left(ext_{jj'}^{\xi}\right). \tag{6}$$

Parameter Ψ_{ξ} relates the two sources of inputs to each other (Eqs. 11.4–11.6). These inputs are the internal input, $h_{jj'}^{\xi}$, and the external input, $ext_{jj'}^{\xi}$. Maximum values of these two sources are defined in questions 10 and 11. Assuming one-layer network, standard BCPNN equations (Sandberg et al., 2002) is given when $\Psi_{\xi}=1$. Parameters γ_{h}^{ξ} and γ_{ext}^{ξ} are internal and external gain respectively. Layer 4 external input is:

$$ext_{jj'}^{L4} = I_{LGN}\left(x, y, c, \delta\theta\right).$$

In the OS study two network configurations has been used for the layer 4 model. The local network configuration is obtained by (h_{ref}^{L4} is the internal input of the reference unit in layer 4):

$$\gamma_{h}^{\xi} = \gamma_{ext}^{\xi}, \quad -\mu \le h_{jj'}^{L4} \le \mu, \quad 0 \le ext_{jj'}^{L4} \le \mu, \quad \mu = \max\left(h_{ref}^{L4}\right),$$

and the full network configuration is obtained similarly:

$$\gamma_{h}^{\xi} = \frac{\gamma_{ext}^{\xi}}{2}, \quad -\mu \le h_{jj'}^{L4} \le \mu, \quad 0 \le ext_{jj'}^{L4} \le \frac{\mu}{2}, \quad \mu = \max\left(h_{ref}^{L4}\right).$$

The external input to a layer 2/3 unit is the summed activity of the two anti-phase pairs located in the layer 4 model below:

$$ext_{jj'}^{L2/3} = \hat{\pi}_{jj'}^{L4} + \hat{\pi}_{jk'}^{L4}, \quad j' \mapsto \phi, k' \mapsto \phi + 180^{\circ}, \tag{7}$$

$$\gamma_{h} = \gamma_{ext}, \quad 0 \le h_{jj'}^{L2/3} \le \mu, \quad 0 \le ext_{jj'}^{L2/3} \le \mu, \quad \mu = \max\left(h_{ref}^{L2/3}\right).$$

Internal input of unit *jj'* is defined according to the standard BCPNN equations (Sandberg et al., 2002) (index ξ is ignored for clarity in equations below):

$$h_{jj'} = \beta_{jj'} + \sum_{i}^{N} \log\left(\sum_{i'}^{M_i} w_{ii'jj'} P_{X_i}(x_{ii'}) \right).$$

The bias of unit *jj'* is:

$$\beta_{jj'} = \log(P(y_{jj'})),$$

and the weight that connects the 'presynaptic' unit *ii'* to unit *jj'* is:

$$w_{ii'jj'} = \frac{P(x_{ii'}, y_{jj'})}{P(x_{ii'})P(y_{jj'})}.$$

Convergence to the attractor state is defined through the following equation:

$$\tau_c \frac{dh_{jj'}(t)}{dt} = \beta_{jj'}(t) + \sum_{i}^{N} \log\left(\sum_{i'}^{M_i} w_{ii'jj'} f(h_{ii'}(t)) \right) - h_{jj'}(t),$$

where τ_c is 'membrane time constant' of units. The inner sum above denotes input from one of *N* hypercolumn-modules in the network.

At the end of each retrieval step the total activity within a hypercolumn-module is normalized to one (Eq. 11.8). By doing this, the total activity within the hypercolumn-modules, and consequently the network is controlled:

$$\hat{\pi}_{jj'} = f(H^{\xi}_{jj'}) = \frac{e^{H^{\xi}_{jj'}}}{\sum_{j'} e^{H^{\xi}_{jj'}}}. \qquad (8)$$

In learning mode units receive solely external input. Weights and biases are updated through following equations:

$$\hat{\pi}_{ii'} = ext^{\xi}_{ii'} \qquad (9)$$

$$\frac{d\Lambda_{ii'}(t)}{dt} = \alpha([(1-\lambda_0)\hat{\pi}_{ii'}(t) + \lambda_0] - \Lambda_{ii'}(t)) \qquad (10)$$

$$\frac{d\Lambda_{ii'jj'}(t)}{dt} = \alpha([(1-\lambda_0^2)\hat{\pi}_{ii'}(t)\hat{\pi}_{jj'}(t) + \lambda_0^2] - \Lambda_{ii'jj'}(t)) \qquad (11)$$

$$\beta_{ii'}(t) = \log(\Lambda_{ii'}(t) + \lambda_0) \qquad (12)$$

$$w_{ii'jj'}(t) = \frac{\Lambda_{ii'jj'}(t)}{\Lambda_{ii'}(t)\Lambda_{jj'}(t)} \qquad (13)$$

To avoid logarithmic zero $\lambda_0 = 10^{-8}$ is introduced. This parameter mimics the background activity as well. Parameter α is defined as the inverse of the learning time constant τ_L. Plasticity is induces when $\alpha > 0$, (network is non-plastic if $\alpha = 0$.

Acknowledgements

This work was supported by CUGS (the Swedish National Graduate School in Computer Science).

References

Ahmed BA, Anderson JC, Douglas RJ, Martin KA, Nelson JC (1994) Polyneural innervation of spiny stellate neurons in cat visual cortex. J. Comp. Neurol. 341:39–49.

Albrecht DG, Hamilton DB (1982) Striate cortex of monkey and cat: contrast response function. J. Neurophysiol. 48:217–237.

Albrecht DG, Geisler WS, Frazor RA, Crane AM (2001) Visual cortex neurons of monkey and cats: temporal dynamics of the contrast response function. J. Neurophysiol. 88:888–913.

Albus K, Wolf K (1984) Early postnatal development of neuronal function in the kitten's visual cortex: J. Physiol. (Lond.) 348:153–185.

Allman JM, Meizin F, McGuiness E (1985) Stimulus specific responses from beyond the classical receptive field: neurophysiological mechanisms for local-global comparisons in visual neurons. Annu. Rev. Neurosci. 5:407–430.

Amir Y, Harel M, Malach R (1993) Cortical hierarchy reflected in the organization of intrinsic connections in macaque monkey visual cortex. J. Comp. Neurol. 334:19–46.

Ben-Yishai R, Bar-Or RL, Sompolinsky H (1995) Theory of orientation tuning in visual cortex. Proc. Natl. Acad. Sci. USA 92:3844–3848.

Ben-Yishai R, Hansel D, Sompolinsky H (1997) Traveling waves and the processing of weakly tuned inputs in a cortical network module. J. Comput. Neurosci. 4: 57–77.

Blakemore C, Van Sluyters RC (1975) Innate and environmental factors in the development of the kitten's visual cortex. J. Physiol. 248:663–716.

Blasdel GG, Fitzpatrick D (1984) Physiological organization of layer 4 in macaque striate cortex. J. Neurosci. 4:880–95.

Bonds AB (1989) The role of inhibition in the specification of orientation selectivity of cells in the cat striate cortex. Vis. Neurosci. 2:41–55

Bosking WH, Zhang Y, Schofield B, Fitzpatrick D (1997) Orientation selectivity and the arrangement of horizontal connections in tree shrew striate cortex. J. Neurosci. 17:2112–2127.

Buisseret P, Imbert M (1976) Visual cortical cells: their developmental properties in normal and dark-reared kittens. J. Neurophysiol. 255:511–525.

Bullier J, Henry GH (1979) Laminar distribution of first order neurons and afferent terminals in cat striate cortex. J. Neurophysiol. 42:1271–1281.

Buxhoeveden DP, Casanova MF (2002) The minicolumn hypothesis in neuroscience. Brain 125:935–951.

Chapman B, Gödecke I, Bonhoeffer T (1999) Development of orientation preference in the mammalian visual cortex. J. Neurobiol. 41:18–24.

Chapman B, Stryker MP (1993) Development of orientation selectivity in ferret visual cortex and effects of deprivation. J. Neurosci. 13:5251–5262.

Chapman B, Stryker MP, Bonhoeffer T (1996) Development of orientation preference maps in ferret primary visual cortex. J. Neurosci. 16:6443–6453.

Chapman B, Zahs KR, Stryker MP (1991) Relation of cortical cell selectivity to alignment of receptive fields of the geniculocortical afferents that arborize within a single orientation column in ferret visual cortex. J. Neurosci. 11:1347–1358.

Chisum HJ, Mooser F, Fitzpatrick D (2003) Emergent properties of layer 2/3 neurons reflect the collinear arrangement of horizontal connections in tree shrew visual cortex. J. Neurosci. 23:2947–2960.

Crair MC, Gillespie DC, Stryker MP (1998) The role of visual experience in the development of columns in cat visual cortex. Science 279:566–570.

Çürüklü B, Lansner A (2002) An abstract model of a cortical hypercolumn, in: IEEE Proc., International Conference on Neural Information Processing 80–85.

Çürüklü B, Lansner A (2003) Quantitative assessment of the local and long-range horizontal connections within the striate cortex, in: IEEE Proc. Computational Intelligence, Robotics and Autonomous Systems.

Çürüklü B, Lansner A (2004) A Model of the Summation Pools within the Layer 4 (Area 17). The Annual Computational Neuroscience Meeting 2004, Baltimore, USA.

Das A (1996) Orientation in visual cortex: a simple mechanism emerges. Neuron 16:447–480.

Dean AF (1981) The relationship between response amplitude and contrast for cat striate cortical neurons. J. Physiol. 318:413–427.

DeAngelis GC, Freeman RD, Ohzawa I (1994)Length and width tuning of neurons in the cat's primary visual cortex. J. Neurophysiol. 71:347–374.

Derrington AM, Fuchs AF (1979) Spatial and temporal properties of X and Y cells in the cat lateral geniculate nucleus. J. Physiol. 293:347–364.

Durack JC, Katz LC (1996) Development of horizontal projections in layer 2/3 of ferret visual cortex. Cerebral Cortex 6:178–183.

Einstein G, Davis TL, Sterling P (1987) Pattern of lateral geniculate synapses on neuron somata in layer IV of the cat striate cortex. J. Comp. Neurol. 260:76–68.

Ferster D (1986) Orientation selectivity of synaptic potentials in neurons of cat primary visual cortex. J. Neurosci. 6:1284–1301.

Ferster D (1988) Spatially opponent excitation and inhibition in simple cells of the cat visual cortex, J. Neurosci., 8:1172–1180.

Ferster D (1990) X- and Y-mediated synaptic potentials in neurons of areas 17 and 18 of cat visual cortex. Vis Neurosci 4:115–133.

Ferster D, Chung S, Wheat H (1996) Orientation selectivity of thalamic input to simple cells of cat visual cortex. Nature 380:249–252.

Ferster D, Lindstrom S (1983) An intracellular analysis of geniculo-cortical connectivity in area 17 of the cat. J. Physiol. (Lond.) 342:181–215.

Ferster D, Miller KD (2000) Neural mechanisms of orientation selectivity in the visual cortex. Annual Reviews of Neurosci. 23:441–471.

Fitzpatrick D (1996) The functional organization of local circuits in visual cortex: insights from the study of tree shrew striate cortex. Cerebral Cortex 6:329–341.

Frégnac Y, Imbert M (1978) Early development of visual cortical cells in normal and dark-reared kittens: the relationship between orientation selectivity and ocular dominance. J. Physiol. 278:27–44.

Garey LJ, Powell TPS (1971) An experimental study of the termination of the lateral geniculo-cortical pathway in the cat and monkey. Proc. R. Soc. Lond. [Biol.] 179:41–63.

Gilbert CD, Wiesel TN (1983) Clustered intrinsic connections in cat visual cortex. J. Neurosci. 3:1116–1133.

Gilbert CD, Wiesel TN (1985) Intrinsic connectivity and receptive field properties in visual cortex. Vis. Res. 25:365–374.

Gödecke I, Kim DS, Bonhoeffer T, Singer W (1997) Development of orientation preference maps in area 18 of kitten visual cortex. Eur. J. Neurosci. 9:1754–1762.

Hawken M, Parker AJ (1984) Contrast sensitivity and orientation selectivity in lamina IV of the striate cortex of old world monkeys. Exp. Brain Res. 54:367–72.

Hirsch JA, Alonso J-M, Pillai C, Pierre C (2000) Simple and complex inhibitory cells in layer 4 of cat visual cortex. Soc. Neurosci. Abstr. 26:1083.

Hirsch JA, Martinez LM, Pillai C, Alonso J-M, Wang Q, Sommer FT (2003) Functionally distinct inhibitory neurons at the first stage of visual cortical processing. Nat. Neurosci. 6:1300–1308.

Holst A (1997) The use of a Bayesian neural network model for classification tasks. PhD Thesis Department of Numerical Analysis and Computing Science, Royal Institute of Science, Stockholm, Sweden, TRITA-NA-P9708.

Hornung JP, Garey LJ (1981) The thalamic projection to the cat visual cortex: ultrastructure of neurons identified by Golgi impregnation or retrograde horseradish peroxidase transport. Neuroscience 6:1053–1068.

Howell ER, Hess RF (1978) The functional area for summation to threshold for sinusoidal gratings. Vision Res., 18:369–374.

Hubel DH, Wiesel TN (1962) Receptive fields, binocular interaction and functional architecture in the cat's visual cortex, J. Physiol., 160:106–154.

Hubel DH, Wiesel TN (1963) Receptive fields of cells in striate cortex of very young, visually inexperienced kittens. J. Neurophysiol. 26:994–1002.

Hubel DH, Wiesel TN (1977) The functional architecture of the macaque visual cortex, The Ferrier lecture. Proc. Royal. Soc. B. 198:1–59.

Humphrey AL, Norton TT (1980) Topographic organization of the orientation column system in the striate cortex of the tree shrew (Tupaia glis). I. Microelectrode recording. J. Comp. Neurol. 192:531–547.

Jones JP, Palmer LA (1987) The two-dimensional spatial structure of simple cell receptive fields in cat striate cortex. J. Neurophysiol. 58:1187–1211.

Kaplan E, Shapley RM (1982) X and Y cells in the lateral geniculate nucleus of macaque monkey. J Physiol. London 330:125–143.

Kayser AS, Miller KD (2002) Opponent inhibition: a development model of layer 4 of the neocotical circuit. Neuron 33:131–142.

Kisvárday ZF, Tóth E, Rausch M, Eysel UT (1997) Orientation-specific relationship between populations of excitatory and inhibitory lateral connections in the visual cortex of the cat. Cerebral Cortex 7:605–618.

Krimer LS, Goldman-Rakic PS (2001) Prefrontal Microcircuits: Membrane properties and excitatory input of local, medium, wide arbor interneurons. J. Neurosci., 21:3788–3796.

Kritzer MF, Cowey A, Somogyi P (1992) Patterns of inter- and intralaminar GABAergic connections distinguish striate (V1) and extrastriate (V2, V4) visual cortices and their functionally specialized subdivisions in the Rhesus monkey. J Neurosci 12:4545–4564.

Lansner A, Ekeberg Ö (1987) An associative network solving the "4-bit adder problem". In: Caudill M, Butler C (editors). IEEE First International Conference on Neural Networks. Pp II–549.

Lansner A, Ekeberg Ö (1989) A one-layer feedback artificial neural network with a bayesian learning rule. Int. J. Neural Syst. 1:77–78.

Lansner A, Holst A (1996) A higher order bayesian neural network with spiking units. Int. J. Neural Syst. 7:115–128.

Lauritzen TZ, Miller KD (2003) Different roles for simple-cell and complex-cell inhibition in V1. J. Neurosci. 23:10201–10213.

LeVay S (1986) Synaptic organization of claustral and geniculate afferents to the primary visual cortex of the cat. J. Neurosci. 6:3564–3575.

LeVay S, Gilbert CD (1976) Laminar patterns of geniculocortical projections in the cat. Brain Res. 113:1–19.

Lund JS, Angelucci A, Bressloff PC (2003) Anatomical substrates for functional columns in macaque monkey primary visual cortex. Cerebral Cortex 12:15–24.

Orban GA Neuronal operation in the visual cortex. Berlin: Springer Verlag, 1984.

Maffei L, Fiorentini A, Bisti S (1973) Neural correlate of perceptual adaptation to gratings. Science 182:1036–1038.

Malach R, Amir Y, Harel M, Grinvald A (1993) Relationship between intrinsic connections and functional architecture revealed by optical imagining and in vivo targeted biocytin injections in primate striate cortex. Proc. Natl. Acad. Sci. USA 90:10496–10473.

Martin KAC (2002) Microcircuits in visual cortex. Current Opinion in Neurobiology 12:418–425.

Martin KAC, Whitteridge D (1984) Form, function and intracortical projections of spiny neurons in the striate visual cortex of the cat. J. Physiol. (Lond.) 353:463–504.

McDonald CT, Burkhalter A (1993) Organization of long-range inhibitory connections within rat visual cortex. J Neurosci 13:768–781.

McLaughin D, Shapley R, Shelley M, Wielaard DJ (2000) A neuronal network model of macaque primary visual cortex (V1): orientation selectivity and dynamics in the input layer 4Cα. Proc. Natl. Acad. Sci. USA 97:8087–8092.

Miller KD, Erwin E, Kayser A (1999) Is the development of orientation selectivity instructed by activity? J. Neurobiol. 41:44–57.

Morrone MC, Burr DC, Maffei L (1982) Functional implications of cross-orientation inhibition of cortical visual cells. I. Neurophysiological evidence. Proc. R. Soc.London Ser. B 216:335–54

Mountcastle VB (1957) Modality and topographic properties of single neurons of cat's somatic sensory cortex. J. Neurophysiol. 20:408–438.

Mountcastle VB (1978) An organizing principle for cerebral function. In: Edelman GM, Mountcastle VB (editors). The mindful brain. MIT Press 7–50.

Mountcastle VB (1997) The columnar organization of the neocortex. Brain 120:701–722.

Pei X, Vidyasagar TR, Volgushev M, Creutzfeldt OD (1994) Receptive field analysis and orientation selectivity of postsynaptic potentials of simple cells in cat visual cortex. J. Neurosci. 14:7130–7140.

Peters A, Payne BR (1993) Numerical relationships between geniculocortical afferents and pyramidal cell modules in cat primary visual cortex. Cereb. Cortex 3:69–78.

Polat U, Norcia AM (1998) Elongated physiological summation pools in the human visual cortex, Vision Res., 38:3735–3741.

Polat U, Sagi D (1993) Lateral interactions between spatial channels: Suppression and facilitation revealed by lateral masking experiments. Vision Res., 33:993–999.

Polat, U, Sagi, D (1994) The architecture of perceptual spatial interactions. Vision Res., 34:73–78.

Polat U, Sagi D (1994) Spatial interactions in human vision: From near to far via experience-dependent cascades of connections. Proceedings of the National Academy of Science USA, 91:1206–1209.

Polat U, Tyler CW (1999) What pattern the eye sees best, Vision Res., 37:887–895.

Powell TPS, Mountcastle VB (1959) Some aspects of the functional organization of the cortex of the postcentral gyrus of the monkey: a correlation of findings obtained in a single unit analysis with cytoarchitecture. Bull Johns Hopkins Hosp. 105:133–162.

Reid RC, Alonso JM (1995) Specificity of monosynaptic connections from thalamus to visual cortex. Nature 378:281–284.

Robson JG, Graham N (1981) Probability summation and regional variation in contrast sensitivity across the visual field. Vision Res., 21:409–418.

Rockland KS (1985) Anatomical organization of primary visual cortex (area 17) in the ferret. J. Comp. Neurol. 241:225–236.

Rockland KS, Lund JS (1982) Widespread periodic intrinsic connections in the tree shrew visual cortex. Science 215:1532–1534.

Rockland KS, Lund JS (1983) Intrinsic laminar lattice connections in primate visual cortex. J. Comp. Neurol. 216:303–318.

Roerig B, Chen B (2002) Relationships of local inhibitory and excitatory circuitry to orientation preference maps in ferret visual cortex. Cereb Cortex, 12:197–198.

Sandberg A (2003) Bayesian attractor neural networks of memory. PhD Thesis Department of Numerical Analysis and Computing Science, Royal Institute of Science, Stockholm, Sweden, TRITA-NA-0310.

Sandberg A, Lansner A, Petersson FM, Ekeberg Ö (2002) A Bayesian attractor network with incremental learning, Network: Computing in Neural Systems, 13:179–194.

Schmidt KE, Kim D-S, Singer W, Bonhoeffer T, Löwel S (1997) Functional specificity of long-range intrinsic and interhemisphic connections in the visual cortex of strabismic Cats. J. Neurosci. 17:5480–5492.

Somers D, Dragoi V, Sur M (2002) Orientation selectivity and its modulation by local and long-range connections in visual cortex. in: Payne BR, Peters A (ed.). The cat primary visual cortex. Academic Press.

Somers D, Nelson SB, Sur M (1995) An emergent model of orientation selectivity in cat visual cortical simple cells. J. Neurosci. 15:5448–5465.

Sompolinsky H, Shapley R (1997) New perspectives on the mechanisms for orientation selectivity. Current Opinion in Neurobiology 7:514–522.

Stratford KJ, Tarczy-Hornoch K, Martin KA, Bannister NJ, Jack JJ (1996) Excitatory synaptic inputs to spiny stellate cells in cat visual cortex. Nature 382:258–261.

Troyer TW, Krukowski AE, Miller KD (1998) Contrast-invariant orientation tuning in cat visual cortex: thalamocortical input tuning and correlation-based intracortical connectivity. J. Neurosci. 18:5908–5927.

Troyer TW, Krukowski AE, Miller KD (2002) LGN input to simple cells and contrast-invariant orientation tuning: an analysis, J. Neurophysiol., 87:2741–2752.

White LE, Coppola DM, Fitzpatrick D (2001) The contribution of sensory experience to the maturation of orientation selectivity in ferret visual cortex. Nature 411:1049–1052.

Wielaard DJ, Shelley M, McLaughin D, Shapley R (2001) How simple cells are made in a nonlinear network model of the visual cortex. J. Neurosci., 21:5203–5211.

Wiesel TN, Hubel DH (1974) Ordered arrangement of orientation columns in monkeys lacking visual experience. J. Comp. Neurol. 158:307–318.

Winfield DA, Powell TPS (1983) Laminar cell counts and geniculo-cortical boutons in area 17 of cat and monkey. Brain Res. 227:223–229.

Yousef T, Bonhoeffer T, Kim D-S, Eysel UT, Tóth E, Kisvárday ZF (1999) Orientation topography of layer 4 lateral networks revealed by optical imagining in cat visual cortex (area 18), E. J. of Neurosci., 11:4291–4308.

Yousef T, Bonhoeffer T, Kim D-S, Eysel UT, Tóth E, Kisvárday ZF (1999) Orientation topography of layer 4 lateral networks revealed by optical imagining in cat visual cortex (area 18), E. J. of Neurosci., 11:4291–4308.